# Exploiting the Retrograde Transport of Disarmed Toxins for the Delivery of Exogenous Antigens into the MHC class 1 Presentation Pathway.

**Karen Louise Noakes**

BSc (Hons) Biochemistry (Warwick)

**A Thesis submitted for the Degree of Doctor of Philosophy.**

**Department of Biological Sciences**

**University of Warwick**

**Coventry, CV4 7AL**

**U.K.**

**March 1999.**

# CONTENTS

LIST OF FIGURES

# LIST OF TABLES

## ABBREVIATIONS

| | |
|---|---|
| amp | ampicillin |
| ATP | adenosine triphosphate |
| APCs | antigen-presenting cells |
| BFA | brefeldin A |
| C-terminal | Carboxyl-terminal |
| CMV | Human cytomegalovirus |
| CTL | cytotoxic T lymphocyte |
| DEAE | diethylaminoethyl |
| DMEM | Dulbecco's modified Eagle's medium |
| DMSO | dimethylsulphoxide |
| DNA | deoxyribonucleic acid |
| DT | Diphtheria toxin |
| *E.coli* | *Escherichia coli* |
| EDTA | diaminoethanetetra-acetic acid sodium salt |
| ER | endoplasmic reticulum |
| ERAD | ER-associated protein degradation pathway |
| FCS | fetal calf serum |
| FITC | Fluorescein-5-isothiocyanate |
| $Gb_3$ | globotriaosylceramide |
| HEPES | N-2hydroxypiperazineN-2ethanesulphonic acid |
| Ii | invariant chain |
| IFN-γ | interferon-gamma |
| IPTG | isopropyl β-D-thiogalactoside |
| kb | kilobase |
| kDa | kilo Dalton |
| Ma | influenza Matrix peptide 58-66 |
| MHC | Major Histocompatibility Complex |
| MES | 2-[N-morpholino]ethane sulphonic acid |
| M | molar |
| mA | milliamperes |
| NP | Nucleoprotein 366-374 |

| | |
|---|---|
| N-terminal | Amino-terminal |
| OD | optical density |
| PAGE | polyacrylamide gel electrophoresis |
| PBS | Phosphate buffered saline |
| PCR | polymerase chain reaction |
| PMSF | phenylmethylsulphonyl fluoride |
| PE | *Pseudomonas* exotoxin A |
| RIP(s) | Ribosome inactivating protein(s) |
| RNA | ribonucleic acid |
| rRNA | ribosomal RNA |
| rpm | revolutions per minute |
| RTA | ricin A-chain |
| RTB | ricin B-chain |
| *S. cerevisiae* | *Saccharomyces cerevisiae* |
| SDS | sodium dodecyl sulphate |
| SLT | *Escherichia coli* Shiga-like toxin-1 |
| ST | Shiga toxin |
| TAP | transporter associated with antigen processing |
| TCR | T cell receptor |
| TEMED | NNN'N tetramethyl diamine |
| TGN | *trans*-Golgi Network |
| Th | T helper (lymphocytes) |
| Tris | tris(hydroxymethyl)aminomethane |
| TNF | tumor necrosis factor |
| UV | ultra violet |
| v/v | volume for volume |
| w/v | weight for volume |
| w/w | weight for weight |
| [$^{125}$ I] | $^{125}$ iodine |
| [$^{35}$S]dATP | $^{35}$ sulphur-labelled dATP |
| [$^{35}$S]Met | $^{35}$sulphur-labelled methionine |
| µCi | Microcurie(s) |

## ACKNOWLEDGEMENTS

Thanks to Dr Lynne Roberts, for her encouragement and guidance in this project and for giving me the opportunity to work in an area of research which has been very enjoyable and interesting.

Dr Enzo Cerundolo for his vital role as immunologist, providing advice and ideas on this project and allowing me to work in his lab at the IMM, Oxford. Thanks also to Prof. Mike Lord who has also shown interest and shared ideas in this project.

Thanks to all past and present members of the 'Ricin Group', if I haven't received technical advice from you, then I've probably 'borrowed' a solution from you (even if you didn't know it!). I'd like to extend my thanks to the whole of the MCB research group (especially the *pombe* boys upstairs) who have also been very helpful and to Jane Pritchard for being a supportive house-mate whilst writing-up.

To members of the Molecular Immunology Group, IMM, Oxford. Special thanks to Hélène Teisserenc, who helped me with the CTL assays and without whom, I would have spent considerable more time on the M40, driving between labs.

Technical assistance was also received in this project from Dr Marshall Pope (mass spectrometry data) and Dr Alan Morris (FACS analysis). Hela-A2 cells were a kind gift from Dr Hans Stauss (Hammersmith Hospital, London) and globotriose-Sepharose provided by Prof. David Crout (Warwick).

I would also like to acknowledge my family for their continued interest and encouragement in my work, my parents Tony and Janet Noakes, Paul and Katie and my grandparents Cliff and Bette Roberts.

And finally, a big thank-you to Marcus Hughes for his support in writing this thesis.

# DECLARATION

I hereby declare that the work described in this thesis was conducted by myself, unless otherwise specified, under the supervision of Dr Lynne Roberts at the University of Warwick. All sources of information have been specifically acknowledged by means of a reference. None of the information contained herein has been used in any previous application for a degree. This research was funded by a BBSRC studentship.

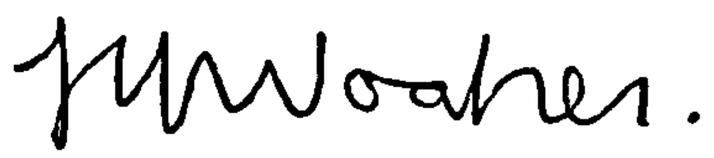

Karen L. Noakes

# ABSTRACT

The targeting of exogenous antigen into the MHC class 1-restricted presentation pathway is required for the induction of cytotoxic T lymphocytes (CTL) which have been shown to be an important component of the protective response to intracellular antigens and also induce immunity to tumour cells. Thus, induction of a CTL response is an important goal in vaccine research and a number of delivery systems are being investigated.

Certain cytotoxic proteins that catalytically modify substrates in the cytosol of mammalian cells undergo retrograde vesicular transport from the cell surface to the endoplasmic reticulum before translocating into the cytosol. In this study, Shiga-like toxin 1 (SLT) from *Escherichia coli* 0157:H7 was used to deliver an antigenic peptide for presentation by major histocompatibility complex (MHC) class I molecules. The SLT A chain was genetically fused with a nonamer peptide derived from influenza virus Matrix protein, positioned at either the N- or C-terminus of the toxin (designated SLT N-Ma or C-Ma). The SLT coding sequence was also mutated to convert an active site glutamate into aspartate to significantly reduce ribosome-inactivating activity, and hence the inherent cytotoxicity of the toxin chimeras. Recombinant holotoxins carrying the viral peptide were expressed in *E. coli* and purified to homogeneity before use. HLA-A2-transfected HeLa cells were allowed to internalize the disarmed toxin-peptide chimeras and were used as targets of influenza Matrix-specific cytotoxic T lymphocytes (CTL). HLA-A2-matched cells, unable to internalize SLT, were used as negative controls.

Results from this study show that SLT N-Ma but not SLT C-Ma is capable of sensitizing HeLa A2 cells for lysis by cytotoxic T -lymphocytes (CTL) whilst no killing of SLT-resistant cells has been observed. Treatment of cells with the Golgi stack-disrupting agent brefeldin A successfully blocked the presentation of the M58-66 epitope at the cell surface, confirming that the antigenic peptide was liberated intracellularly.

This strategy was repeated for ricin A-chain, placing a nonamer peptide derived from influenza virus nucleoprotein at either the N-terminus or within an external loop of the toxin A-chain (designated RTA N-NP or ClaI-NP). Fusion proteins were expressed in *E.coli* and purified, followed by reassociation with ricin B-chain. Preliminary results have failed to show the delivery of peptide antigen to class-1 molecules by the ricin chimeras. This work is ongoing.

This thesis demonstrates that Shiga-like toxin-1, known to be endocytosed from the cell surface to the ER lumen and then transferred to the cytosol of eukaryotic cells, can intersect the MHC class 1 presentation pathway and effectively carry antigenic peptide to class 1 molecules *in vitro*. This approach opens up new possibilities for the generation of $CD8^+$ T-cell vaccines for use against infectious agents, cancer and autoimmune disorders.

# CHAPTER 1

# INTRODUCTION

# Chapter 1

# Introduction

## 1.1 General Overview

The basis for the immune response against virally infected or transformed cells is the recognition by cytotoxic T lymphocytes (CTL) of antigenic peptides. These are derived from cytosolic proteins and presented on the cell surface by major histocompatibility complex (MHC) class 1 molecules. The main steps in this process are the degradation of both self and foreign proteins to short peptides mainly by proteasomes located in the cytosol, translocation of peptides into the lumen of the endoplasmic reticulum (ER) and their assembly with MHC class 1 molecules. Following secretion as a MHC-peptide complex to the cell surface, the complex is recognised as presenting self or foreign peptides and an appropriate immune response made, ultimately leading to the death of virally infected or tumour cells (Cerundolo and Braud, 1996).

Thus, as a general rule, MHC class-I molecules present endogenously derived peptide epitopes from cytosolic and nuclear proteins to CD8+ T lymphocytes (CTL) whereas peptides derived from exogenous, e.g. bacterial proteins are generated in the endocytic pathway and presented by MHC class II molecules to CD4+ T helper (Th) lymphocytes (Pieters, 1997). The two T cell responses lead to an effect that is appropriate to the type of infection. Induction of CD4+ T helper cells stimulates their production of cytokines, one effect of which is to activate B-cells to produce antibodies. This response is effective in the clearance of extracellular pathogens. In

contrast activated CTL secrete proteolytic enzymes resulting in the direct lysis of bound antigen presenting cells. This action prevents or at least controls an intracellular pathogenic infection by removing infected cells.

Since CTL are an important component of the protective and therapeutic immune response to viral infections and tumours (Zinkernagel *et al.*, 1996, Meir *et al.*, 1995, Romero *et al.*, 1998) different vaccine strategies are being developed that allow the presentation of soluble exogenous antigens by MHC class 1 molecules and stimulation of CTL. Whereas direct immunisation with a viral protein tends to lead to antigen endocytosis and a subsequent MHC class II response, delivery of exogenous antigens into the cytosol and their introduction into the MHC class 1 pathway may lead to the generation of protective CTL.

Previous studies have used toxins such as diphtheria (DT), anthrax and *Pseudomonas* exotoxin A (PE) to deliver peptide epitopes into the MHC class 1 pathway (Donelly *et al.*, 1993, Goletz *et al.*, 1997, Ballard *et al.*, 1996, 1998). With one exception (Goletz *et al.*, 1997), the intracelluar routing pathway or the location of processing of the toxin fusion proteins was not known or investigated.

In this study ribosome inactivating proteins (RIPs), namely Shiga-like toxin 1 (SLT) and ricin have been tested for their ability to deliver viral peptides into the MHC class 1 processing pathway. The intracellular uptake pathway taken by SLT and ricin, which involves transport from the cell surface to the endoplasmic reticulum (ER), has been well defined. Based on this knowledge the routing of the toxin

chimera and its processing, either directly in the ER lumen or after translocation of the toxin-A chain, has been investigated.

This introduction will first describe ribosome inactivating proteins with relation to how they may parisitise intracellular transport pathways in order to intoxicate cells. The current knowledge of the MHC class 1 pathway will then be discussed. Finally, various vaccine approaches will be reviewed and their potential against certain viral pathogens and tumour cells discussed.

## 1.2 Protein toxins produced by plants and bacteria

### 1.2.1 Functionally analogous A-B toxins

Some plants and bacteria produce proteins that are potently toxic to mammalian cells. These toxins all act by catalytically modifying essential cellular components, many leading to the inhibition of protein synthesis. To reach their targets, these toxins must bind and gain entry into cells. To achieve this they exist as a family of bipartite A-B toxins consisting of a catalytically active polypeptide A-chain associated with one or more cell-binding subunits (B-chain) (Figure 1.1).

These toxins bind to receptors on the surface of susceptible cells and enter by endocytosis in a clathrin-dependent or independent manner, depending on the chosen receptor. The toxins must then translocate across an intracellular membrane in order to reach their cytosolic target substrates. Translocation can be achieved from acidified

Shiga toxin / Shiga-like toxin-1

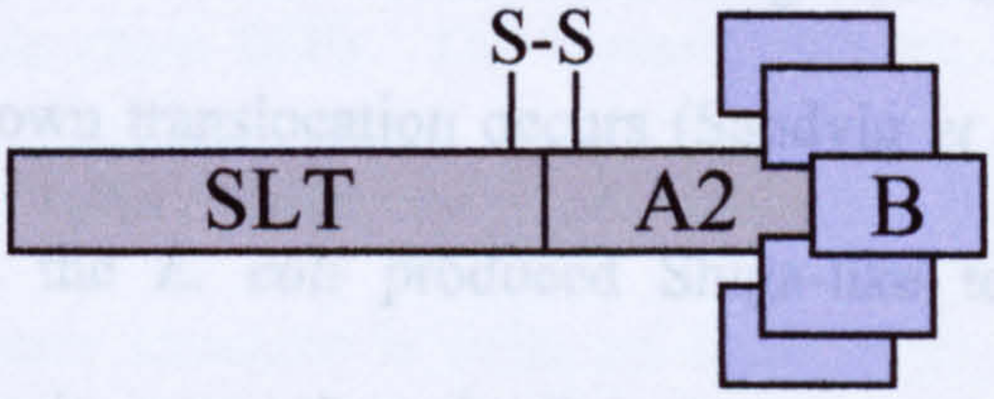


ricin

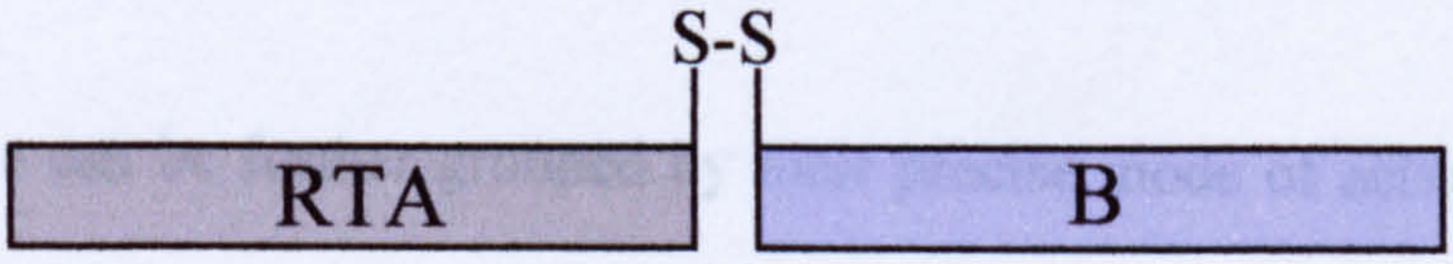


cholera toxin

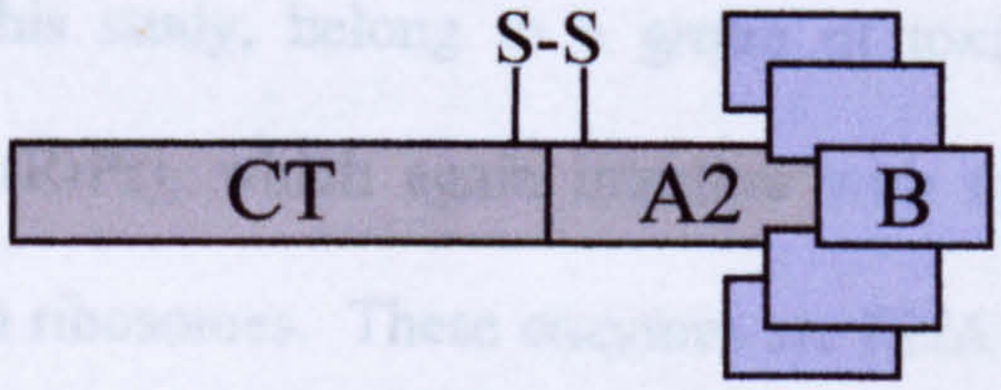


diphtheria toxin

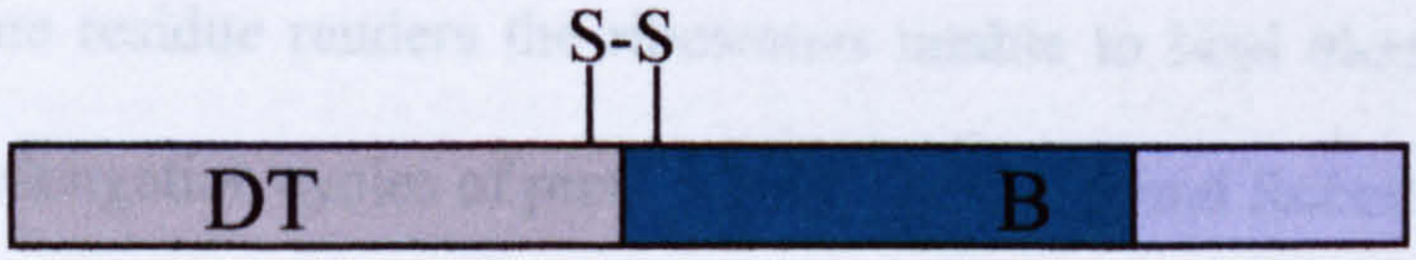


*Pseudomonas* exotoxin A

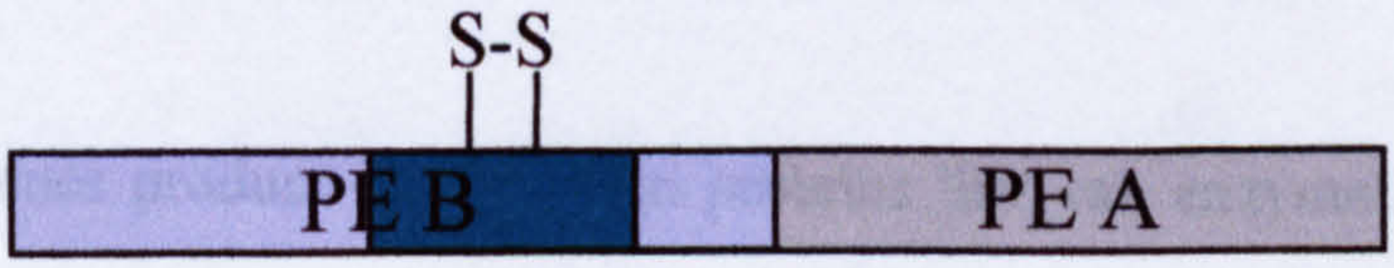


***Figure 1.1 Schematic representation of a selection of A-B plant and bacterial toxins***

Cell binding domains are labelled in blue and known translocation domains in green. Catalytic domains are labelled in grey. Disulfide bonds that covalently link a trypsin-sensitive site or two fragments are labelled. Shiga/ Shiga-like toxin and ricin represent members of ribosome inactivating proteins (RIPs) by their RNA *N*-glycosidase activity. Cholera, diphtheria and *Pseudomonas* exotoxin A are members of a toxin family that function in the ADP-ribosylation of target molecules.

endosomes, as demonstrated by diphtheria toxin. Others are transported beyond endosomes in a retrograde manner via the trans Golgi network (TGN) to the ER from which it has been shown translocation occurs (Sandvig *et al*, 1992). These toxins include Shiga toxin, the *E. coli* produced Shiga-like toxins, *E.coli* heat-labile enterotoxin, cholera toxin, pertussis toxin, *Pseudomonas* exotoxin A and ricin.

Protein toxins can be further grouped by their precise mode of action. DT and PE catalytically inhibit protein synthesis by irreversibly modifying elongation factor-2 by ADP ribosylation of a critical modified histidine (termed diphtamide). SLT and ricin, the toxins in this study, belong to a group of toxins known as ribosome inactivating proteins (RIPs), which again interfere with the ability of elongation factors to interact with ribosomes. These enzymes are RNA specific N-glycosidases and their target lies within the 60 S subunits of 80 S ribosomes. Removal of a specific adenine residue renders the ribosomes unable to bind elongation factor-2, thus blocking elongation cycles of protein synthesis (Lord and Roberts, 1991).

### 1.2.2 Structures and modes of action of ribosome inactivating proteins

Many plant tissues produce single chain proteins that can enzymatically remove a specific adenine residue from ribosomal RNA. Classified by their structure, they are termed type I RIPs, consisting of a single catalytic polypeptide, around 30kDa in size and include toxins such as pokeweed antiviral protein (PAP). Type II RIPs are defined as consisting of a catalytic polypeptide (A-chain) joined by a disulfide bond to a cell-binding polypeptide chain (B-chain) which in the case of all plant RIPs, such as ricin, is a galactose-binding lectin whose molecular weight is also around

30kDa. The A-chain of these type II plant RIPs is structurally and functionally homologous to the single chain RIPs. The bacterial toxins, *Shigella* toxin and the related Shiga-like toxins from certain strains of *E.coli* also fall into this category of type II RIPs although their structure is different from other A-B toxins described, with the catalytic A-chain interacting non covalently with a pentamer of B-chains ($AB_5$).

### 1.2.3 Structure of Shiga-like toxin-1

Shiga-like toxin-1 (SLT) from *E.coli* 0157:H7 is a Shiga toxin (ST) analogue comprising an enzymatic A chain (32,225 kDa) non-covalently associated with a pentamer of B subunits (7,691 kDa each). Comparison of deduced amino acid sequences between ST and SLT has shown the toxins differ by a single amino acid at position 45 (threonine in ST and serine in SLT) (Calderwood *et al.*, 1987). The structure of the holotoxin has been solved by X-ray crystallography (Fraser *et al.*, 1994) (Figure 1.2). Each B subunit is folded into one α-helix and 6 β-strands. The helices are surrounded by antiparallel β-sheets, formed by three strands from each pair of neighbouring B subunits. An α-helix at the C-terminus of the A subunit penetrates the hydrophobic pore created by the B pentamer. A helical segment of hydrophobic residues, Leu 282, Gly 283, Ala 284, Ile 285, Leu 286 and Met 287, extends 11Å into the 20Å pore. Approximately 2000Å of the A subunit is buried by the B pentamer. Half of this is due to the contact between the C-terminal helix and the B subunits (Fraser *et al.*, 1994).

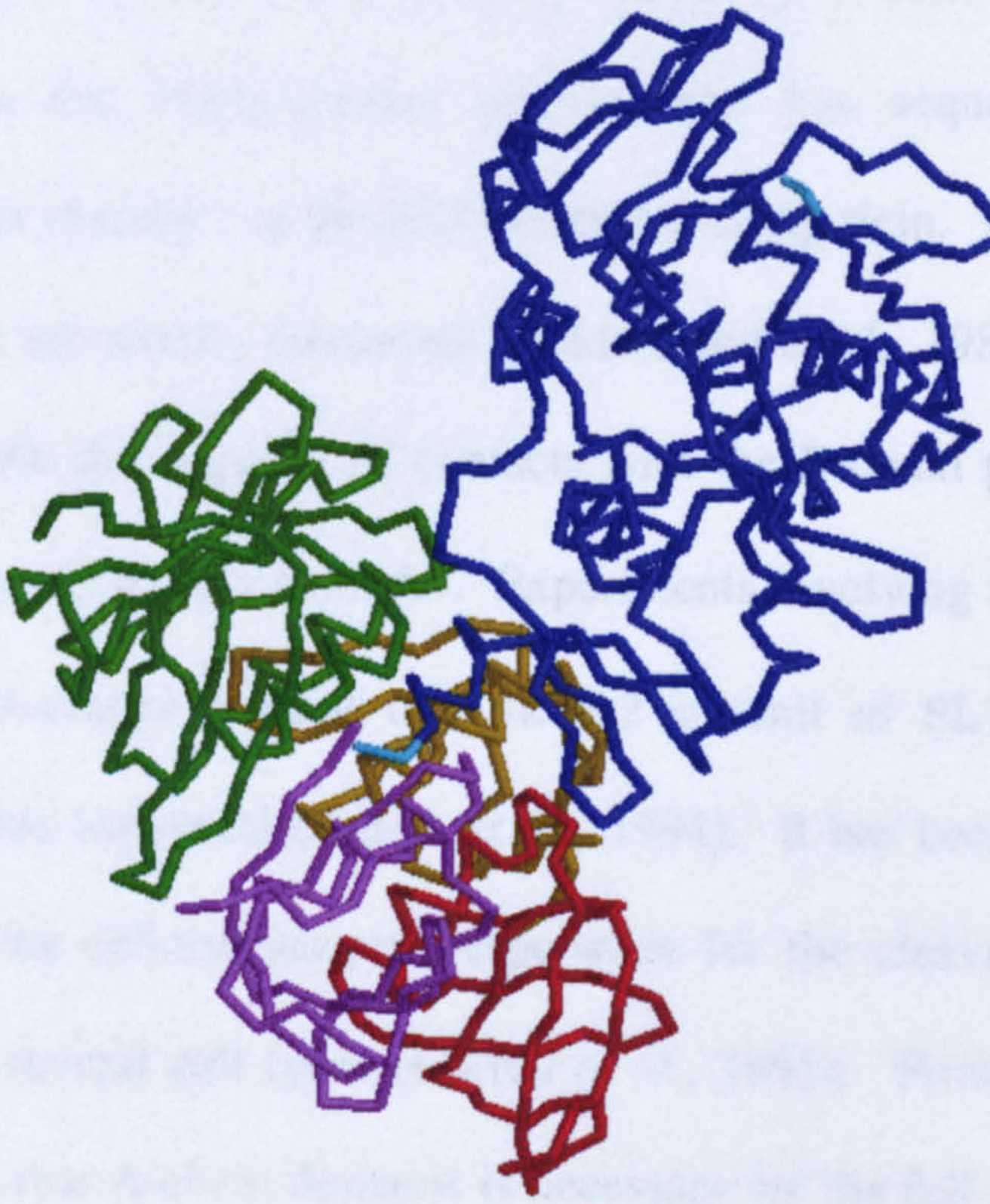

***Figure 1.2 Structure of Shiga toxin α-carbon backbone***

Shiga toxin structure (Fraser *et al.*, 1994), represented as a α-carbon backbone drawing with Shiga toxin A-chain in blue. The N- and C-terminus of the A-chain are shown in light blue to highlight the location of peptide fusions.

The A-chain contains a trypsin-sensitive site, resulting in the generation of two fragments A1 and A2 that are covalently linked by a disulfide bond. The A1 fragment carries the N-glycosidase activity and has sequence and structural similarity to other members of the RIP family including ricin. Many residues found in the active-site are strictly conserved (Calderwood *et al.*, 1987). Residues of the A2 fragment make the majority of contacts with the B-chain pentamer along with contacts made by a β-hairpin from A1. Experiments involving the assembly of SLT with truncated A-chains suggest that the A2 subunit of SLT is crucial for the formation of stable holotoxin (Austin *et al.*, 1994). It has been shown that Golgi-located furin is the cellular enzyme responsible for the cleavage of the trypsin – sensitive site in several cell types (Garred *et al.*, 1995). Proteolytic cleavage and separation of the two A-chain domains is necessary for the full activity of the toxin. The crystal structure of ST shows residues 258-262 of A2 lie adjacent to the active site cleft and the side chain of methionine 260 is inserted into the active site, effectively blocking access to the substrate (Fraser *et al.*, 1994).

Mutations affecting the catalytic activity of SLT-1 have been studied by placing the gene for SLT-1 A-chain under the control of an inducible promoter in *Saccharomyces cerevisiae* (Deresiewicz *et al.*, 1992). Induction of the cloned element was lethal to the host and this was the basis for the selection of point mutations affecting the activity of SLT-1 A-chain that had lost the ability to kill *S. cerevisiae*. Three aromatic residues were identified in the putative active-site cleft: Tyr 77, Tyr 114 and Trp 203, homologous to aromatic residues previously identified in ricin (Tyr 80, Tyr 123 and Trp 211). These conserved residues in SLT and ricin

(studied as single mutations) decrease the activity of both toxins in the region of 7-20 fold (Deresiewicz *et al.*, 1992; Ready *et al.*, 1991; Bradley *et al.*, 1990).

Other conserved residues have been studied, most notably those that are located at the base of the active-site cleft, Glu 177, Ala 178 and Arg 180 in ricin (homologous to Glu 167, Ala168 and Arg 170 in SLT-1). In a study by Hovde *et al.* (1988), the glutamic acid residue at position 167 in SLT was selected for mutation as carboxylate side-chains are known to be crucial in the catalytic mechanisms of a number of enzymes, including other classes of toxins such as diphtheria toxin and *Pseudomonas* exotoxin A. The change of glutamic acid 167 to aspartic acid (The SLT mutation used in this study) retains the carboxyl function of the residue but alters its spatial position in the SLT A-chain. This mutation caused a 1000-fold reduction in activity, when assessed by an assay based on protein synthesis inhibition. The corresponding change glutamic acid 177 to aspartic acid in ricin decreased catalytic activity 80-fold based on a similar protein synthesis inhibition assay (Schlossman *et al.*, 1989). Further structural studies of ricin are discussed below.

### 1.2.4 Structure of ricin

The best characterised of the related plant toxins is ricin, a major protein in the endosperm of the seed of the castor oil plant, *Ricinus communis.* Ricin is synthesised as a precursor, preproricin, made up of a 35 residue presequence followed by the 267 residues of the catalytic A-chain (RTA), a 12 residue linker and the 262 residues of the cell-binding B-chain. During biogenesis the signal peptide is

cleaved followed by co-translational modifications, including N-glycosylation at four sites (two in each of the mature chains) and the formation of four disulphide bonds within the B-chain and another which links the mature RTA and B-chain upon the subsequent removal of the linker. Mature ricin has a mass of 66kDa (RTA 30kDa and RTB 29kDa).

The structure of ricin was determined by X-ray crystallography to a resolution of 2.8Å (Montford *et al.*, 1987) (Figure 1.3). Further structural analyses have been published at greater resolutions including RTA resolved at 1.8Å by Weston *et al.*, (1994) and X-ray analysis of a bound substrate analogue. These have revealed the importance of 15 residues in RTA which are essential for association between the two chains and along with biochemical analysis, characterised certain residues in the active site (refer to section 1.2.3) involved in the catalytic mechanism of the toxin.

The A-chain contains eight α-helices and eight β-strands that can be divided into three domains. The first domain consists of a six-stranded β-sheet, the second domain is helical in structure, forming the central core of the protein while the third domain contains the residues involved in the interface with the B-chain. The structure of the A-chain is maintained in the absence of the ricin B-chain (RTB). RTB contains two domains originating from gene duplication (with 32% homology), each of them having a binding site for carbohydrates such as galactose (Lord *et al.*, 1994).

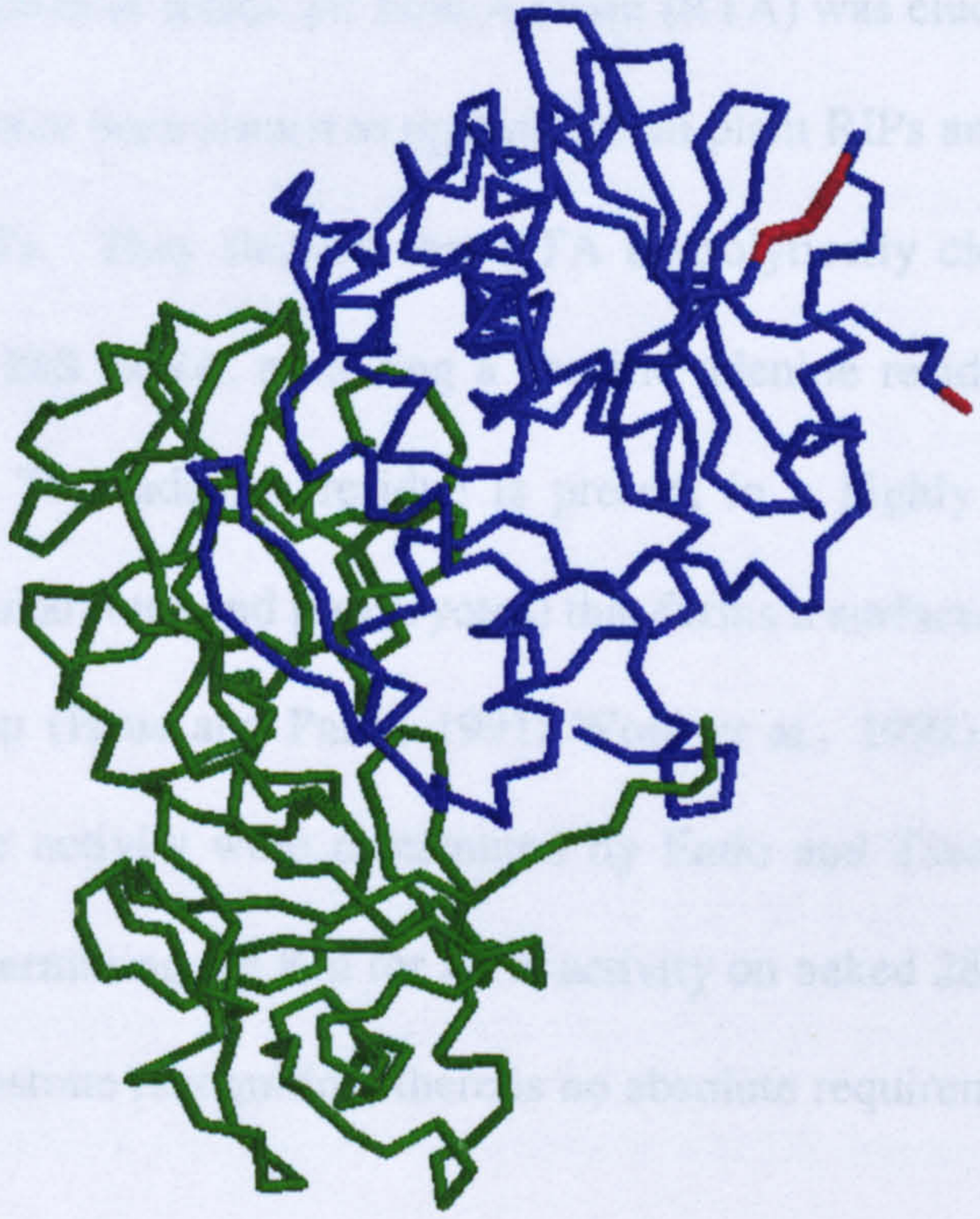

***Figure 1.3 Structure of ricin α -carbon backbone***

Ricin structure (Montford *et al*., 1987), represented as a α-carbon backbone drawing with ricin A-chain in blue and ricin B-chain in green. The N-terminus and *Cla*I site of the A-chain are highlighted in red to depict the location of peptide fusions.

### 1.2.5 Mode of action

The specific mechanism of action for ricin A-chain (RTA) was elucidated by Endo *et al.* (1987) but has since been shown to operate for all plant RIPs and for the bacterial toxins, ST and SLTs. They showed that RTA hydrolytically cleaves a single N-glycosidic bond in 28S rRNA, removing a specific adenine residue (A 4324 in rat liver 28S rRNA). This adenine residue is present in a highly conserved rRNA sequence (in both eukaryotes and prokaryotes) that forms a surface exposed 'GAGA' tetra-nucleotide loop (Heus and Pardi, 1991; Wool *et al.*, 1992). The kinetics of RNA N-glycosidase activity were determined by Endo and Tsurugi (1988) which included studies determining the Km for RTA activity on naked 28S rRNA. The data indicated that in substrate recognition, there is no absolute requirement for ribosomal proteins.

RIP-depurinated ribosomes are deficient at two stages in protein synthesis. The formation of the 80S initiation complex during initiation is slowed down 6-fold and the translocation step of the elongation cycle is blocked, detailed in Osborn and Hartley (1990). Several type 1 RIPs, including PAP, show activity towards not only eukaryotic ribosomes but also prokaryotic ribosomes (Hartley *et al.*, 1991). RTA is able to modify naked *E.coli* 23S rRNA but not whole prokaryotic ribosomes, suggesting that prokaryotic ribosomal proteins interfere with access to the rRNA substrate.

## 1.3 Toxin entry: Retrograde transport through the secretory pathway

### 1.3.1 Introduction

The structures, mechanism of action and kinetics of RNA glycosidase activity having been elucidated, studies in recent years have focused on how AB-toxins gain entry into cells. Those toxins that are unable to translocate from endosomes have been shown to travel further along the protein transport pathway, in a retrograde direction, to the ER (Figure 1.4).

Recently it has been speculated that these toxins may take advantage of the recently discovered ER-associated protein degradation (ERAD) pathway. This pathway disposes of misfolded or unassembled proteins in the ER lumen by exporting them, via Sec61p translocons for degradation in the cytosol (Brodsky and McCracken, 1997).

Current knowledge of these cellular intoxication processes and retrograde transport pathways will be discussed in relation to the toxins in this study, SLT and ricin. Other catalytic toxins enter cells by the same mechanisms and reference will be made to them where appropriate.

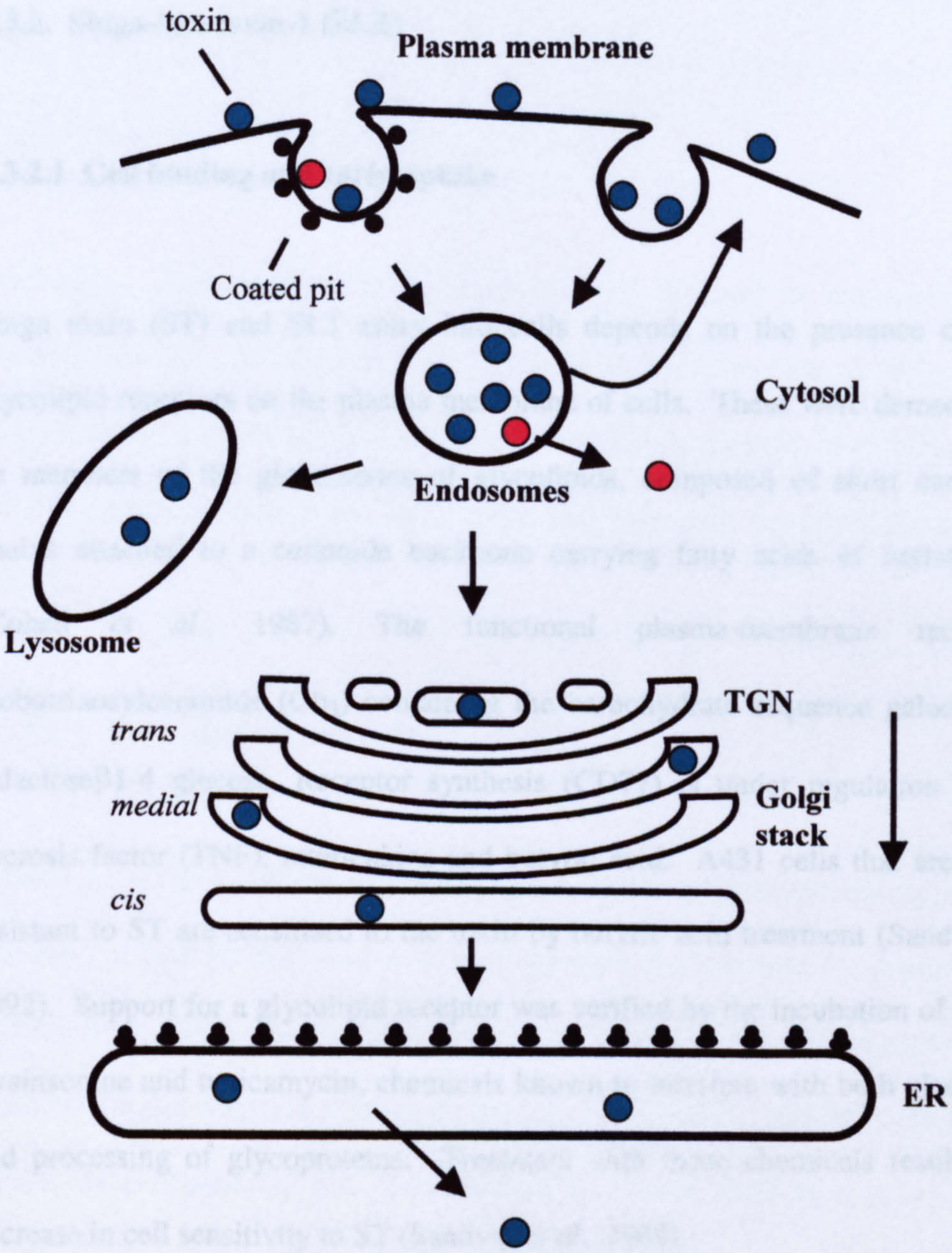


***Figure 1.4 Retrograde transport of endocytosed toxins***

Schematic representation of retrograde transport of toxins in mammalian cells. Toxins bind to receptors on the surface of susceptible cells and enter by endocytosis in a clathrin-mediated (ricin, PE, SLT, DT) or clathrin-independent (ricin) manner to reach the endosomal system. Endosomes are the site of translocation for toxins such as diphtheria toxin (shown in red). Toxins such as Shiga toxin, ricin and *Pseudomonas* exotoxin A (shown in green) are transported to the trans Golgi network (TGN) from where they undergo retrograde vesicular transport to the ER, the site of translocation for the catalytic A fragment of the toxin. Only a small proportion of the endocytosed toxin may take this pathway, the majority is either recycled back to the cell surface from endosomes or transported to lysosomes for degradation.

### 1.3.2. Shiga-like toxin-1 (SLT)

#### 1.3.2.1 Cell binding and early uptake

Shiga toxin (ST) and SLT entry into cells depends on the presence of specific glycolipid receptors on the plasma membrane of cells. These were demonstrated to be members of the globo-series of glycolipids, composed of short carbohydrate chains attached to a ceramide backbone carrying fatty acids of variable length (Cohen *et al.*, 1987). The functional plasma-membrane receptor is globotriaosylceramide ($Gb_3$) containing the carbohydrate sequence galactose α1-4 galactoseβ1-4 glucose. Receptor synthesis (CD77) is under regulation by tumor necrosis factor (TNF), interleukins and butyric acid. A431 cells that are normally resistant to ST are sensitised to the toxin by butyric acid treatment (Sandvig *et al.*, 1992). Support for a glycolipid receptor was verified by the incubation of cells with swainsonine and tunicamycin, chemicals known to interfere with both glycosylation and processing of glycoproteins. Treatment with these chemicals resulted in no decrease in cell sensitivity to ST (Sandvig *et al.*, 1989).

In the same study Sandvig *et al.* (1989) reported that ST enters cells in a clathrin-dependent manner. Horseradish peroxidase-tagged ST was detected in coated pits by electron microscopy. ST is seen to be evenly bound all over the cell surface at low temperature but after a short incubation at 37°C, aggregates in clathrin coated pits and is endocytosed. Depleting cytosolic $K^+$ or lowering the cytosolic pH, which inhibits clathrin-mediated endocytosis, inhibits toxin entry into cells (Sandvig *et al.*, 1996). It is not known how a glycolipid might act in receptor-mediated endocytosis

endocytosis through coated pits, but it may interact with a protein already anchored to a pit. In contrast, two other lipid-binding toxins, cholera and tetanus toxin are internalised in a clathrin-independent manner.

Following internalisation, Shiga toxin can be detected in endosomes where it colocalizes with the transferrin receptor, a classical marker of early endosomes (Johannes *et al.*, 1997). Evidence described below suggests that ST and SLT are then transported first to the Golgi stack and then onto the endoplasmic reticulum (ER).

### 1.3.2.2. Intracellular transport

There are several different routes that can be followed from the endosome. A large fraction of both ST/SLT and ricin is transported to lysosomes for degradation (Van Deurs *et al.*, 1988). A large fraction of endocytosed ricin is also recycled to the cell surface but this does not seem to be the case for ST/SLT. In experiments where the toxin was prebound, the cell surface is cleared of toxin (Sandvig *et al.*, 1989; 1991). A relatively small fraction of both ricin and ST/SLT is transported to the TGN and onto the Golgi stack. This transport step appears essential for intoxication. Recently it has been shown that, uniquely, ST is transported from early endosomes directly to the TGN bypassing the usual route from early endosomes via late endosomes to the TGN (Johannes *et al.*, 1997).

For some toxins such as diphtheria, this further transport step is unnecessary, translocation into the cytosol occurring directly from acidified endosomes. The low

pH in endosomes induces a conformational change in diphtheria that triggers translocation of the A-chain (Silverman *et al.*, 1994). Other toxins that translocate from endosomes include anthrax, botulinum and tetanus.

The first demonstration that internalised protein can be transported to the Golgi apparatus came when cholera toxin, conjugated to HRP was seen to localise there (Joseph *et al.*, 1978). In more extensive experiments, ST conjugated to HRP was delivered to the Golgi complex with endocytosed material being examined in electron microscope sections (Sandvig *et al.*, 1989; 1991). Using butyric acid-sensitised A431 cells treated with ST-HRP conjugates, electron micrographs revealed toxin visible in endosomes, lysosomes, throughout the Golgi complex and, for the first time, in the ER (Sandvig *et al.*, 1992). The most recent study of ST transport visualised ST-HRP conjugates again in the ER of T47D (human breast carcinoma) cells. Here the toxin was seen in the ER without the need for butyric acid treatment of the cells (Garred *et al.*, 1995). In addition, the isolated ST B-chain, again conjugated to HRP, has been shown to be transported back to the ER (Sandvig *et al.*, 1994), indicating that this subunit of the toxin is required for the complete retrograde transport of SLT to the ER. The visualisation of ST localised to the ER by electron microscopy does not signify that this fraction of toxin is physiologically significant. However the appearance of ST in the ER of sensitised A431 cells correlated well with the acquisition of sensitivity to toxin. This and work with brefeldin A suggested that routing to the ER was functionally important.

Studies with brefeldin A (BFA), known to disrupt Golgi stacks (described in section 1.3.2.4), have shown that when cells are treated with BFA they are protected against

ST and ricin (Sandvig *et al.*, 1991). In addition, in cells incubated with ricin and ST at 18-20°C, the delivery of toxin to the Golgi apparatus is blocked. Such cells show greatly reduced sensitivity to the toxins (Sandvig *et al.*, 1989). In contrast, diphtheria toxin that is translocated from endosomes, remains very potent in both BFA-treated cells and in cells incubated at this lower temperature (Sandvig *et al.*, 1984).

### 1.3.2.3 Cellular responses to brefeldin A

Brefeldin A (BFA) is a fatty acid derivative made by several fungi which induces the rapid redistribution of Golgi stacks into the ER. The Golgi fuses with the ER, leaving no definable Golgi stack structure. This effect is reversible and removal of BFA results in the reformation of the Golgi. Whilst blocking transport of secretory proteins out the Golgi, low concentrations of BFA has no effect on cellular processes such as endocytosis, lysosomal degradation or protein synthesis (Misumi *et al.*, 1986). BFA prevents bulk movement of material from the ER to the Golgi system (Lippincott-Scwartz *et al.*, 1990) which would include MHC class-1 molecules. It follows also that proteins being endocytosed via the trans Golgi network (TGN) to the ER will also be blocked by BFA. The BFA-induced reduction in cytotoxicity of those RIPs following a retrograde pathway via the Golgi has been well documented (Sandvig *et al.*, 1991; Sandvig and van Deurs, 1996).

### 1.3.3 Ricin

#### 1.3.3.1 Cell binding and early uptake

The binding of ricin to the surface of target cells is mediated by the B-chain. RTB has an affinity for a range of complex oligosaccharides terminating in α1-4 galactose and these residues, found on surface-expressed glycoproteins and glycolipids, are displayed by a huge number of cell-types and cell-lines. On HeLa cells, for example, it is estimated there are $3x10^7$ potential binding sites for ricin. Most eukaryotic cells are susceptible to ricin, the most notable exceptions being *S.Cerevisiae* and BHK cells which appear unable to bind toxin at the cell surface. Native ricin and RTA also possess the ability to bind and enter cell types by virtue of its own carbohydrate side-chains. A limited number of cell lines express mannose receptors at the cell surface, allowing ricin and RTA (containing exposed mannose residues) to bind to them. Mannose receptor-mediated uptake of ricin has been described in both macrophages (Simmons *et al.*, 1986) and rat liver endothelial cells (Magnusson *et al.*, 1993).

Ricin provided some of the first evidence that there is more than one mechanism for endocytosis (van Deurs *et al.*, 1987). The binding and internalisation of ricin into Vero cells was first visualised using a ricin-gold conjugate (van Deurs *et al.*, 1985). Binding of the conjugate, shown to be as efficient as binding of native toxin, was visualised in clathrin-coated pits. Other experiments recognised that clathrin-independent endocytosis was also involved in the uptake of ricin (Moya *et al.*, 1985). Coated pit formation in HEp-2 cells was blocked by hypotonic shock and potassium

ion depletion and treated cells then challenged with toxin. In contrast to DT and ST/SLT, (which are endocytosed solely by clathrin-coated pits), radiolabelled ricin was seen to internalise and kill cells at 50% of that seen in untreated cells.

Ricin can enter cells via a clathrin-independent mechanism that does not involve caveolae (Simpson *et al.*, 1998). The use of sterol binding drugs, such as nystatin, to disrupt caveolae formation was shown to have no effect on the sensitivity of cells to ricin. The overexpression of dynamin and Rab5, GTPases involved in the regulation of clathrin-mediated endocytosis, were also shown by Simpson *et al.* (1998) to have no effect on the intoxication of cells by ricin. The lack of inhibition of ricin toxicity in the presence of excess mutant GTPases supports a clathrin-independent mechanism of endocytosis. Other results have shown an inhibition of toxicity from the overexpression of a mutant dynamin. This observation may not necessarily be due to the inhibition of ricin endocytosis but affecting an additional transport step from endosomes to the Golgi apparatus (Llorente *et al.*, 1998).

### 1.3.3.2 Endocytosis beyond endosomes

The trafficking of ricin beyond endosomes was initially followed, as for ST/SLT, by electron microscopy. Unlike ST, ricin-HRP conjugates were not visualised in the ER but did show labelling of the Golgi stacks (van Deurs *et al.*, 1986). Evidence to support the theory that like ST/SLT, ricin may also travel from the Golgi complex to the ER came from biochemical experiments showing the protection of brefeldin A-treated cells against ricin (Yoshida *et al.;* 1991, Sandvig *et al.*, 1991). In other studies, cells overexpressing trans-dominant GTPase mutants, involved in the

regulation of Golgi transport and ER export, show significantly reduced ricin cytotoxicity (Simpson *et al.*, 1995).

Experiments with PE mutants provided an explanation of how retrograde transport from the Golgi to the ER might occur for PE and also ricin. The last five C-terminus residues of the PE A-chain (REDLK) may act as a KDEL-like ER retrieval signal, interacting with recirculating KDEL-receptors that normally recycle escaped ER resident proteins containing the KDEL motif. Deletions or substitutions predicted to prevent interaction with the KDEL receptor (but having no effect on the catalytic activity of the toxin) reduce the cytotoxicity of PE (Chaudhary *et al.*, 1990). Indeed replacing the REDLK sequence with KDEL produced a mutant even more cytotoxic than wild-type PE (Chaudhary *et al.*, 1990).

Ricin does not possess a KDEL-related sequence but the addition of a KDEL retrieval signal to the C-terminus of RTA significantly enhances cytotoxicity (Wales *et al.*, 1992). Ricin must therefore encounter recirculating KDEL receptors that are predominantly located in the early Golgi. Ricin may undergo retrograde transport from the TGN to the ER by binding to a recycling galactosylated component which might itself carry a KDEL retrieval signal or interact with another molecule containing a KDEL-like motif. The Shiga toxin B-chain does not require the direct interaction with a KDEL receptor since the addition of KDEL to this toxin makes no difference to the kinetics of entry or to toxin potency (Johannes *et al.*, 1997). It is proposed that the glycosphingolipid receptors of ST may be able to carry Shiga toxin from the cell surface to the ER themselves.

Recently, direct biochemical evidence has shown that endocytosed ricin reaches the ER (Rapak *et al.*, 1997). Ricin A-chain was modified to contain a tyrosine sulfation site and three potential N-glycosylation sites. Reassociated mutant ricin was incubated with cells in the presence of $Na_2{}^{35}SO_4$. A proportion of the holotoxin molecules became labelled with radioactive sulphate, indicating that this fraction of toxin had been transported through the Golgi stack. Such labelling of ricin could be prevented by the treatment of cells with BFA. A fraction of sulphated toxin also becomes core glycosylated, conclusively indicating for the first time that transport involved passage to the ER. Interestingly, only free glycosylated A-chain was subsequently seen in the cytosol, indicating that transport to the ER is necessary for translocation into the cytosol. A similar biochemical approach has been used to confirm that Shiga B-chain also reaches the ER via the Golgi apparatus (Johannes *et al.*, 1997).

## 1.4 The ER as the site of toxin translocation into the cytosol

In recent years it has become apparent that proteins that fail to fold or assemble correctly in the ER lumen can be transported the ER membrane to the cytosol where they are degraded by proteasomes (Hiller *et al.*, 1996; Werner *et al.*, 1996). The mechanisms of this ER-associated protein degradation (ERAD) have been studied using both yeast and mammalian cells.

Human cytomegalovirus (CMV) takes advantage of this export machinery to down regulate antigen presentation at the cell surface by class 1 MHC molecules. The US11 gene product of CMV causes the dislocation of the transmembrane MHC class

1 heavy chain from the ER membrane to the cytosol and its subsequent degradation by proteasomes (Wiertz *et al.*, 1996a). Co-immunoprecipitation studies indicated that the MHC class 1 heavy chain in CMV-infected cells may be exported through the Sec61p translocon (Wiertz *et al.*, 1996b) and direct evidence for the involvement of Sec61p has been demonstrated in yeast (Pilon *et al.*, 1997; Plemper *et al.*, 1997).

If toxins were to be perceived as misfolded or unassembled proteins, they may well be able to translocate across the ER membrane by the ERAD pathway. It is unclear whether the A and B-chains of toxins such as PE, ST or ricin disslocate in the ER before translocation or in the cytosol after the translocation of holotoxin. It may be that when the toxins reach the ER lumen, thiol exchange catalyzed by protein disulfide isomerase causes dissociation of the disulfide-linked A and B subunits. This has been demonstrated to be the case for cholera toxin (Orlandi *et al.*, 1997).

It is known that dissociation of the toxin A and B-chains exposes hydrophobic regions present in the A-chain and in the case of ricin, point mutations in this region reduce cytotoxicity but have no effect on the catalytic activity of RTA (Simpson *et al.*, 1995). Exposure of this hydrophobic region may promote unfolding of the A-chain, leading to possible export to the cytosol by the ERAD system. Evidence exists for the partial unfolding of RTA during cell entry (Argent *et al.*, 1994). What factors might promote disulfide-bond reduction and unfolding in the ER remain unknown. Recent work using Sec61p mutants in S. *Cerevisiae* suggests that RTA is translocated from the ER to the cytosol via the Sec61p translocons (Simpson *et al.*, unpublished observations). If this proves to be the case, this would be the first

example of a native rather than an aberant protein, that becomes ejected from the ER lumen to the cytosol.

If this pathway of entry into the cytosol for certain toxins is correct then some of the exported toxin must refold into a biologically active conformation in order to kill the cell. To do this, toxin must avoid rapid degradation by proteasomes to which the ERAD pathway ultimately leads. Recent evidence suggests that this may be achieved by ribosome-induced refolding of a fraction of the dislocated toxin, a process which, at the same time, leads to inactivation of the ribosome chaperone (Argent, unpublished observations).

## 1.5 MHC-restricted antigen recognition

### 1.5.1 Overview of MHC class-I and class-II antigen presentation pathways

The fundamental difference between the two MHC antigen presentation pathways is that peptide processing and loading onto MHC class I and class II molecules occurs in different intracellular compartments (Cresswell, 1994). MHC class 1 molecules bind peptides derived from the processing of cytosolic proteins that are translocated from the cytosol into the ER where they form a MHC-peptide complex. Class II MHC molecules bind peptides derived from exogenous antigens that are either internalized by phagocytosis or enter cells by endocytosis, to be processed within the endocytic pathway (Figure 1.5).

***Figure 1.5 Schematic representation of MHC class-I and class-II antigen presentation pathways.***

Basic intracellular pathways of peptide loading onto MHC class-I ( ) and class-II ( ) molecules. Class-I associated peptides are generated by proteasomal degradation and transported into the ER by TAP (transporter associated with antigen processing), where they are loaded onto class-I molecules. The peptide-class-I complex is then transported to the cell surface. Class-II-Ii complexes are transported into the endosomal system from the TGN (trans Golgi network). Class-II restricted peptides are derived from extracellular proteins internalised via the endocytic pathway. Processing of the invariant chain ( ) and endocytosed proteins occurs in endosomes, allowing the formation of peptide-class-II complexes which are then transported to the cell surface. Class-I molecules are shown in red, class-II molecules in blue.

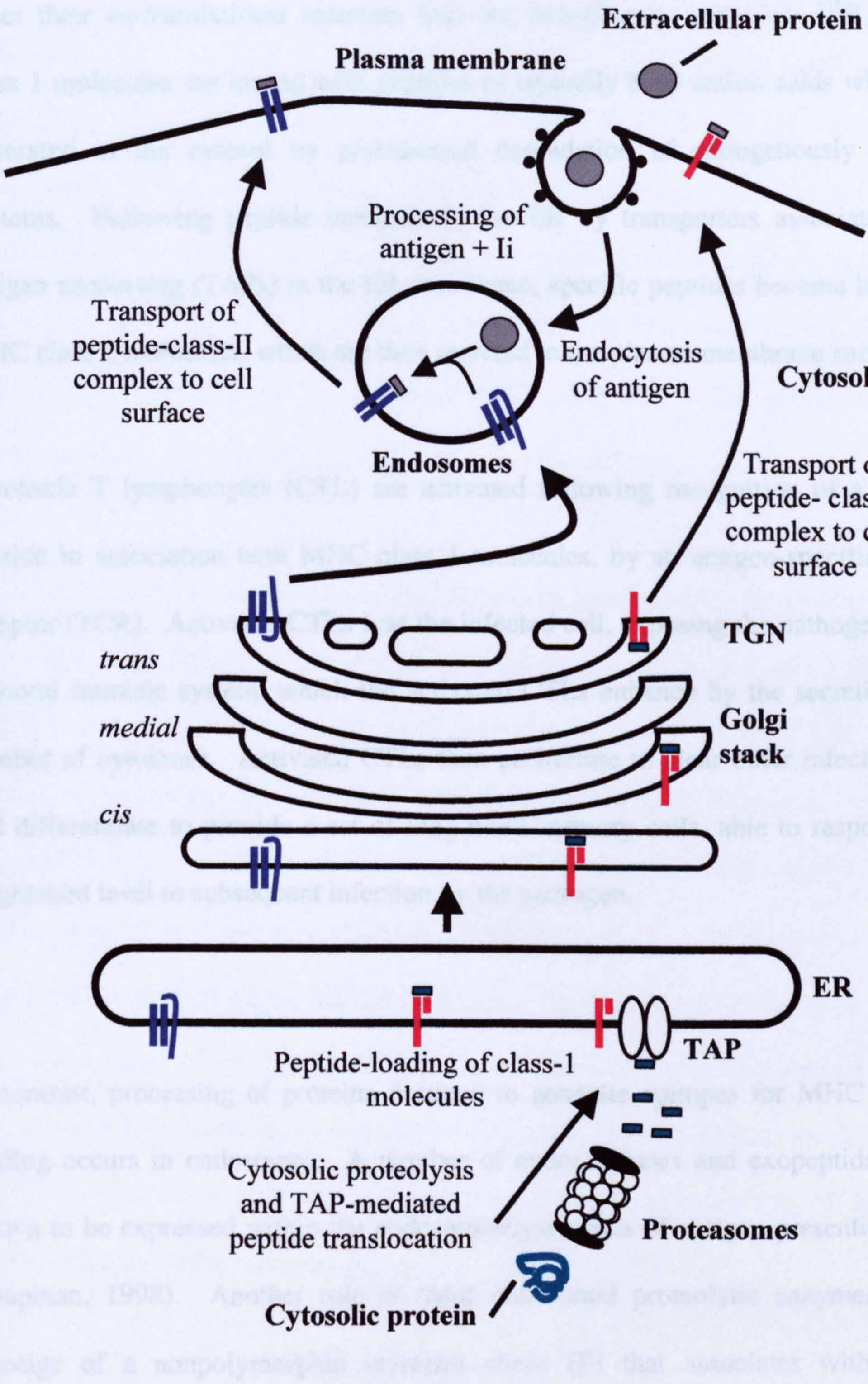


***Figure 1.5 Schematic representation of MHC class-I and class-II antigen presentation pathways.***

After their co-translational insertion into the endoplasmic reticulum (ER), MHC class 1 molecules are loaded with peptides of typically 8-10 amino acids which are generated in the cytosol by proteasomal degradation of endogenously derived proteins. Following peptide transport to the ER by transporters associated with antigen processing (TAPs) in the ER membrane, specific peptides become bound to MHC class 1 molecules, which are then secreted to the plasma membrane surface.

Cytotoxic T lymphocytes (CTL) are activated following recognition of a foreign peptide in association with MHC class 1 molecules, by an antigen-specific T cell receptor (TCR). Activated CTLs lyse the infected cell, exposing the pathogen to the humoral immune system, which the activated CTLs enhance by the secretion of a number of cytokines. Activated CTLs then proliferate to clear other infected cells and differentiate to provide a set of long-lived memory cells, able to respond at a heightened level to subsequent infection by the pathogen.

In contrast, processing of proteins destined to generate epitopes for MHC class-II binding occurs in endosomes. A number of endoproteases and exopeptidases are known to be expressed within the endosomes/lysosomes of antigen presenting cells (Chapman, 1998). Another role of these endosomal proteolytic enzymes is the cleavage of a nonpolymorphic invariant chain (Ii) that associates with newly synthesised MHC class-II $\alpha$ and $\beta$-chains in the ER. The invariant chain acts as a chaperone, promoting the proper assembly of MHC class-II dimers and preventing the premature loading of ER-resident peptides. A lumenal domain within the invariant chain termed CLIP (Class-II associated Invariant Peptide) protects the

peptide-binding groove. MHC class-II dimers associate with the chaperone to form trimers, which themselves associate to form a trimer resulting in a nanomeric complex (Cresswell, 1994). Correct trafficking of MHC class-II complexes is dependent on the invariant chain. Trafficking to endosomes requires N-terminal Ii cytoplasmic sequences. The rapid degradation of the invariant chain is necessary for the endosomal loading of peptides and rapid transport to the cell surface (Brachet *et al.*, 1997). If this degradation is delayed, MHC class-II:Ii complexes are transported to lysosomes, from where they move slowly to the cell surface.

Although a number of major proteases, have been implicated in the processing of the invariant chain, selective irreversible inhibition of a minor protease, cathepsin S, blocks the complete processing of Ii and the generation of the CLIP fragment therefore indicating an important role for this enzyme (Reise *et al.*, 1996). Degradation of Ii begins at the luminal C-terminal domain, required for the association of nanomeric complexes (Bijlmakers *et al.*, 1994), promoting their dissociation to MHC class-II:Ii heterotrimers. Proteolytic processing of Ii results in the generation of a MHC class-II:CLIP complex, able to interact with a nonpolymorphic MHC-like dimer termed HLA-DM which catalyses the dissociation of CLIP from MHC class-II molecules, enabling peptide loading of the empty peptide-binding MHC groove (Sloan *et al.*, 1995).

Once bound to MHC class-II dimers, the protein fragments can be repeatedly nicked by proteases, the core peptide being protected from proteolysis by the MHC-binding groove itself. Unlike MHC class-I molecules, the MHC class-II heterodimers may

therefore aid in the generation of antigenic diversity to a protein by participating in the processing of the antigens (Deng *et al.*, 1993).

MHC class-II-peptide complexes are then transported to the plasma membrane where they can be recognised by CD4+ T helper cells. This leads to the production of a number of cytokines, activating B-cells to produce antibodies and signalling for activated CTLs to differentiate and provide a set of long-lived memory cells.

The two MHC pathways are not entirely discrete and there are exceptions to the rule. Endogenous peptides derived from cytosolic proteins, generated in the ER can also associate with class-II molecules (Nuchtern *et al.*, 1990; Weiss *et al.*, 1991). Similarly epitopes generated from phagocytosed proteins may gain access to the MHC class 1 pathway (Watts, 1997). In transgenic mice, CD8+ T cells can also recognize peptides in association with MHC class-II molecules (Kirberg *et al.*, 1994).

### 1.5.2 MHC class-I and class-II structures

The major histocompatibility complex is a collection of genes within a long continuous stretch of DNA on chromosome 6 in humans and on chromosome 17 in mice. The region is highly polymorphic, many alleles existing at each locus, and encodes for MHC class-I and class-II molecules including a number of soluble serum proteins and enzymes associated with the immune process.

MHC class-I molecules consist of a large polymorphic glycoprotein α-chain (45kDa) non-covalently associated with a smaller invariant $\beta_2$–microglobulin protein (12kDa) (Figure 1.6). The α-chain is a transmembrane glycoprotein, containing a hydrophobic transmembrane segment, a hydrophilic cytoplasmic tail and three external domains ($\alpha_1$,$\alpha_2$ and $\alpha_3$). The $\alpha_1$ and $\alpha_2$ domains interact to form a deep groove of eight antiparallel β strands spanned by two long α-helical regions, which is the peptide-binding site. The peptide-binding site is closed at both ends, limiting the size of peptide that can be accommodated.

MHC class-II molecules share a similar structure to MHC class-1 molecules, being membrane-bound glycoproteins that contain external domains, a transmembrane segment and a cytoplasmic anchor. MHC class-II molecules contain an α and β-chain that associate non-covalently, the $\alpha_1$ and $\beta_1$ domains forming the peptide-binding region (Figure 1.7).

The peptide-binding groove of MHC class-I molecules restricts peptide lengths to 8-10 residues. Peptides that have been eluted and sequenced from a variety of human and mouse class-I molecules are listed in Table 1.1. The carboxyl terminus and the second residue from the amino terminus are conserved anchor residues, interacting with invariant pockets in the binding groove. Over the majority of the binding groove there is considerable flexibility, MHC class-I molecules being able to bind a range of peptides. Water molecules have been found to fit around the spaces between the binding groove and peptide, optimising the interaction between MHC and peptide (Smith *et al.*, 1996).

*side view*

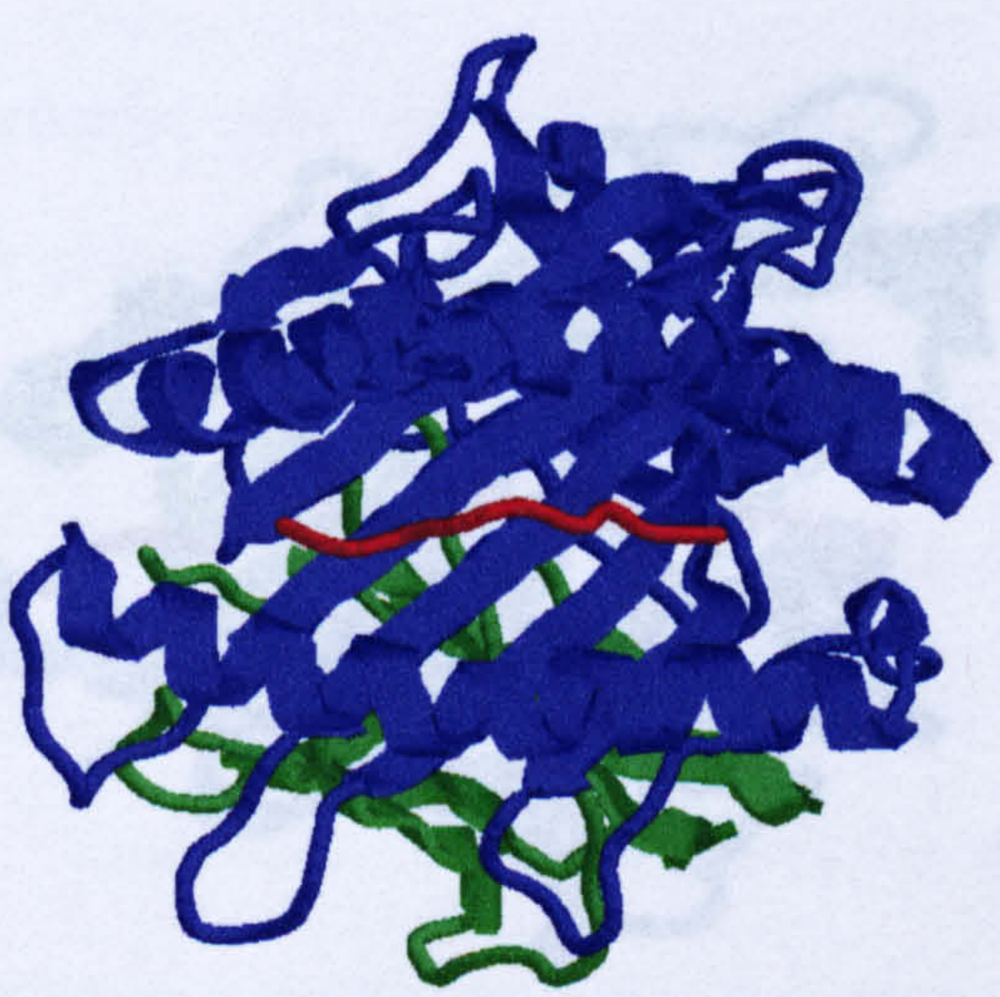

*top view*

***Figure 1.6 Structure of human class-1 molecule HLA B35 with bound HIV-2 gag peptide.***

Ribbon diagram of human class-1 molecule complexed with HIV-2 gag peptide (single letter code-TPYDINQML) (Smith *et al.*, 1996) The class-1 heavy chain is shown in blue with $\beta_2$microglobulin chain in green. The peptide bound in the class-1 groove is highlighted in red.

*side view*

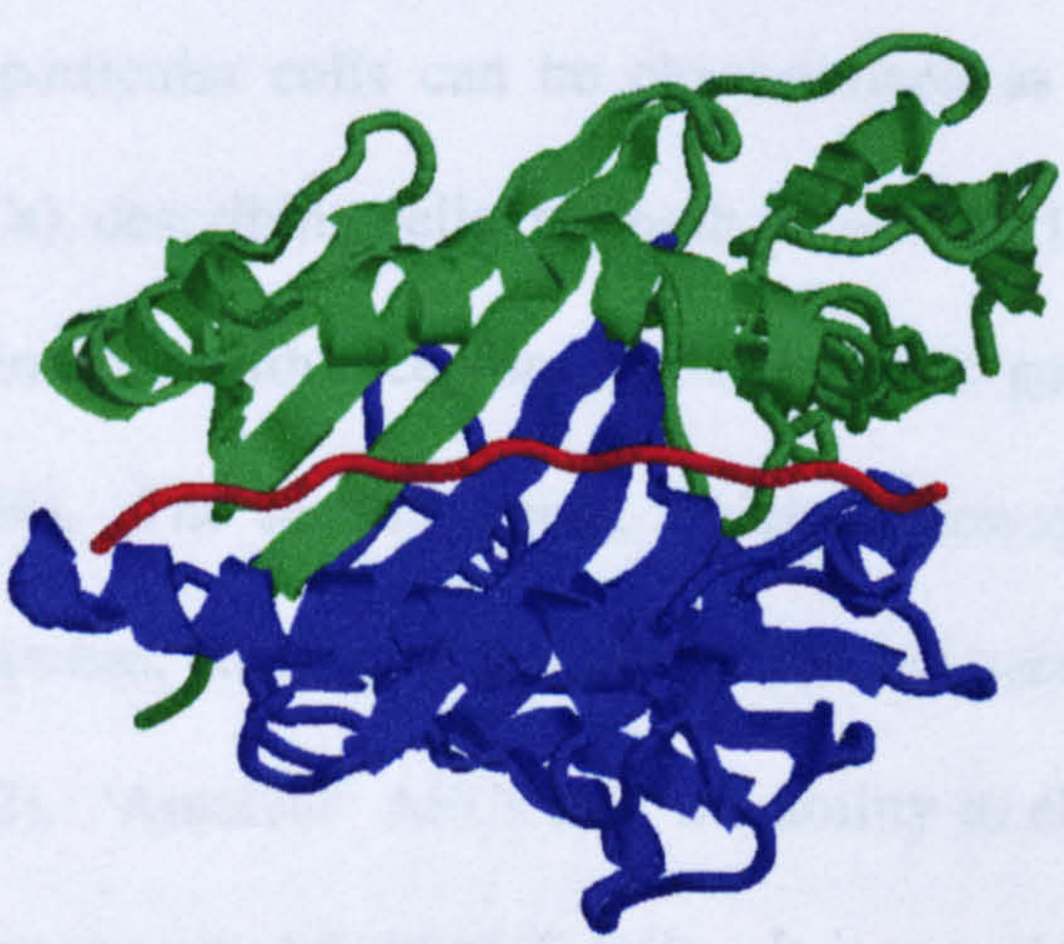

*top view*

***Figure 1.7 Structure of human class-II molecule HLA I-AD with bound influenza haemagglutinin peptide.***

Ribbon diagram of mouse class-II molecule complexed with influenza haemagglutinin peptide (single letter code-PVSKMRMATPLMEA) (Scott *et al.*, 1998). The α-chain is shown in blue, the β-chain in green. The peptide bound in the class-II groove is highlighted in red.

In contrast the MHC class-II peptide-binding groove is more open in structure, allowing a variation in length of bound peptides (13-18 residues) but containing typically nine residues of conserved secondary structure, bound within the class-II groove with additional, relatively free amino and carboxyl-terminal residues (Jardetzky *et al.*, 1996). Thus predictions of potential T-cell epitopes in antigens of known sequence can be made using known binding motifs.

### 1.5.3 Antigen-presenting cells

While nearly all tissues express MHC class-I molecules, the expression of class-II molecules is generally restricted to certain cell types, including B lymphocytes, dentritic cells from various tissues and some populations of mononuclear phagocytes. These particular cells can be characterised as professional antigen-presenting cells (APCs), describing cells that both present MHC-peptide and express surface proteins that interact with receptors on the T cell to generate a second signal (Mellman *et al.*, 1998). The second signal, which is non-specific, is required to initiate the T cell response, stabilising the interaction between the T cell and APC (Schwartz *et al.*, 1992). 'Amateur' APCs lack the ability to elicit 'signal 2' and are recognized only by previously activated T cells. It is possible that amateur APCs may present peptide to T cells that subsequently become activated by a professional APC recruited to the site of infection (Tighe *et al.*, 1998).

| Class-1 molecule /epitope | Conserved residues /peptide sequence | Class-1 molecule /epitope | Conserved residues /peptide sequence |
|---|---|---|---|
| **Human HLA A2** | **2 C** | **HLA A11** | **2 C** |
| Flu Ma 56-68 | GILGFVFTL | EBV EBNA4 | IVTDFSVIK |
| HTLV1Tax 11-19 | SLFGYPVYV | HIV gag 325-333 | AIFQSSMTK |
| HCMV gB 619-628 | IAGNSAYEYV | HIV nef 74-82 | PLRPMITYK |
| HBV Ncp 18-27 | FLPSDFFPSV | p53 343-351 | ELNEALELK |
| HIV-1 pol 476-484 | ILKEPVHGV | | |
| HIV-1 gag 77-85 | SLYNTVATL | | |
| | | **Mouse** | |
| **HLA B35** | **2 C** | **H-2D$^b$** | **2 5 C** |
| PF cp26 368-375 | KPKDELDY | Flu NP 366-374 | ASNENMDAM |
| PF ls8 1850-1857 | KPNDKSLY | SV40-T 207-215 | AINNYAQKL |
| HIV-1 nef 74-81 | VPLRPMTY | HPV E7 47-57 | RAHYNIVTF |
| HIV-2 gag 245-253 | NPVPVGNIY | LCMVGP1 | KAVYNFATC |
| CMV pp65 123-131 | IPSINVHHY | LCMVNP | FQPQNGCFI |
| **HLA B8** | **3 5 C** | **H-2K$^b$** | **2 5 C** |
| Flu NP 386-394 | ELRSRYWAI | Ovalbumin257-264 | SIINFEKL |
| EBV EBNA3 339-347 | FLRGRAYGI | VSV NP 53-60 | RGYVYQGL |
| HIV gag p17 24-32 | GGKKKYKLK | SV NP 324-332 | FAPGNYPAL |
| HIV pol 185-193 | DPKVKQWPL | Insulin 31-39 | CGSHDVEAL |
| HIV gag p24 331-339 | DCKTILKAL | | |

*Table 1.1 Sequences of MHC class-1 binding peptide epitopes*

A selection of class-1 binding epitopes are listed, together with the peptide sequence and conserved anchor residues (emboldened). One anchor residue is always at the carboxyl- terminus (denoted C), a second anchor residue is commonly found at postion 2 but may be present at position 3 or 5 of the peptide.

Key: Flu, influenza A virus; SV, Sendai virus; HPV, human papilloma virus; VSV, vesicular stomatis virus; PF, *Plasmodium falciparum*; LCMV, lymphocytic choriomeningitis; HTLV, human T cell leukaemia; HCMV, human cytomegalovirus; HBV, hepatitis B virus; HIV, human immunodeficiency virus; EBV, Epstein-Barr virus.

## 1.6 MHC class-I presentation pathway

### 1.6.1 Mechanisms of MHC class-I restricted antigen processing

The majority of class-I restricted antigen processing is attributed to the activity of proteasomes, large multicatalytic cylindrical proteases which are located in the cytosol and nucleoplasm (Figure 1.8). They are the major non-lysosomal protein degradation enzymes in eukaryotic cells. The core 20S proteasome consists of four seven-membered rings, with the catalytic sites centred in the central cavity. Regulatory complexes (19S) can bind to the ends of the cylinder to form 26S proteasomes. The 26S proteasomes recognise ubiquitinated substrates by their 19S subunit but can also degrade non-ubiquitinated proteins by ATP-dependent mechanisms (Rivett, 1998).

The evidence for proteasome involvement in antigen presentation came about from the use of peptide aldehydes that inhibited the proteolytic activities of proteasomes (as well as other proteases such as the cytosolic cysteine protease calpain) and blocked the presentation of antigens introduced into the cytosol by MHC class-1 molecules (Rock *et al.*, 1994; Harding *et al.*, 1995; Hughes *et al.*, 1996).

Several types of inhibitors of the proteasome have been identified. Peptide aldehydes are reversible substrate analogues and transition-state inhibitors of the proteasome and also certain lysosomal cysteine proteases and calpains. Lactacystin is more specific than peptide aldehydes, acting again as a pseudo-substrate. It shows higher specificity but can also inhibit lysosomal cathepsin A. Lactacystin has been

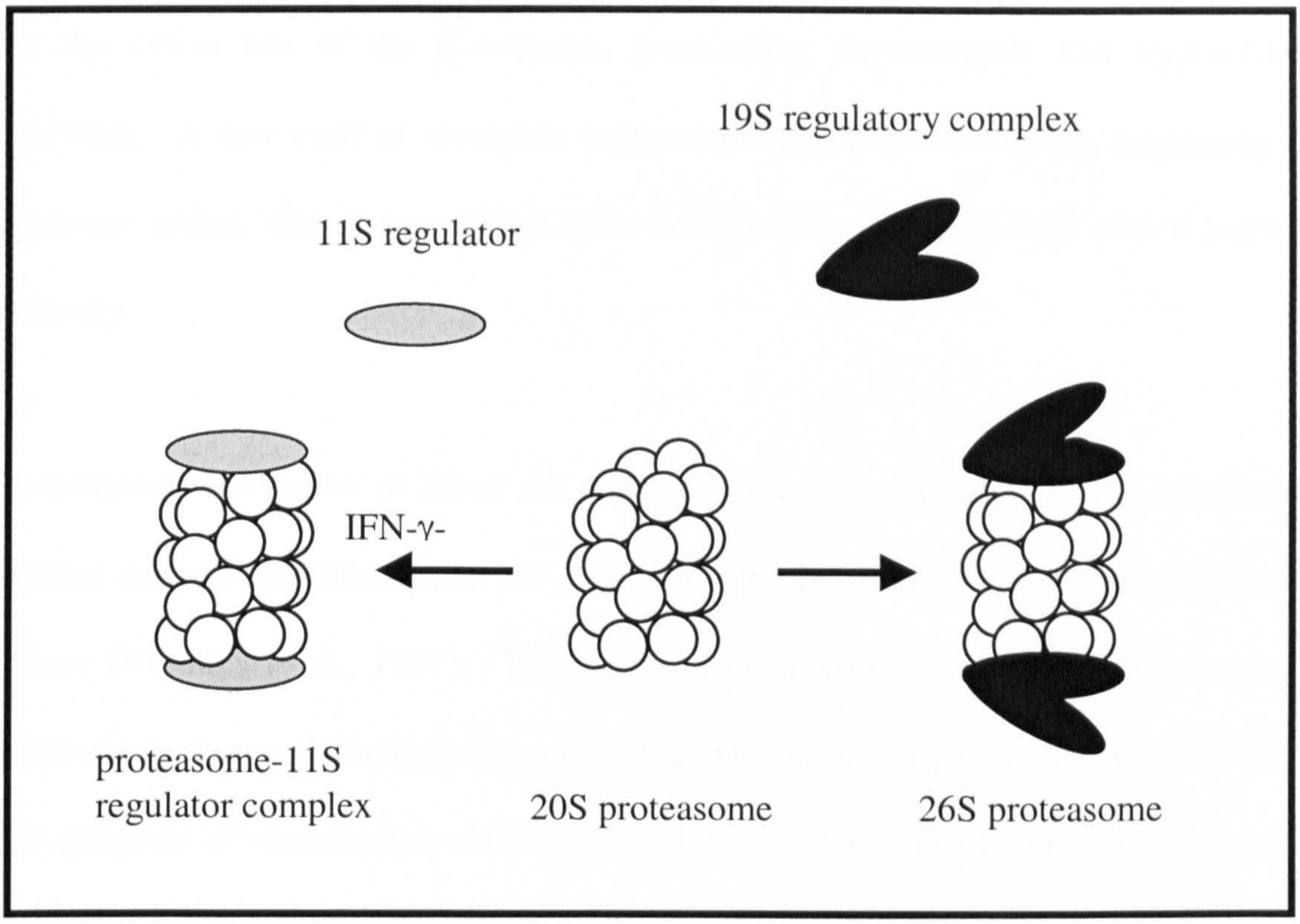


***Figure 1.8 Proteasome association with regulatory complexes in animal cells.***

The core 20S proteasomes has a hollow cylindrical structure, the catalytic sites contained inside the central cavity. Regulatory complexes can bind to both ends of the cylinder. The 11S regulator (PA28) is inducible by interferon-γ and has been implicated in antigen processing, while the binding of 19S regulatory complexes results in the formation of the 26S proteasome, required for ubiquitin-dependent protein degradation (and also for the ATP-dependent degradation of some non-ubiquitinated proteins).

shown to inhibit proteasome function by linking covalently to the hydroxyl groups on the active site of the β subunits, inactivating chymotryptic and tryptic-like activities. A new class of reversible proteasome inhibitors now exists, containing a boronate group, that do not inhibit other cellular proteases and bind with a higher potency.

Lactacystin was shown to block the presentation of certain epitopes in human and murine cells (Cerundolo *et al.*, 1997) but only partially block or have no affect on others (Vinitsky *et al.*, 1997). This suggests the involvement of non proteasomal cytosolic proteases in the generation of MHC class-I binding peptides. Research into the adaption of mammalian cells with inhibitor- induced inactivated proteasomes, suggests that other proteolytic systems can compensate for the loss of proteasomal activity (Glas *et al.*, 1998).

Other implications into the role of proteasomes in antigen processing came about from the recognition that two proteasomal subunits (termed LMP2 and LMP7) are encoded for by genes located in the MHC (Brown *et al.*, 1991) and that LMP-2 and LMP-7-deficient mice show defects in the processing of certain antigenic peptides (van Kaer *et al.*, 1994; Fehling *et al.*, 1994). Both LMP2 and LMP7 replace two constitutive proteasome subunits upon induction by interferon-γ. Incorporation of these subunits into proteasomes has been reported to alter the substrate specificity of the proteasome (Driscoll *et al.*, 1993), with preference to the generation of peptides suitable for antigen presentation. IFN-γ stimulation was reported to reduce the generation of peptides with acidic carboxy-terminal residues and to favour the generation of peptides with hydrophobic or basic carboxyl-termini (Gaczynska *et al.*,

1993; 1994) although other groups have reported different changes (Boes *et al.*, 1994; Kuckelhorn *et al.*, 1995).

Another IFN- γ inducible subunit has been implicated with antigen processing. The 20S proteasome can associate at both ends with the 11S (PA28) activator complex enhancing the cleavage of short peptide substrates *in vitro* and the class-I mediated presentation of two viral epitopes *in vivo* (Groettrup *et al.*, 1996). Complexes containing these IFN-γ inducible subunits have been termed immunoproteasomes (Tanaka *et al.*, 1997). PA28 replaces the 19S regulatory complex of the 26S proteasome that is responsible for the recognition and degradation of ubiquitinated substrates.

The involvement of the ubiquitin pathway in antigen presentation is inconclusive at the present. Initial observations by Townsend *et al,*. (1988) suggested that ubiquitin tagging enhanced the presentation of an influenza nucleoprotein epitope, other work has found antigen presentation to be ubiquitin-independent (Michalek *et al.*, 1996).

The distribution of immunoproteasomes in the cytosol has been investigated by Rivett *et al.*, (1998) using antibodies against LMP2 and LMP7. Proteasomes containing these subunits have been found to localise around the ER, suggesting that in addition to altering the catalytic abilities of proteasomes, LMP2 and LMP7 may target immunoproteasomes to the ER. It is still not known how peptides that are released from proteasomes are directed to TAP peptide transporters in the ER membrane and without degradation. Having found TAP to be localised near the ER,

it may be that immunoproteasomes can bind directly to TAP for efficient transport of peptides.

### 1.6.2 Transporters associated with antigen processing (TAPs)

Transporters associated with antigen processing (TAPs) are noncovalent complexes of two homologous subunits TAP1 and TAP2 that belong to the superfamily of ATP-binding cassette transporters (Figure 1.9a). Like the proteasomal subunits LMP2/LMP7 and PA28, the TAP subunits are encoded in the MHC. Each TAP subunit has an N-terminal hydrophobic region with multiple transmembrane spanning domains and a cytosolic C-terminal ATP-binding domain.

Studies demonstrating the ability of TAP to translocate peptides across the ER membrane, have involved the use of TAP-containing microsomes or cells with permeabilized plasma membranes to follow the fate of radiolabelled peptides (Neefjes *et al.*, 1994). By radiolabeling with photoactivatable peptides containing crosslinkers, it has been established that both TAP1 and TAP2 subunits contribute to peptide binding (Nijenhuis et al., 1996) which, unlike peptide translocation, is ATP independent.

TAP transporters preferentially transport peptides of 8-12 residues, the sequence specificity of these peptides varying between species (Neefjes *et al.*, 1995). The transport specificity of TAP meets the requirements needed for the binding of

A) Schematic representation of TAP1/TAP2 heterodimer.

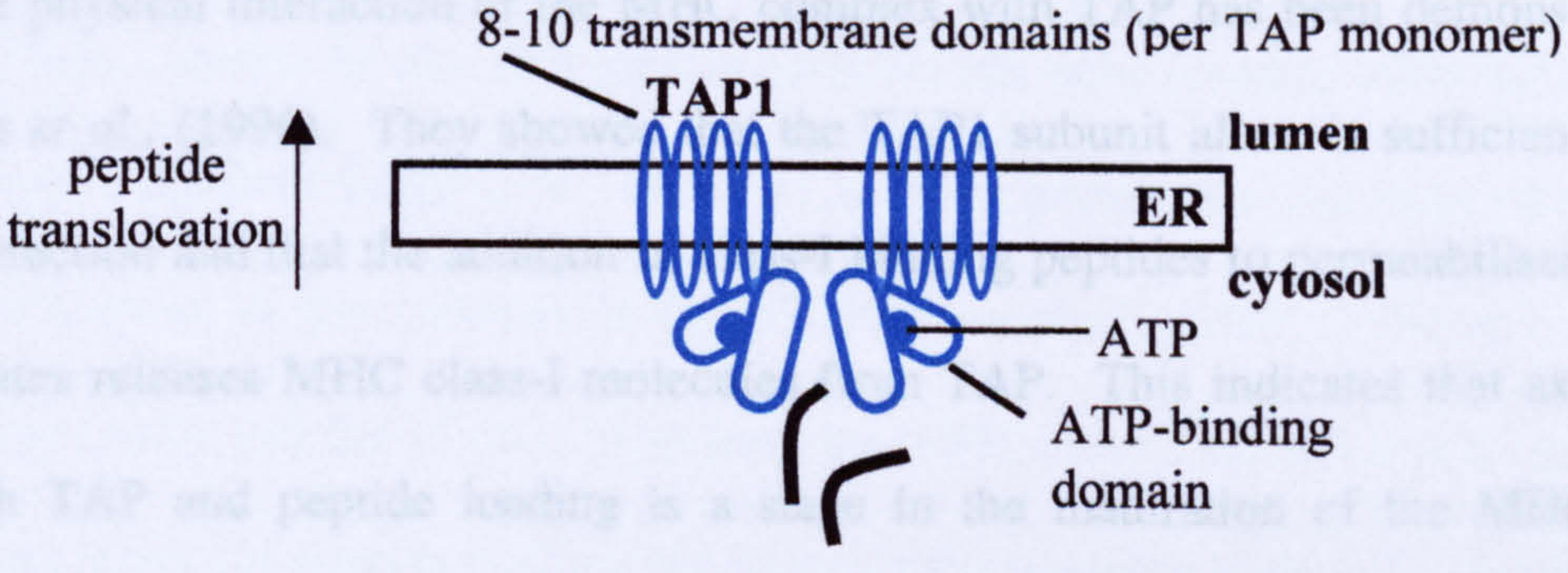


B) Maturation of human class-1 molecules in the ER.

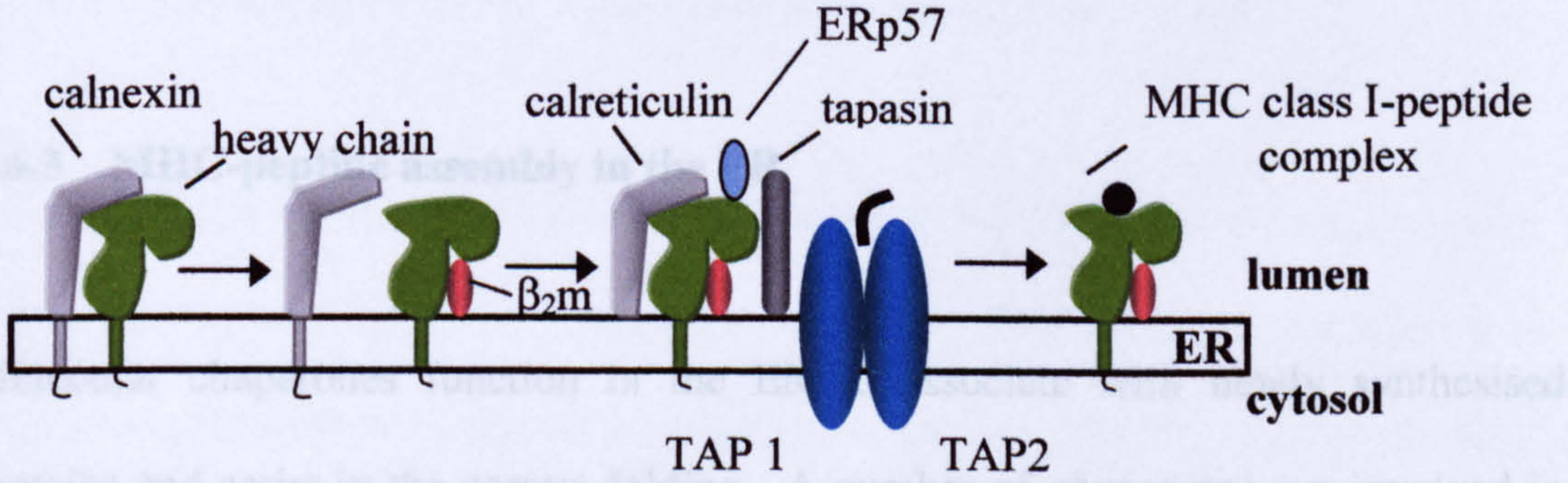


***Figure 1.9 Peptide assembly with MHC class-1 molecules***

Hypothetical sketches of the TAP transporter and the interaction of a number of chaperones in MHC class-1-peptide assembly A) Cross-section of TAP heterodimer spanning the ER membrane. Eight to ten transmembrane segments (per TAP monomer) are predicted with the ATP-binding domains extending into the cytosol. B) Newly synthesised class-1 heavy chains initially associate with calnexin which promotes their assembly with $\beta_2$ microglobulin light chains. Empty class-1 heterodimers then associate with calreticulin (the soluble homologue of calnexin), Erp57 and form a complex with tapasin. Tapasin enables empty class-1 heterodimers to associate with TAP. Upon loading of peptide, the MHC class-1-peptide complexes are released for transportation to the cell surface.

peptides by MHC class-I molecules, selectively transporting peptides suitable for class-1 antigen presentation.

The physical interaction of the MHC complex with TAP has been demonstrated by Suh *et al.*, (1996). They showed that the TAP1 subunit alone is sufficient for this interaction and that the addition of class-I binding peptides to permeabilised cells or lysates releases MHC class-I molecules from TAP. This indicates that association with TAP and peptide loading is a stage in the maturation of the MHC class-I complex. Other components have been found to transiently associate with MHC class-1 molecules and aid in the assembly of peptide-loaded MHC complexes, their role in this process is described below.

### 1.6.3 MHC-peptide assembly in the ER

Molecular chaperones function in the ER to associate with newly synthesised proteins and assist in the correct folding. A number of chaperones are involved in the maturation of MHC-peptide complexes (Figure 1.9b). Calnexin is the first chaperone that class-I heavy chains encounter after their biosynthesis in the ER membrane (Degen *et al.*, 1992). Calnexin is a type-I membrane protein with its substrate-binding domain located in the ER. Calnexin facilitates the folding and disulfide bridge formation of heavy chains, promoting its association with $\beta_2$-microglobulin. Calnexin is then replaced by its soluble homologue, calreticulin (calreticulin showing homology to the luminal domain of calnexin). It has been shown that calreticulin then remains associated with the heavy chain-$\beta_2$m heterodimers during the transient interaction with TAP (Sadasivan *et al.*, 1996).

A further glycoprotein (48kDa) was found in a complex with TAP, MHC and calreticulin, termed tapasin (Sadasivan *et al.*, 1996). Tapasin may form a bridge between heavy chains and TAP, being able to bind each independently. The affinity of heavy chains for the TAP-tapasin complex has been found to differ between MHC class-1 allelles (Neisig *et al.*, 1996). The latest protein that has been identified as a component of this complex is ERp57 (Hughes *et al.*, 1998). The role of tapasin, calreticulin and Erp57 may be to keep the MHC class-1 complex in a conformation state ready for peptide binding and to retain the complex in the ER. Peptide binding then causes the dissociation of these accessory proteins.

### 1.6.4 Processing of MHC class-I restricted antigens in the ER

It is currently thought that cytosolic proteasomal degradation is the major source of peptides for MHC class-I binding (section 1.7.1). This has been concluded from a number of observations that show proteasome-specific inhibitors reduce the level of antigen presentation to CTLs. In addition, cell mutants lacking TAP transporters for peptide translocation into the ER have reduced levels of class-I molecules at the cell-surface indicating that the majority of antigenic peptides are generated in the cytosol. However there are examples of alternative antigen processing, suggesting that degradation may also take place in the ER. Peptides associated with class-1 molecules in TAP-negative cells, have been found to be derived from signal sequences that have direct access to the ER and are liberated by signal peptidase. Secretory and transmembrane proteins, that are co-translationally inserted into the ER, are known to generate epitopes in TAP-negative cells although, several of these

have been shown to have been translocated from the ER by Sec61p (section 1.2) and processed in the cytosol (Mosse *et al.*, 1998).

Studies with minigenes encoding peptide epitope precursors, preceded by the influenza hemagglutinin ER translocation sequence, have shown that processing of polypeptides of at least 40 residues can occur in the ER of TAP-negative cell-lines but that the proteolysis of larger proteins is limited (Elliot *et al.*, 1995). The release of epitopes from the C-terminus is more efficient than from the N-terminus of such precursors processed in the ER, suggesting the involvement of N-aminopeptidases (Snyder *et al.*, 1997).

These studies indicate that processing of MHC class-I restricted antigens can occur in a proteasome-independent manner and that alternative processing mechanisms may exist in the ER.

### 1.6.5 Cell surface presentation of MHC-peptide complexes

It is generally assumed that once the MHC-peptide complex leaves the ER, progression to the cell surface is rapid (Jackson *et al.*, 1994). Studies with mammalian cells that overexpress MHC class-I heavy chains and $\beta_2$-microglobulin have found that the expression of MHC class-I molecules at the cell surface may be regulated (Joyce, 1997). They found that only 2 to 20% of the overexpressed (50-fold) class-I molecules were stably expressed at the plasma membrane even though the majority formed complete MHC-peptide complexes. Almost all of the MHC class-I molecules became sialylated, indicating trafficking as far as the Golgi. Their

regulation at the cell surface may be achieved by the rapid internalisation and recycling of class-I molecules from, and back to the plasma membrane. Alternatively, sorting may occur in the TGN (Joyce, 1997).

### 1.6.6 Cellular responses to interferon-γ

The elevation of MHC class-1 molecules expressed on the cell surface involves the upregulation of many genes, most encoded in the MHC, that play a role in the antigen presentation pathway. The expression of the $\beta_2$m and MHC heavy chain genes are upregulated by IFN-γ as well as by IFN-α/β and TNF-α.

The transporter associated with antigen processing (TAP) is a heterodimeric member of the ATP-binding cassette transporter family and is essential for the transport of peptides from the cytosol to the ER for loading onto MHC class 1 molecules. Both genes encoding the two subunits of TAP (TAP 1 and TAP 2) map to the class II region of the MHC and are inducible by IFN-γ.

The proteasome β-subunits LMP-2 and LMP-7 both map in the class II region of the MHC, in close proximity to the TAP genes. The replacement of constitutive β-subunits in the proteasome with IFN-γ inducible β-subunits (including MECL-1 which is encoded elsewhere in the genome) results in the modification of proteolytic cleavage preference, increasing the suitability of peptides for class 1 loading. The proteasome activator (PA28), which enhances the yield of peptides of a size and structure optimal for TAP transport and class 1 loading is also upregulated by IFN-γ.

ER luminal proteins have also been found to be upregulated by IFN-γ. Tapasin, mapping in or near the MHC, is required for the normal assembly and loading of MHC class 1 molecules. A number of chaperones including gp96 have been implicated in taking a role in protecting peptides entering the ER from degradation and helping their loading onto MHC class 1 molecules.

## 1.7 Towards development of $CD8^+$T-cell vaccines

Activated CTL are an important component of the protective and therapeutic immune response to viral infections and tumours. A number of approaches to generate safe CTL-based vaccines are being studied. Direct immunisation, with a viral protein or synthetic peptide tends to lead to antigen endocytosis and association with MHC class-II complexes. Live or attenuated viral vaccines, that are processed and presented by the MHC class-I pathway, are potentially pathogenic and a risk to the recipient. The reversion of an attenuated vaccine strain to a virulent phenotype is particularly important when considering pathogens such as HIV.

These safety issues have forced the development of subunit or inactivated virus vaccines, self proteins expressing antigenic peptide or the delivery of exogenous proteins (for presentation by MHC class-1 molecules) by liposome complexes or synthetic lipopeptides (reviewed by Bona *et al.*, 1998). In many cases, these vaccines have not elicited the necessary humoral, cellular and mucosal response, necessary for long-term memory andto confer life-long protection in immunized individuals.

However, promising vaccine vectors have been developed in recent years that are now reaching the stage of clinical trials. Plasmid DNA-based vaccines have been shown to elicit strong humoral and cellular immune responses in rodents and non-human primates. DNA, encoding antigens under the control of a eukaryotic promoter, is adhered to gold particles to increase its mass before being injected through the skin using a helium driven gun to accelerate the particles. The DNA is incorporated into the skin's antigen presenting cells, which produce antigenic proteins that illicit an immune response (PowderJect Pharmaceuticals, UK).

This technology has been combined with another promising vaccine vehicle candidate, recombinant vaccinia viruses expressing antigens derived from pathogens. Prime-boost immunization strategies in mice have been carried out, comparing combinations of recombinant vaccinia virus strains and plasmid DNA. The modified virus Ankara (MVA) strain of vaccinia has been attenuated such that MVA is replication-restricted (losing 31kb of DNA) and has been used safely on humans during a smallpox immunization program (Mayr *et al.*, 1978).

Using plasmid priming and recombinant MVA boosting in mice, complete protection against *Plasmodium berghei*, the rodent virus model for malaria, has been observed (Schneider *et al.*, 1998). This protection was associated with high levels of activated CTLs in the spleen and was dependent on the specific order of vaccine delivery (DNA priming and MVA boost). A similar vaccination programme has been used to enhance the induction of HIV-specific CTL in mice (Hanke *et al.*, 1999).

$CD8^+$ T cell vaccination is only suitable against viral infections or intracellular pathogens known to raise a strong CTL response in their host. Pathogens known to raise such a response (and have a global impact on health) include HIV, malaria (as noted above), rotavirus, Ebola virus (Xu *et al.*, 1998) and the intracellular bacterial pathogen, *Mycobacterium tuberculosis* (Kaufmann, 1999). In contrast, influenza virus tends to raise a humoral antibody response to infection.

In addition to viral vaccines, $CD8^+$ T cell immunotherapy has been successfully used to elicit anti-tumour responses in certain cancers that are poor stimulators of an immune response, or that may have induced tolerance towards tumour cells. As well as the use of recombinant viral and bacterial vaccines (adenovirus, vaccinia and *Listeria monocytogenes* are common vectors), dendritic cell (DC)- based vaccines are under investigation. Autologous DCs, pulsed with tumour lysate or MHC class-1 restricted melanoma peptides are used as antigen carriers for tumour vaccination. An alternative approach to the priming of DCs with peptides is to transfect cells with tumour-derived RNA, an advantage being that RNA encodes multiple epitopes for many HLA alleles (Smita *et al.*, 1998).

T-cell based vaccines have also been shown to suppress certain autoimmune diseases and inhibit allergic responses, involving the administration of increased doses of allergen- encoding vaccines to induce T cell tolerance (reviewed by Tighe *et al.*, 1998).

## 1.8 Aims of project

To develop a model system whereby an antigenic peptide fused to a 'carrier' toxin is delivered to MHC class-I molecules assembled in the ER. This would lead to the subsequent presentation of the intracellular peptide at the cell surface and the elicitation of an antigen-specific cytotoxic T lymphocyte (CTL) response.

The toxins used , Shiga-like toxin-1 from *E.coli* 0157:H7 (SLT) and ricin, are members of a family of ribosome inactivating proteins (RIPs), that undergo retrograde vesicular transport from the cell surface to the ER, before translocating into the cytosol. To be useful, disarmed toxins with defective or deleted catalytic domains must be utilised in order that target cells are not destroyed in the process of peptide delivery. For SLT, this was achieved by using a mutant with an active site mutation (E167D). The activity of E167D SLT, purified to homogeneity from *E.coli* by receptor-ligand based chromatography, was assessed by *in vitro* ribosome-inactivation assays and *in vivo* cytotoxicity comparisons with wild-type SLT. The SLT A chain was genetically fused with a well defined nonamer peptide derived from influenza virus Matrix protein (Ma, 58-66), positioned at either the N- or C-terminus of the toxin.

The active-site mutations R180H and E177D in ricin were expressed both individually and as a double mutant in an attempt to engineer a holotoxin completely devoid of activity. Influenza Matrix peptide 58-66 (Ma) and influenza Nucleoprotein 366-374 (NP) were placed at the N-terminus of RTA. NP was also placed within an external loop (residue 113-114), accessible by a *Cla* 1 site to study

the possible effect of positioning of the peptide within the toxin. The toxin fusion proteins constructed are shown schematically in Figure 1.10.

It is now evident that both SLT and ricin undergo retrograde transport from the cell surface to the ER (described in section 1.3). Recent evidence suggests that the toxins may then exploit the ER export machinery normally associated with the ejection of aberrantly folded ER proteins to the cytosol for degradation by proteasomes. Processing of the toxin chimeras may therefore occur at two stages during this progression either directly in the ER by ER-resident proteases or in the cytosol. Once in the cytosol the toxin chimeras may follow the conventional proteasome degradation pathway or be processed by other cytosolic proteases. The intracellular routing of the novel wtSLT-peptide fusion proteins and the location of peptide loading of MHC class-1 molecules were investigated by treating cells with the Golgi stack-disrupting agent brefeldin A. Cells were also treated with the proteasome-specific inhibitor lactacystin to examine the processing requirements of the SLT-peptide fusions.

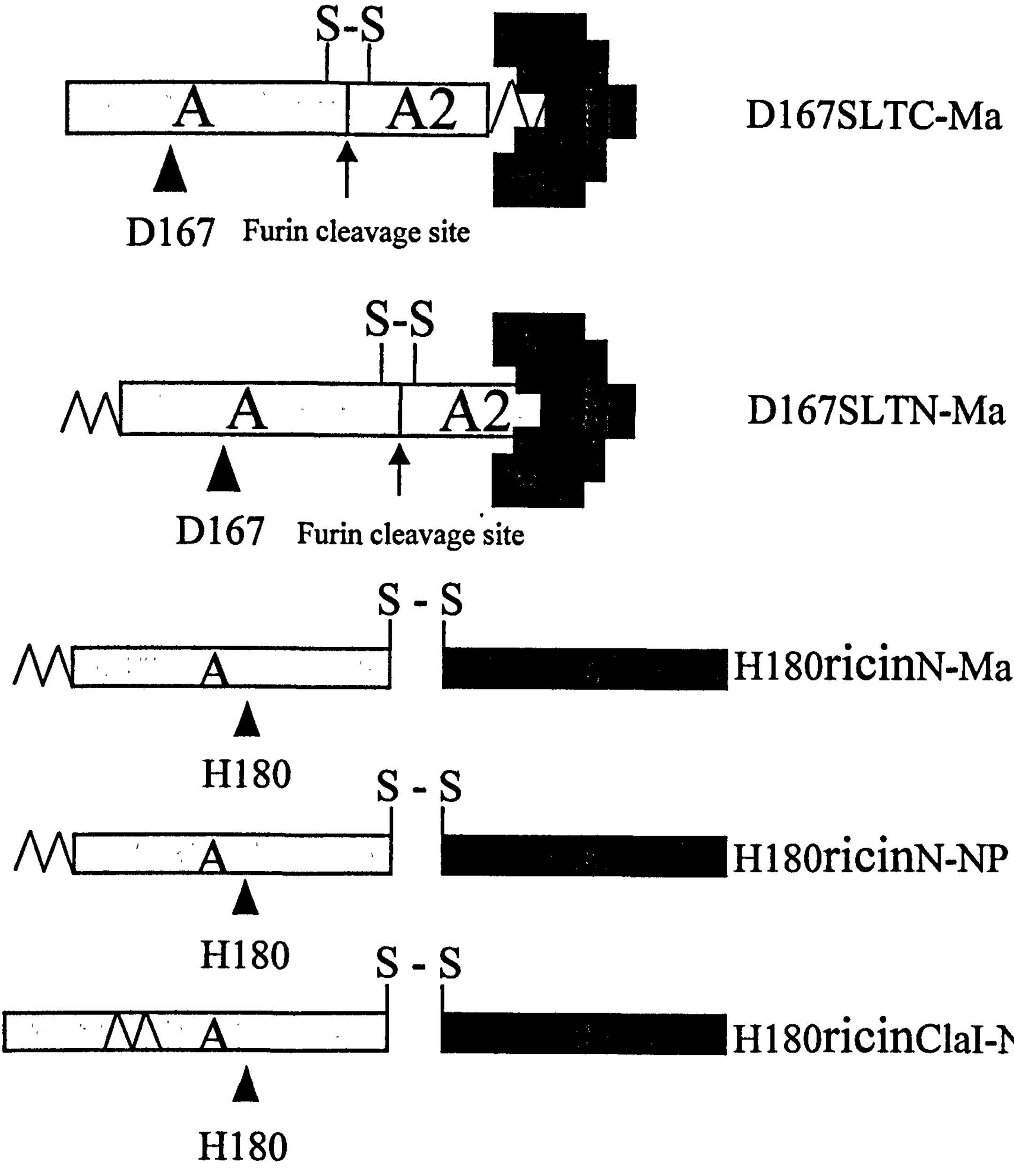


*Figure 1.10 Schematic representation of toxin-peptide fusion proteins constructed in this study*

The catalytic A-chain is shown in grey (▲, refers to a catalytic site mutation), the cell-binding B-chain in green. The position of the peptide is denoted by the zig-zag and is either influenza Matrix peptide 58-66 (Ma) or influenza Nucleoprotein 366-374 (NP). Disulfide bonds that covalently link a trypsin-sensitive site or two fragments are labelled.

# CHAPTER 2

# MATERIALS AND METHODS

# Chapter 2

# Materials and Methods

## 2.1 Suppliers and reagents

### 2.1.1 Suppliers

The majority of reagents used were obtained from BDH Chemicals Ltd (UK), Fisons (USA) or Sigma (UK) and were of analytical grade if available. Suppliers of other reagents are listed below.

*Aldrich (USA)*

Tween 20

*Amersham (UK)*

Hybond™C nitrocellulose, Hybond™N nitrocellulose, α-[$^{35}$S] dATP (1000Ci/mmol), [$^{35}$S] methionine (3000Ci/mmol), γ-[$^{32}$P]-ATP (5000Ci/mmol).

*Bio 101 inc. (USA)*

Geneclean II kit.

*Boehringer Mannheim (UK)*

Adenosine triphosphate, Sequencing grade trypsin, Protease inhibitor cocktail tablets.

*Calbiochem (UK)*

lactacystin

*Chivers and Sons Ltd. (UK)*

Dried skimmed milk powder.

*Difco (USA)*

Bacto-agar, bacto-tryptone.

*Gibco BRL (USA)*

RPMI 1640 medium, Dulbecco's Modified Eagle's medium, Geneticin G418 Sulphate, trypsin-EDTA solution, agarose, restriction enzymes and REact™ buffers, T4 DNA ligase, T4 polynucleotide kinase, medium-range molecular weight markers.

*Inland Laboratories (USA)*

Ricin-B-chain

*Johnson-Matthey (UK)*

Silver nitrate

*Kodak (UK)*

LX24 developer, Unifix

*NBL Gene Sciences Ltd.(USA)*

40% Acrylamide-Bisacrylamide

*Oxoid (UK)*

Yeast extract.

*Pharmacia Biotech (Sweden)*

CM-Sepharose, DEAE-Sephacel, PD-10 desalting column.

*Polaroid (UK)*

665/667 photographic film.

*Promega (USA)*

BCIP, NBT, rabbit reticulocyte lysate.

*Qiagen (Germany)*

QIAprep spin plasmid kit, QIAprep, Maxi plasmid kit.

*Sigma Immunochemicals*

Donkey anti-sheep antibody (conjugated to alkaline phosphatase), goat anti-mouse IgG Fab-specific FITC-conjugate antibody.

*USB(USA)*

Sequenase T7 DNA polymerase.

*Whatman (UK)*

3MM chromatography paper

*Zenecca Pharmaceuticals(UK)*

Recombinant ricin-A chain

### 2.1.2 Standard reagents

Standard solutions and media were prepared as in Sambrook *et al,*. (1989).

Phosphate-buffered saline (PBS) (137mM sodium chloride, 0.27mM potassium chloride, 10.4mM disodium hydrogen phosphate, 1.8mM potassium dihydrogen phosphate).

### 2.1.3 Aniline reagent

Aniline was prepared from aniline which had been distilled twice, 1ml of this was mixed with 7ml of distilled water and 0.5ml glacial acetic acid in a sterile glass universal. The pH of the aniline was adjusted to pH4.5 by the addition of glacial acetic acid drop-wise and the final volume made up to 11ml with water. Aniline reagent was stored in the dark at 4°C.

## 2.2 Growth and Maintenance of Cells

### 2.2.1 Maintenance of *Escherichia coli* Strains

The genotype of the strains of *E.coli* used were:

TG2 *supE hsd* Δ5 *thi* ρ(*lac-proAB*) Δ(*srl-recA*)306::Tn*10*(*tet* $^{r}$)
F'[*traD*36 *proAB*$^{+}$ *lacI*$^{q}$ *lacZ* ΔM15]

71-18 *supE thi* Δ(*lac-proAB*) F'[*proAB*$^{+}$ *lacI*$^{q}$ *lacZ*ΔM15

*E.coli* strains JM109, TG2 and 71-18 were maintained on Luria-Bertani (LB) plates (10g/l bacto-tryptone, 5g/l yeast extract, 10g/l sodium chloride, 2% (w/v) bacto-agar) by streaking and subsequent incubation at 37°C overnight.

**Maintenance of Mammalian Tissue Culture Cells**

**The mammalian cell lines used were as follows:**

| | |
|---|---|
| **HeLa** | **human cervix epitheloid carcinoma** |
| **HeLa-A2** | **HeLa cells stably transformed with an HLA-A2 haplotype [stably transformed using the pcdNA3.1/HIS Xpress™ expression system (*Invitrogen*, UK)]** |
| **Vero** | **African Green Monkey kidney fibroblast** |
| **Skmel-29** | **human melanoma, HLA-A2 haplotype** |
| **L** | **murine fibroblast, H2-D$^{b}$ haplotype** |

HeLa and Vero cells were grown in Dulbecco's Modified Eagle's Medium (DMEM) supplemented with 5% heat inactivated foetal calf serum, 2mM glutamine, 50 IU/ml penicillin, 300μg/ml streptomycin. LO[6] were grown in DMEM supplemented as above with 10% heat inactivated foetal calf serum. SKmel-29 cells were grown in RPMI 1640 medium (supplemented with 10% heat inactivated foetal calf serum, 2mM glutamine, 50 IU/ml penicillin, 300μg/ml streptomycin). HeLa-A2 cells were also grown in RPMI 1640 medium with the same supplements plus 800μg/ml (powder weight) Geneticin G-418 sulphate, a selective antibiotic which maintains the HLA-A2 gene insertion.

The cells were grown in vented flasks at 37°C in a 5% $CO_2$ air humidified incubator. Adherent cells were passaged by washing with PBS and the addition of 5ml of 0.25% trypsin/0.02% versene (0.02% EDTA, 0.1% phenol red/ PBS pH 7.4) at 37°C until the cells were released from the flask. Cells were pelleted at 250xg in a Beckman GPR centrifuge (GH3.7 rotor) at room temperature for 5 minutes and resuspended in fresh media. Cells were stored frozen under liquid nitrogen in a freezing mix (90% heat inactivated foetal calf serum, 10% DMSO).

CTLs were maintained in Iscove's medium (5% human serum, 100U/ml IL-2) and restimulated every 3 weeks. CTLs ($5x10^5$) were stimulated with matched peripheral blood lymphocytes ($2x10^6$) and B cells ($5x10^5$) in 2ml Iscove's medium (5% human serum, 100U/ml IL-2, 5μg/ml pHA) and allowed to proliferate for one week, replacing with fresh media.

## 2.3 DNA Preparation and Cloning Techniques

### 2.3.1 General Molecular Biology Techniques

The preparation of plasmid and M13 DNA and the transformation of competent cells were undertaken as described in Sambrook *et al.*, (1989) unless stated. Small-scale preparation of plasmid DNA was performed using the QIAprep Spin Plasmid kit according to the manufacturer's protocol. All restriction endonucleases and DNA modification enzymes were used in accordance with the manufacturer's instructions. DNA digests and PCR products were separated by agarose gel electrophoresis (2.3.3) and gel-purified prior to subsequent cloning steps using the Stratech Geneclean II kit following the recommended instructions.

### 2.3.2 Phenol/Chloroform Extraction and precipitation of DNA/RNA

The DNA/RNA to be extracted was made up to a minimum volume of 200µl with TE unless otherwise stated. To this 0.5 volumes of Tris-saturated phenol was added and mixed by vortexing followed by 0.5 volumes of chloroform and further mixing. The organic and aqueous layers were separated by microcentrifugation at 13000xg for 5 minutes and the upper aqueous layer removed to another eppendorf tube. The extraction process was repeated 3 times followed by DNA/RNA precipitation.

The DNA solution to be precipitated was mixed with 0.1 volumes of 3M sodium acetate pH6.0 and 2 volumes of ice-cold absolute ethanol on dry ice for at least 15 minutes.

The RNA solution to be precipitated was mixed with 0.1 volumes of 7M ammonium acetate and 2.5 volumes of ice-cold absolute ethanol on dry ice for at least 15 minutes.

The DNA/RNA pellet was recovered by centrifugation at 17,800xg in a Heraeus refrigerated microcentrifuge for 20 minutes and the pellet washed with 100µl 70% ethanol by centrifugation as above for 5 minutes. The pellet was dried in a vacuum desiccater and resuspended in TE or water.

### 2.3.3 Preparation of Competent Cells

A 5ml overnight culture of *E.coli* was used to inoculate 50ml LB medium and grown in a shaking-incubator at 37°C/250rpm until it had reached an $OD_{600}$ 0.6 (approx. 2 hours). The culture was transferred to a pre-cooled 50ml centrifuge tube and the cells harvested by centrifugation at 1500xg in a Beckman GPR bench centrifuge (GH3.7 rotor) for 10 minutes at 4°C. The pellets were gently resuspended in 25ml calcium chloride (0.5M)/15% glycerol and incubated on ice for 30 minutes. Cells were harvested as before and the pellet resuspended in 5ml calcium chloride (0.5M)/15% glycerol. The cells were left for a minimum of one hour at 4°C before use in transformation (and for a maximum of 24 hours before being frozen at -70°C).

### 2.3.4 Separation of DNA fragments by Agarose Gel Electrophoresis

0.8% w/v agarose/0.5xTBE gels containing 0.05% (w/v) ethidium bromide were used for the separation and isolation of DNA fragments (Sambrook *et al.*, 1989). Gels were cast in a horizontal electrophoresis tank and a 40-80mA current applied. DNA migration was visualised by short-wave ultra-violet illumination and photographed by a UVP (TMW-200) transilluminator (Upland, USA), gel-documentation system.

### 2.3.5 Oligonucleotide Site-Directed Mutagenesis

Single-stranded M13 wtSLT DNA was mutated using an oligonucleotide-directed Sculptor T7-polymerase mutagenesis kit (Amersham) according to the manufacturer's instructions. The active site mutant E167D SLT was prepared using the phosphorylated oligonucleotide 5' ACA GCT GAT GCT TTA CG 3'. Mutated single-stranded M13 DNA was transformed into competent 71-18 cells. Potential mutants were screened using a *Hind*III digest. The mutation of GAA to GAT destroys a unique *Hind*III site in the SLT sequence. Mutants linearise whereas non-mutated DNA releases a ~580bp fragment.

### 2.3.6 DNA sequencing

Single stranded M13 DNA and denatured plasmid DNA was sequenced using a Sequenase™ T7 DNA Polymerase kit version 2.0 (United States Biochemical). The kit was used in accordance with the manufacturer's instructions. Typically 1μg of

single stranded M13 DNA or 2μg of plasmid DNA was sequenced per reaction. Single stranded M13 DNA was obtained by the small-scale PEG precipitation method of DNA preparation (Sambrook *et al.*, 1989). Plasmid DNA was prepared using the QIAprep spin miniprep kit (2.3.1) or large-scale plasmid DNA prepared using the alkaline lysis method (Sambrook *et al.*, 1989). Plasmid DNA prepared using the alkaline lysis method was further purified for sequencing by mixing the DNA with glassmilk using the Stratech Geneclean II kit, following the recommended instructions for DNA purification. Plasmid DNA was denatured by diluting into a 90μl volume of water and the addition of 10μl of 10M sodium hydroxide for 5 minutes at room temperature. The denatured DNA was precipitated by the addition of 10μl of 5M ammonium acetate and 250μl ice-cold ethanol, centrifuged for 15 minutes at 4°C, washed with 70% ethanol and recentrifuged for 5 minutes at 4°C. Sequencing was carried out referring to the manufacturer's protocol and the samples run on polyacrylamide sequencing gels (2.2.6).

### 2.3.7 Sequencing Gels

6% w/v polyacrylamide/urea gels were used for the separation of sequencing products. The gel mix (24g of urea dissolved in 16.75ml of water, 5ml of 10x TBE, 7.5ml of 40% acrylamide/2% N, N'-methylene bis-acrylamide) was polymerized by the addition of 250μl of 10% ammonium persulphate and 29μl of TEMED and poured into 38cm x 15cm taped gel plates. The gels were pre-warmed and the sequencing samples electrophoresed at 40W for 1-3 hours. The gels were then dried and exposed to Fuji RX X-ray film overnight. Films were developed under

darkroom conditions with LX24 developer (1:4 dilution), washed and fixed with Unifix (1:4 dilution).

### 2.3.8 Polymerase Chain Reaction (PCR).

Specific mutagenic PCR conditions are described in Results (sections 3.3 and 6.2/6.3). All reactions were carried out using a Hybaid thermocycler with a typical 100µl reaction mix consisting of 84µl of water, 10µl of 10x PWO buffer, 2µl of stock dNTP's (each at 10mM), 1µl sense primer (1mg/ml), 1µl antisense primer (1mg/ml), plasmid DNA (between 1 and 5 ng/µl), 0.5µl of PWO polymerase. PCR products were purified by gel isolation (2.3.1) prior to further enzyme reactions.

## 2.4 Expression of Recombinant Proteins in *E.coli.*

### 2.4.1 Expression of wild-type SLT-1 holotoxin and SLT fusion proteins

Recombinant SLT fusions were expressed in *Escherichia coli* and purified by globotriose-Sepharose affinity chromatography. A 10ml culture of *E.coli* TG2 harbouring pUC19 plasmid containing SLT gene was grown overnight at 37°C, then used to inoculate 1l of LB media and grown to an optical density of 0.6 (2-3 hours). Expression of SLT was induced by the addition of 1mM isopropyl 1-thio-β–D-galactoside (IPTG) to the culture and incubated for 3 hours at 37°C. Cells were harvested by centrifugation at 700xg for 30 minutes at 4°C and the periplasmic extract collected by osmotic-lysis of the cells. Cell pellets were resuspended in 20ml

tris/sucrose buffer (20% sucrose (w/v), 300mM Tris-HCl pH8.0, 1mM ethylenediaminetetra-acetic acid disodium salt (EDTA), 0.5mM magnesium chloride) and left at room temperature for 10 minutes. Cells were pelleted at 4400xg for 5 minutes at 4°C and resuspended in 10ml 1mM ice-cold Tris-HCl pH7.5. Cells were incubated on ice for 10 minutes then recentrifuged at 17500xg for 15minutes at 4°C. The supernatant periplasm was filter-sterilized and applied to a 1ml globotriose-Sepharose affinity column (refer to 2.5.1).

### 2.4.2 Expression of Ricin A-chain and RTA fusion proteins

The expression of recombinant RTA was carried out exactly as described by Day *et al.*, (1996).

## 2.5 Protein Purification

### 2.5.1 Purification of SLT-1 by Affinity Chromatography

Recombinant holotoxins were purified to homogeneity from *E.coli* by receptor-ligand based chromatography using globotriose (α-D-galactose-(1→ 4)-β-D-galactose-(1→ 4)-β-D-glucose-(1→ )) coupled to a Sepharose matrix. The supernatant containing the *E.coli* periplasmic extract (2.4.1) was applied to a 1ml globotriose-Sepharose affinity chromatography column equilibrated in PBS. The column was washed with 500ml PBS and the SLT-1 eluted with 6M guanidine hydrochloride and collected in 1ml fractions. The absorbance of each fraction was determined at 280nm in a spectrophotometer and the fractions containing protein

were immediately dialysed against PBS, with buffer changes after 6 hours and overnight. The concentration of SLT-1 was determined by spectrophotometry (refer to 2.5.4).

### 2.5.2 Purification of Ricin A-chain by Ion-Exchange Chromatography

Recombinant RTA was purified as described in Day *et al.*, (1996). In addition to the conditions described, various buffers and matrices were used to optimise the purification of RTA fusion proteins, described in Results (section7.5).

### 2.5.3 Reassociation of Ricin A-chain with Ricin B-chain

Typically 50μg of ricin A-chain was mixed with 50μg of ricin B-chain (Inland Labs) or ricin B-chain made from native ricin holotoxin (refer to 2.5.4)in a total volume of 200μl in PBS, by gentle agitation on a tumbler at 4°C for 4 hours. Reassociated holotoxin was then purified from free A-chain by applying to a 0.5ml α-lactose (insolubilized on 6% beaded agarose) column equilibrated with PBS. The holotoxin was loaded onto the column in a final volume of 1ml in PBS and passed through the column a total of 4 times. The column was washed with 5ml PBS and the holotoxin (and free B-chain) eluted with 4ml of 50mM galactose collecting 0.5ml fractions.

### 2.5.4 Preparation of free ricin B-chain

Ricin holotoxin (20mg) in 10mM Tris ph8, 5% β-mercaptoethanol, 0.1M lactose in a total volume of 50ml was stirred overnight at 4°C. The reduced ricin was then loaded onto a 75ml DEAE Sephacel (Pharmacia) column equilibrated in buffer (10mM Tris pH8, 1% β-mercaptoethanol, 0.1M lactose). Free A-chain was washed from the column with 250ml of the same buffer, collecting the wash in 10ml fractions. Ricin B-chain was eluted with a linear 500ml 0.1-0.3 M sodium chloride gradient and the fractions collected analysed by reducing SDS-PAGE.

### 2.5.5 Determination of Protein Concentration

The concentration of recombinant SLT 1 holotoxins (with the exception of SLT-CMa) and ricin A-chains was determined by measurement at 280nm using a Shimadzu UV 160A spectrophotometer. Optical density values at 280nm were converted to protein concentrations from a extinction co-efficient calculated from the formula:

$$\varepsilon_{A280nm} = 12.075x[\text{No. Tyr} + (5x \text{ No. Trp})] / \text{Total No. amino acids.}$$

SLT 1 holotoxin extinction co-efficient = 0.984

Ricin A-chain extinction co-efficient = 0.77

For this formula, the protein concentration calculated from $\varepsilon_{A280nm}$ has been converted to mg/ml.

The concentration of SLT-CMa was determined by scanning densitometry comparisons of the SLT A-chain of known wtSLT holotoxin concentrations (in triplicate), against SLT-CMa after reducing SDS-PAGE and silver staining of samples (refer to 2.5.6). The concentration of this fusion protein was calculated in this way due to the presence of excess B-chain on gels. Assuming the stoichiometry of 1A:5B chains is always correct, the concentration of A-chain is directly proportional to the concentration of holotoxin present as holotoxin is purified by the ability of SLT B-chain to bind to globotriose-Sepharose.

Ricin holotoxins, generated by the association of free RTA with free RTB, were quantified in a similar manner to SLTC-Ma, by ricin A-chain densitometry comparisons of known concentrations of recombinant ricin A-chain. This step is necessary to take account of unassociated ricin B-chain. Reducing SDS-PAGE gels were either silver-stained or coomassie stained and the A-chains quantified on a Molecular Dynamics Computing Densitometer. The concentration of A-chain is directly proportional to the concentration of holotoxin present, as the α-lactose column is washed free of unbound ricin A-chain before the reassociated ricin is eluted.

### 2.5.6 Storage of Recombinant proteins

Recombinant SLT-1 holotoxins and fusion proteins were stored for short periods of time (up to 2 months) in PBS at 4°C or long-term in PBS at -70°C. Recombinant ricin A-chain and fusion proteins were stored long-term at 4°C. Ricin holotoxin and

fusion proteins were routinely stored at 4°C but can be stored at -20°C (in 15% glycerol).

### 2.5.7 SDS-Polyacrylamide gel electrophoresis (SDS-PAGE).

Proteins were routinely separated on 15% polyacrylamide gels described in Sambrook *et al.*, (1989) in reducing or non-reducing conditions where, in the latter, β-mercaptoethanol was omitted from the sample-loading buffer.

Gels were visualised by silver-staining (Merrel *et al.*, 1981) or by Coomassie Brilliant Blue R250 staining (Sambrook *et al.*, 1989).

### 2.5.8 Western Blot Analysis

Protein samples were electrophoresed by SDS-PAGE (2.5.6), then transferred onto a Hybond-C nitrocellulose filter (Amersham) in transfer buffer (25mM Tris, 192 mM glycine, 20% methanol) using a Sigma-Aldrich techware semi-dry blotting system. The blotting apparatus was run at a constant voltage (150V) for 1 hour. The filter was removed to a clean box and blocked with TBS (10mM Tris pH8.0, 150mM sodium chloride) containing 0.1% Tween-20 and 5% dried skimmed milk (TBS-T-M) for 30 minutes with shaking at room temperature. The TBS-T-M was replaced with 40ml of fresh TBS-T-M containing the primary antibody at an appropriate dilution and incubated for 1-4 hours at room temperature. The filter was washed 3

times for 5 minutes with 100ml of TBS-T-M and the secondary antibody conjugated to alkaline phosphatase added to the filter in 20ml of TBS-T-M for 1 hour at room temperature. The filter was washed with TBS-T as before with an additional 3 washes with TBS. The filter was developed by the addition of 33µl of nitroblue tetrazolium (NBT) and 66µl of 5-bromo-1-chloro-3-indolyl phosphate (BCIP) (Promega) in 10ml of alkaline phosphatase buffer (100mM Tris-HCl pH 9.5, 100mM sodium chloride, 5mM magnesium chloride) until staining was complete and the reaction stopped by the addition of 10mM Tris, pH8.0, 5mM EDTA. The filter was dried at room temperature.

## 2.6 *In vitro* Ribosome Inactivation assay

All solutions used in the preparation or treatment of ribosomes and RNA were kept as RNase-free as possible. Equipment (polycarbonate tubes, glass rods, gel tanks) was soaked in 0.1M sodium hydroxide overnight and rinsed with distilled water. Polycarbonate tubes and glass rods were baked before use.

### 2.6.1 Preparation of Rabbit Reticulocyte Ribosomes

1ml of non-nuclease-treated rabbit reticulocyte lysate (Promega) was carefully layered on 1ml of an ice-cold 1M sucrose pad in 1x ENDO buffer (25 mM Tris, pH7.6, 25mM potassium chloride, 5mM magnesium chloride) in a 3ml TL-100 thick-walled polycarbonate tube. This was centrifuged at 412,000 xg (100 000 rpm) in a Beckman TL-100 ultracentrifuge (using a TL-100 rotor) for 45 minutes at 4°C. The supernatant was carefully removed allowing the sucrose pad to be poured away

and the ribosome pellet gently washed twice with 1ml of ice cold 1xENDO by adding the 1xENDO and immediately pouring off. The pellet was gently resuspended in 1ml 1xENDO with a glass rod and recentrifuged as before. The pellet was washed with 1xENDO as previously and resuspended in 100µl final volume ensuring the glass rod is washed free of ribosomes. The concentration of ribosomes was calculated by measuring the optical density of a diluted sample at 280nm using the formula that 1mg/ml of ribosomes is equivalent to 12.5 $OD_{260nm}$ units. Ribosomes were stored in aliquots at -70°C.

### 2.6.2 Nicking of SLT-1 furin-sensitive site prior to incubation with ribosomes.

Before SLT-1 was incubated with ribosomes, the furin-sensitive site located between SLTA1 and A2 was cleaved with trypsin to release the catalytic A1 subunit from A2. Various trypsin concentrations and incubation times were tested with SLT-1 (see results) to ensure 100% cleavage of the site, visualized on reducing SDS-PAGE by a single A-chain band the size of A1 (26KDa).

Sequencing grade trypsin (Boehringer Mannheim) was added at 0.5µg/ml in PBS to 2µg of SLT-1 in a final volume of 10µl then incubated for 1 hour at 37°C. The reaction was stopped by the addition of 1µl of 10mg/ml PMSF in isopropanol and the nicked SLT-1 stored at 4°C until required.

### 2.6.3 Toxin incubation with ribosomes, extraction and aniline-cleavage of depurinated RNA.

Endo and Tsurugi (1988) first described the N-glycosidase activity of SLT-1 and ricin to remove a specific adenine residue from a highly conserved stem-loop region of yeast and mammalian RNA which can be visualized by aniline treatment and the subsequent cleavage of a fragment of rRNA. This method was modified by May *et al.* (1989).

A range of nicked SLT-1 (2.6.2) and ricin dilutions were mixed with 30µg of rabbit reticulocyte ribosomes (2.6.1) in 1x ENDO buffer to a final volume of 20µl (6mM β-mercaptoethanol was added to the SLT-1 samples to reduce the disulphide bridge and release the catalytic A1 subunit) then incubated for 30 minutes at 30°C. Reactions were stopped by the addition of 180µl of 1% SDS. The samples were then phenol/chloroform extracted 3 times before RNA precipitation with ice-cold, 0.1 volumes of 7M ammonium acetate and 2 volumes of absolute ethanol on dry-ice for 15 minutes (2.2.1). The RNA was pelleted, washed by the addition of 70% ethanol, dried under vacuum and resuspended in 20µl of water.

The concentration of RNA was determined by measuring the optical density at 260nm of a diluted sample of each reaction (1.0 $OD_{260nm}$ = 40µg/ml of rRNA). To 3 µg of modified RNA , 20µl of 1M acetic aniline, pH4.5 was added and incubated for 2 minutes at 60°C followed by the addition of 0.1 volumes of ammonium sulphate and 2 volumes of absolute ethanol. The rRNA samples were precipitated as before and the dried pellets resuspended in 20µl of 60% deionized formamide in 0.1x TPE (3.6mM Tris, 3mM sodium dihydrogen phosphate dihydrate, 0.1mM EDTA, pH8) .

Non-aniline treated rRNA controls containing 3µg rRNA were diluted to 20µl with 60% deioninzed formamide/0.1x TPE. The samples were incubated at 65°C for 5 minutes before the addition of 4µl of RNA sample buffer (50% glycerol, 0.1xTPE, 0.05% bromophenol blue). The rRNA samples were resolved on denaturing formamide-agarose gels (2.6.4).

The N-glycosidase activity of the toxins was quantified by measuring the densities of the resolved 28S rRNA reticulocyte ribosomes and 390-ribonucleotide fragment, released upon treatment with aniline. RNA was visualised under U.V., photographed with Polaroid black and white and the negative quantified by a Molecular Dynamics Computing Densitometer. Alternatively northern blot analysis of the RNA was carried out (Methods, 2.6.6), for quantification by a Molecular Dynamics Phosphorimager. The percentage depurination (toxin activity) of the reticulocyte ribosomes was determined by dividing the density of the aniline fragment by the combined densities of the aniline fragment plus the 28S rRNA and multiplying by 100.

### 2.6.4 Extraction of RNA from SLT-1 treated HeLa cells

Typically, 1.5 ml of HeLa cells were plated in flat bottomed 6-well plates at $2.5x10^5$ cells/ml and treated overnight with various concentrations of SLT-1. The cells were washed 3 times with PBS and then dissolved in 0.5ml denaturing buffer (6M guanidine hydrochloride, 20mM MES [4-morpholineethan-sulfonic acid] pH7.0, 20mM EDTA, 50mM β-mercaptoethanol [added just before use]) by incubating at

room temperature for 5 minutes. The cell suspension was then removed to an eppendorf tube and extracted twice with phenol/chloroform (2.2.1) and precipitated with 0.1 volumes of 7M ammonium acetate and 2.5 volumes of absolute ethanol on dry ice for 30 minutes. The RNA was pelleted by centrifugation at 8000xg for 15 minutes at 4°C, washed with 70% ethanol and dried. The pellet was resuspended in 1x DNase buffer (50mM Tris-HCl pH7.5, 1mM magnesium chloride) to a final volume of 100µl and 15 units RNase-free DNase (Gibco BRL) added for 30 minutes on ice. The RNA was phenol/chloroform extracted and precipitated as before and resuspended in 10µl sterile distilled water.

### 2.6.5 Separation of RNA by Formamide-Agarose Gel Electrophoresis

The rRNA samples were loaded onto horizontal denaturing formamide gels (1.2% RNase-free agarose, 50% deionized formamide, 0.1xTPE) and electrophoresed, without submerging, in 0.1x TPE at 24mA until the sample buffer had run half-way across the gel. The gel was stained in 500ml water containing 50µl of 10mg/ml ethidium bromide, shaking for 30 minutes at room temperature, before destaining in water for at least 15 minutes. The RNA was visualised under UV and photographed with Polaroid black and white, positive/negative film.

### 2.6.6 Northern blot analysis

Northern blot analysis was used to visualize the 400 ribonucleotide RNA species produced by cleavage of modified rRNA upon aniline treatment by probing with an

oligonucleotide complementary to the 3' region of rabbit reticulocyte 28S rRNA (with the base sequence 5'CAT AAT CCC ACA GAT GG 3').

Following separation of rRNA on denaturing formamide gels (2.6.5), the gel was then washed in 500ml of 50mM sodium hydroxide for 20 minutes followed by 500ml of 20xSSC (3M sodium chloride, 0.3M tri-sodium citrate pH7) for 45 minutes. The rRNA was then transferred from the gel onto a nitro-cellulose membrane (Hybond-N, Amersham), pre-soaked in 20x SSC, using a vacuum blotting system (Vacugene, Pharmacia) referring to the manufacturer's instructions. The rRNA was transferred for 1 hour after which the membrane was rinsed in 6xSSC and air dried. The transferred rRNA was cross-linked to the membrane using a Stratagene UV Stratalinker.

The oligonucleotide was labelled by phosphorylation using T4 DNA kinase. In a final volume of 20µl, 50pmol of oligonucleotide was incubated with 20µCi of [$^{32}$P]-γ-ATP in 1x kinase reaction buffer (70mM Tris pH 7.6, 10mM magnesium chloride, 5mM DTT) with 1µl of T4 polynucleotide kinase (Gibco BRL) at 37°C for 45 minutes, then at 70°C for 10 minutes. The phosphorylated oligonucleotide was precipitated with 10µl of 3mg/ml sonicated salmon sperm DNA (Pharmacia), 0.1 volumes of 7M ammonium acetate and 2.5 volumes absolute ethanol for 30 minutes on dry ice, then pelleted by centrifugation at 8000g for 30 minutes. The pellet was washed in 70% ethanol and allowed to air dry. The dried pellet was resuspended in 300µl water and used immediately for hybridization.

The membrane cross-linked with rRNA was soaked in hybridisation buffer (6xSSC, 0.3% SDS, 5x Denhardt's reagent [made as a 50x stock: 10mg/ml Ficoll 400, 10mg/ml polyvinylpyrrolidone, 10mg/ml BSA]) before being pre-hybridized by incubation with 10ml of hybridisation buffer containing 30µl of 3mg/ml heat-denatured sonicated salmon sperm DNA for 2 hours at 37°C in a hybridisation bottle placed in a rotating oven (Hybaid). The buffer was then discarded and 10ml of fresh hybridisation buffer containing the phosphorylated oligonucleotide (passed through a DynaGard filter) was added and incubated overnight at 37°C. The buffer containing oligonucleotide was discarded and the membrane washed with 100ml of 2xSSC for 30 minutes at 37°C in the oven. The membrane was wrapped in Clingfilm and placed in a phosphorimager cassette for quantification by a Molecular Dynamics Phosphorimager or exposed to RX X-ray film with an intensifying screen overnight at -70°C.

## 2.7 Cytotoxicity Assay

Cytotoxicity comparison of wt and D167SLT-peptide chimeras against HeLa A2.1 cells and wtSLT against SK-mel-29. Cell were plated in flat bottomed 96-well plates ($1.5*10^4$ cells per well) and left to adhere overnight at 37°C. The cells were then washed with PBS and the toxin dilutions added in RPMI (5% FCS) in a total volume of 150µl per well. Cells were then incubated for 16hrs at 37°C. Cells were washed with PBS and labelled with $^{35}$S-Methionine (1µCi (3000Ci/mmol) per well) for 2 hours. Labelled proteins were then precipitated by washing the cells 3 times with 5% trichloroacetic acid and washing the cells once with PBS. Protein synthesis

was measured by the incorporation of $^{35}$S-Methionine in cells and a percentage calculated in relation to toxin-free control cells from 4 replicate dilution samples.

## 2.8 $^{51}$Cr-release Cytotoxic -T- lymphocyte Assay

HeLa A2 cells were challenged with D167SLT-Ma chimeras (20ng/ml) overnight. The cells were then washed and $^{51}$Cr- labelled (50μCi/million cells) for 1hr at 37°C. Cells were then plated with CTLs at 5:1 and 2:1 effector/target ratios and incubated for 4 hrs at 37°C before $^{51}$Cr-release counting. HeLa-A2 cells were treated with γ-interferon (100U/ml) for 48 hrs before challenging with toxin. Control HeLa-A2 cells were infected with 5 plaque forming units (pfu)/cell of vaccinia-encoded influenza Matrix (M1) for 90 minutes and allowed to express influenza Matrix protein overnight prior to $^{51}$Cr-labelling or infected with the vaccinia at the same time as $^{51}$Cr-labelling. If the latter was the case, cells were incubated with M1 vaccinia and $^{51}$Chromium (50μCi/million cells) for 90 minutes at 37°C, washed and incubated for a further 3 hours at 37°C to allow expression of influenza Matrix protein Cells were treated with lactacystin (100μM in water) for 1 hr and then incubated overnight at a final concentration of 1μM lactacystin in RPMI medium. The lactacystin was washed off the cells with the toxin prior to $^{51}$Cr-labelling. Influenza matrix peptide (0.1μM) was plated with control $^{51}$Cr-labelled HeLa A2.1 cells and CTLs.

# Chapter 3

# The construction of expression plasmids for E167D SLT and SLT-Ma fusions proteins.

## 3.1 Introduction

In order that target cells were not destroyed in the process of peptide delivery, an active site mutant of SLT-1 (glutamate 167 to aspartate; E167D) was prepared by oligonucleotide-directed T7 polymerase mutagenesis. The activity of E167D SLT-1, purified to homogeneity from *E.coli* by receptor-ligand based chromatography, was assessed by *in vitro* ribosome-inactivation assays and *in vivo* cytotoxicity comparisons with wild-type SLT-1 (see Chapter 4).

The ability of SLT-1 to deliver antigenic peptides to class-1 MHC molecules was tested by placing a peptide at the C-terminus and N-terminus of the SLT A-chain. The possible advantage of placing the peptide at the C-terminus of the A-chain was that it left the restricted anchor residue at the C-terminus of the epitope free access to the class-1 MHC groove after B-chain dissociation in the ER lumen. A possible disadvantage of placing the peptide at the C-terminus of the SLT A-chain is that it is not known whether the A2 fragment of the chain is translocated into the cytosol. If this is the case, the epitope would not be available for cytosolic processing by proteasomes. The association between the C-terminus of SLT A-chain and the B pentamer may also make the epitope inaccessible for processing within the ER. By contrast, the N-terminus of the SLT A-chain is sterically unhindered by the presence of the B-chain.

Influenza matrix peptide 58-66 (Ma, GILGFVFTL-single letter code) was chosen as the epitope for the SLT fusion since an HLA-A2.1 stably transfected HeLa cell-line was available to us along with Matrix 58-66-specific CTL. In particular, influenza Matrix peptide consists predominantly of hydrophobic amino-acyl residues and may be more stable when placed at the C-terminus of the SLT A-chain compared to a charged epitope such as influenza Nucleoprotein 366-374 (ASNENMDAM). This is due to the position of the C-terminal end of the SLT A-chain when associated with the B-chain pentamer. The C-terminus of the A subunit, consisting of a helical segment of hydrophobic residues penetrates the pore formed by the B-chain pentameric ring (Fraser *et al.*, 1994). Thus a hydrophobic peptide placed at the C-terminus of the SLT A-chain may be better tolerated.

Approximately 2000Å of the A subunit is buried by the B pentamer (Fraser *et al.*,1994), a result of the contact between the C-terminal helix and the B subunits. The positioning of a peptide at the end of the A-chain may therefore potentially disrupt the non-covalent association between the A-chain and B pentamer.

To ensure that the presence of the peptide did not interfere with normal trafficking of the toxin moiety, M58-66 was also conjugated to the wild type toxin.

## 3.2 Construction of plasmid E167D SLT

M13 wtSLT DNA was mutated using a Sculptor T7-polymerase mutagenesis kit (see Methods, 2.2.4). This protocol is summarised in Figure 3.1. The mutated M13 DNA was then cut with the restriction enzymes *EcoR*1 and *Pst*1 consecutively to release a 1.3 Kb fragment containing the entire bicistronic operon. This was ligated into the SLT expression vector PUC19 that had been digested similarly and dephosphorylated with calf alkaline intestine phosphatase (CIP). The entire SLT insert was sequenced using 8 sequencing primers spanning the SLT sequence and forward/reverse vector primers.

## 3.3 Construction of SLT-Ma expression plasmids.

DNA coding for the influenza Matrix peptide 58-66 (GILGFVFTL) was genetically fused with the 5'- or 3'-terminus of DNA encoding the catalytic A-chain of SLT by mutagenic PCR. The was performed by a two-step PCR strategy. The first step is the amplification of two DNA products in separate reactions. Two primers were designed, one that contains a sequence complementary to the sense genomic sequence and the other a non-complementary sequence, both primers also encoding for the Ma peptide. The two DNA products (one 1Kbp and the other 300bp) are complementary in the region encoding Ma. In the second step of the PCR, the two DNA products are annealed together and end-filled by PWO polymerase alone. The annealed DNA is then amplified by the addition of M13 PCR primers resulting in a 1.5Kbp PCR product which can be digested and ligated back into the expression

*Figure 3.1 Construction of pE167DSLT*

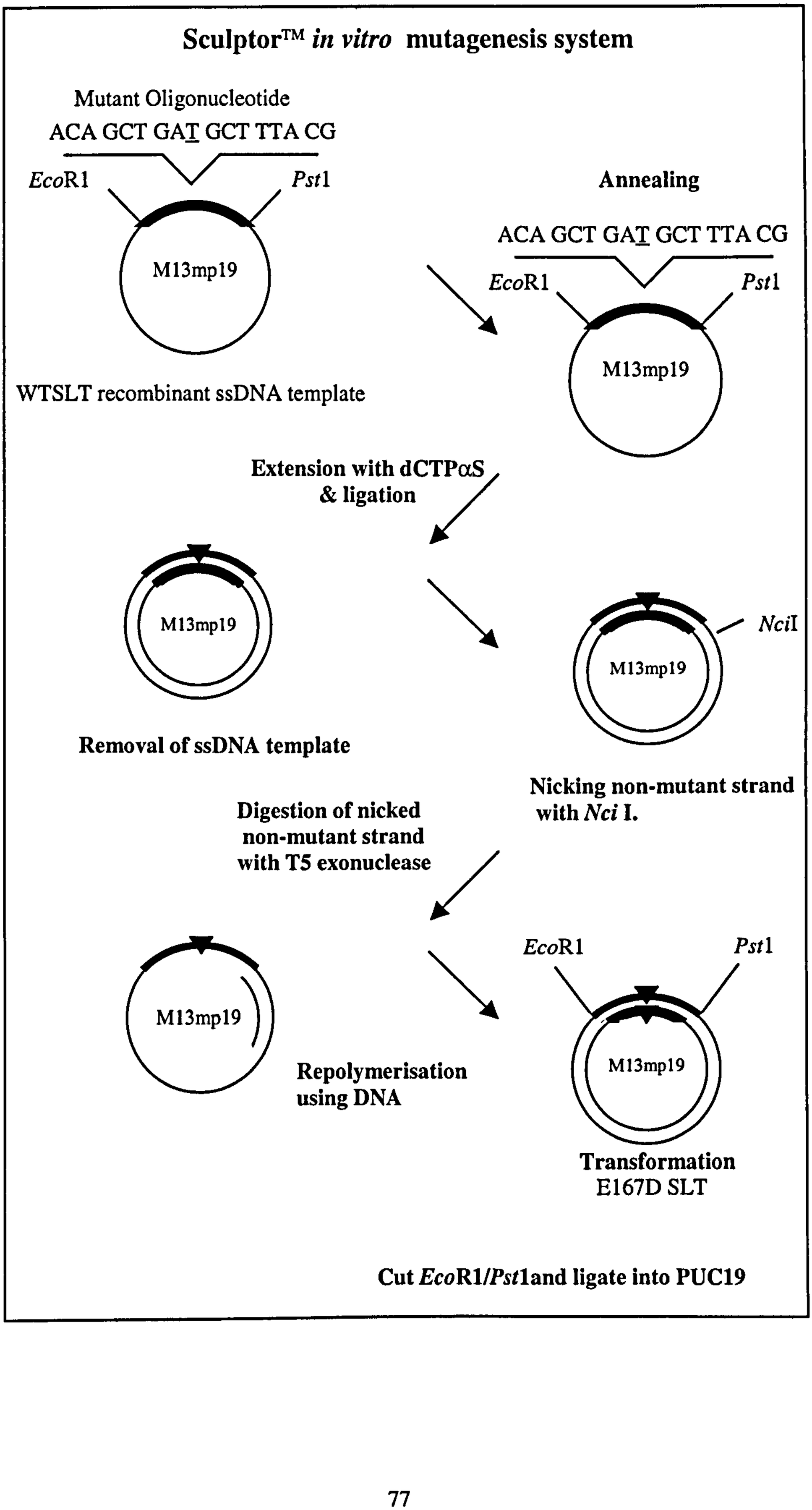

vector. The PCR strategies for SLT-Ma construction are detailed in Figure 3.2 and Figure 3.3. The PCR conditions are shown below in table 3.1.

| | Hot start 94°C | denaturing 94°C | Annealing Variable | Extension * 72°C |
|---|---|---|---|---|
| SLTC-Ma reaction 1 | | 30 s | 1 min 63°C | 1 min |
| SLTC-Ma Reaction 2 | | 30 s | 1 min 63°C | 1 min |
| SLTC-Ma Reaction 3 | 1 min | 30 s | 1 min 45°C | 1 min |
| | (add primers) | 30 s | 1 min 55°C | 1 ½ min |
| SLTN-Ma Reaction 1 | | 30 s | 1 min 65°C | 1 min |
| SLTN-Ma Reaction 2 | | 30 s | 1 min 65°C | 1 min |
| SLTN-Ma Reaction 3 | 1 min | 30 s | 1 min 45°C | 1 min |
| | (add primers) | 30 s | 1 min 55°C | 1 ½ min |

* all reactions were concluded with a 7 min incubation at 72°C to allow full extension.

**Table 3.1** ***PCR conditions for the construction of pSLTC-Ma and pSLTN-Ma.***

PCR reactions were typically carried out in a total volume of 50µl or 100µl (see Methods, 2.2.7) using a Hybaid thermocycler. The products of reactions 1 and 2 (amplified by 30 cycles of PCR) were gel purified (see section 2.3.1) and approximately 1 ng of each DNA used in reaction 3. Reaction 3 consisted of 10 cycles of PCR in the presence of PWO (0.5µl) alone followed by the addition of M13 vector primers and extra PWO (0.5µl) for 30 cycles.

The product of reaction 3 was digested with *Pst*1 and *Eco*R1 and ligated into PUC19 (see Methods, 2.3.1).

## *Figure 3.2 Construction of SLT N-Ma by 2-stage mutagenic PCR*

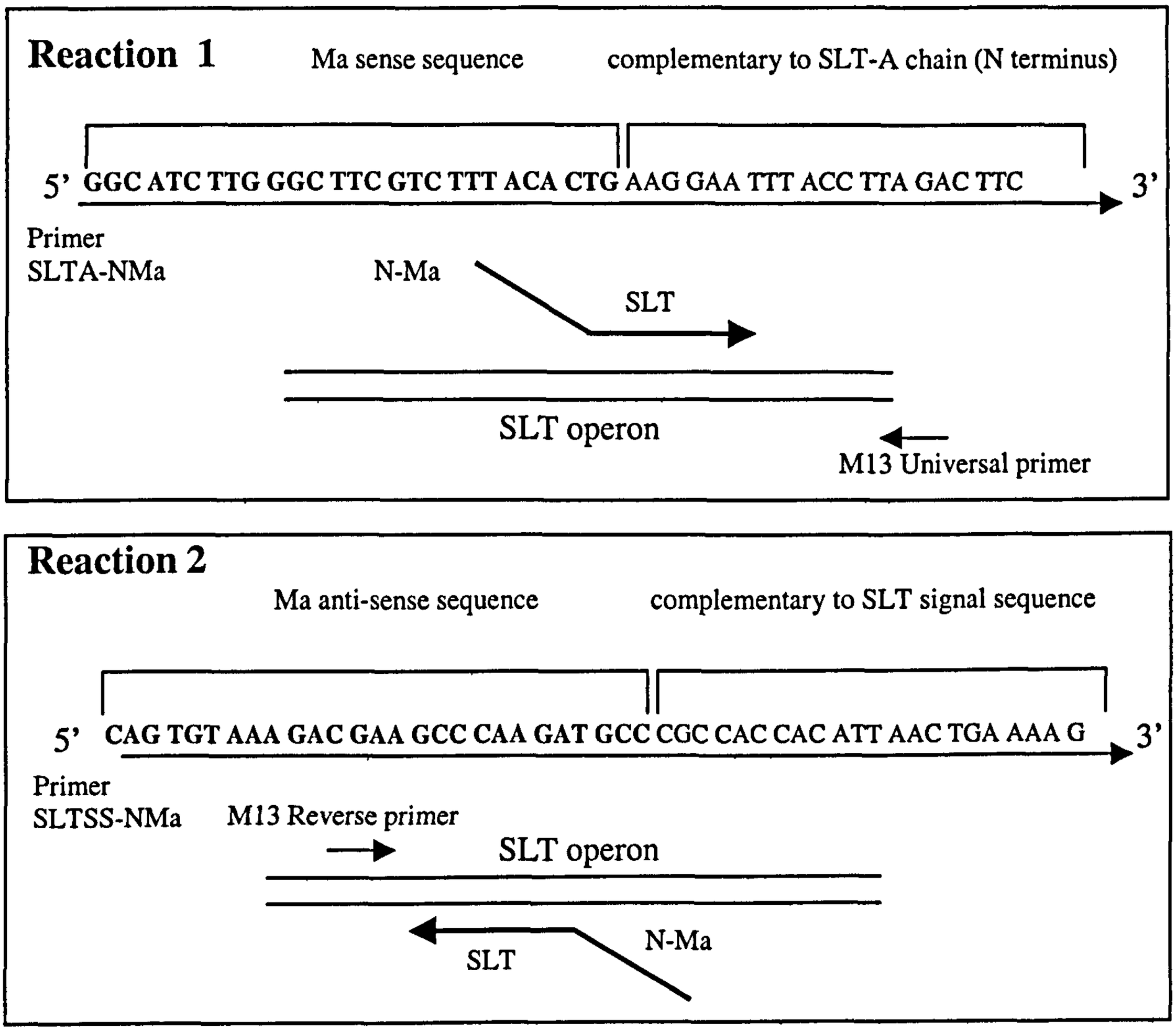

## *Figure 3.3 Construction of SLT C-Ma by 2-stage mutagenic PCR*

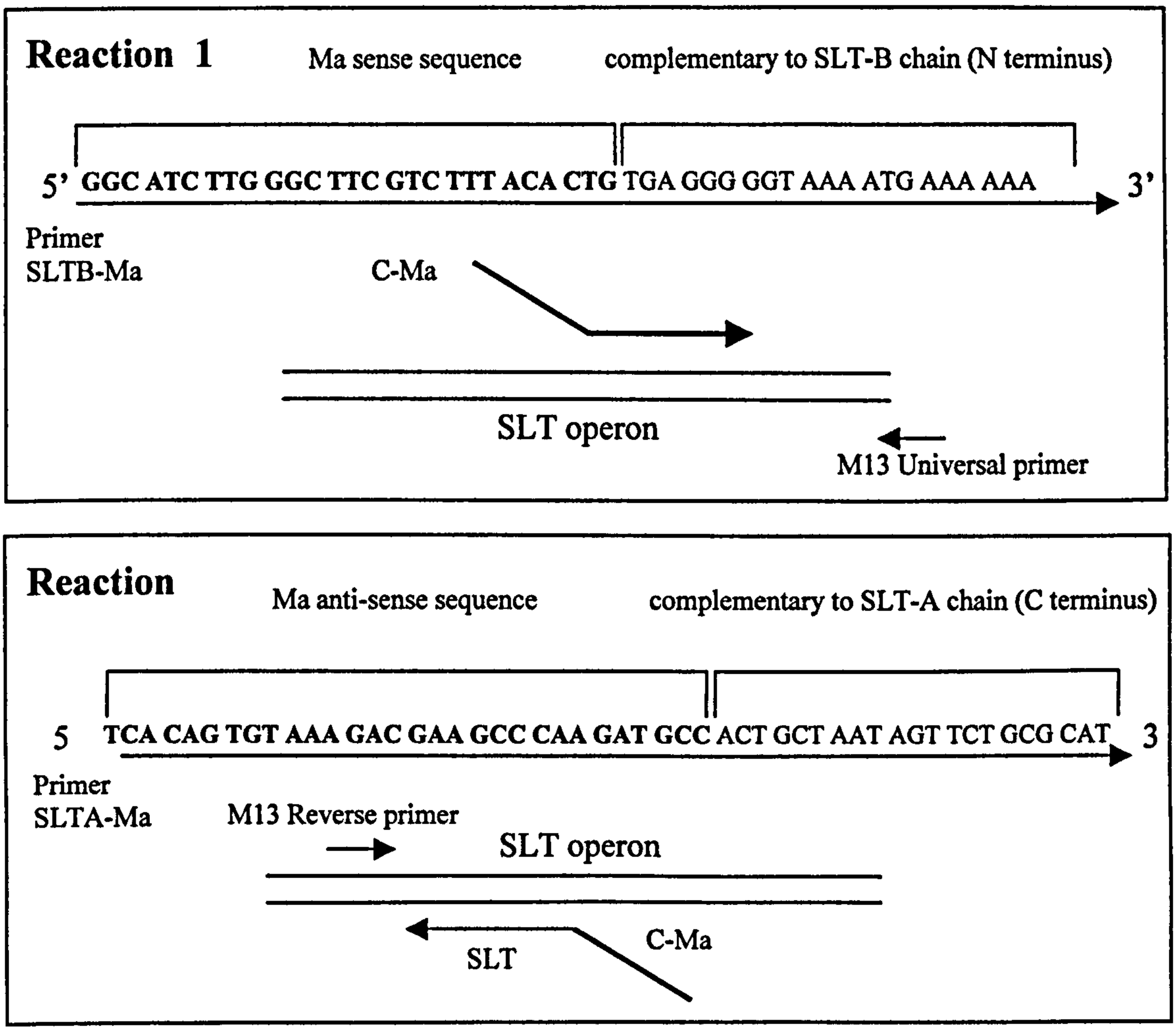

# CHAPTER 4

# THE ACTIVITY ASSESSMENT OF E167D SLT-1 AND CONSTRUCTION OF SLT-1 FUSION PROTEINS

# Chapter 4

# The activity assessment of E167D SLT-1 and construction of SLT-1 fusion proteins.

## 4.1 Introduction

The SLT constructs made were all expressed from the vector pUC19 where expression can be driven by the *lac Z* promoter. The pUC19 expression plasmids contain the full length bicistronic operon for SLT, encoding both the SLT A-chain and B-chain and its associated Shine-Dalgarno and periplasmic targeting sequences. The recombinant protein is targeted to the periplasmic space as this allows the association of A and B chains and disulphide bond formation in a compartment analogous to that in naturally producing strains of *E.coli*.

All manipulations involving pUC19 SLT in the wild-type background must be carried out under category III biological containment conditions as the plasmid contains a holotoxin gene under the control of a strong promoter that constitutively expresses the gene at low levels.

Reassociated SLT was purified by its affinity for globotriose ceramide, the carbohydrate moiety of the SLT-binding receptor. Globotriose ceramide was chemically synthesised and coupled to Sepharose by the laboratory of Professor David Crout (Warwick). This matrix has a high affinity for SLT, binding wild-type holotoxin at approximately 1mg/ml of matrix.

The activity of E167D SLT, purified to homogeneity from *E.coli* by receptor-ligand based chromatography, was assessed by *in vitro* ribosome-inactivation assays and *in vivo* cytotoxicity comparisons with wild-type SLT. This mutant SLT was previously reported to cause a 1000-fold reduction in activity as measured by the ability of crude SLT-containing *E.coli* periplasmic extracts to inhibit protein synthesis by rabbit reticulocyte lysate (Hovde *et al.*, 1988).

## 4.2 Preparation of E167DSLT

E167D SLT was expressed and purified as for wtSLT (refer to Methods, 2.4.1 and 2.5.1). The substitution of glutamate 167 to aspartate had no affect on the level of expression of SLT in TG2 *E.coli* cells and E167D SLT was directed to the periplasm in a soluble form in the same way as wtSLT. E167DSLT was purified to homogeneity by receptor-ligand based chromatography using globotriose coupled to a Sepharose matrix and visualised on 15% reducing- SDS-PAGE gels (Fig 4.1). The concentration of SLT was calculated by optical density measurement at 280nm and using the extinction coefficient, $\varepsilon = 0.984$ (Methods, 2.5.4).

## 4.3 Nicking of SLT-1 furin-sensitive site to release catalytic A1 subunit.

Before activity comparisons between E167DSLT and wtSLT could be made by direct assays on mammalian ribosomes *in vitro*, the catalytic A1 subunit had to be released from A2 which partially blocks the active site and therefore reduces N-glycosidase activity. In the standard protocol of this laboratory, SLT is nicked with 0.1μg/ml sequencing grade trypsin (Boehringer Mannheim) for 7 minutes. Early

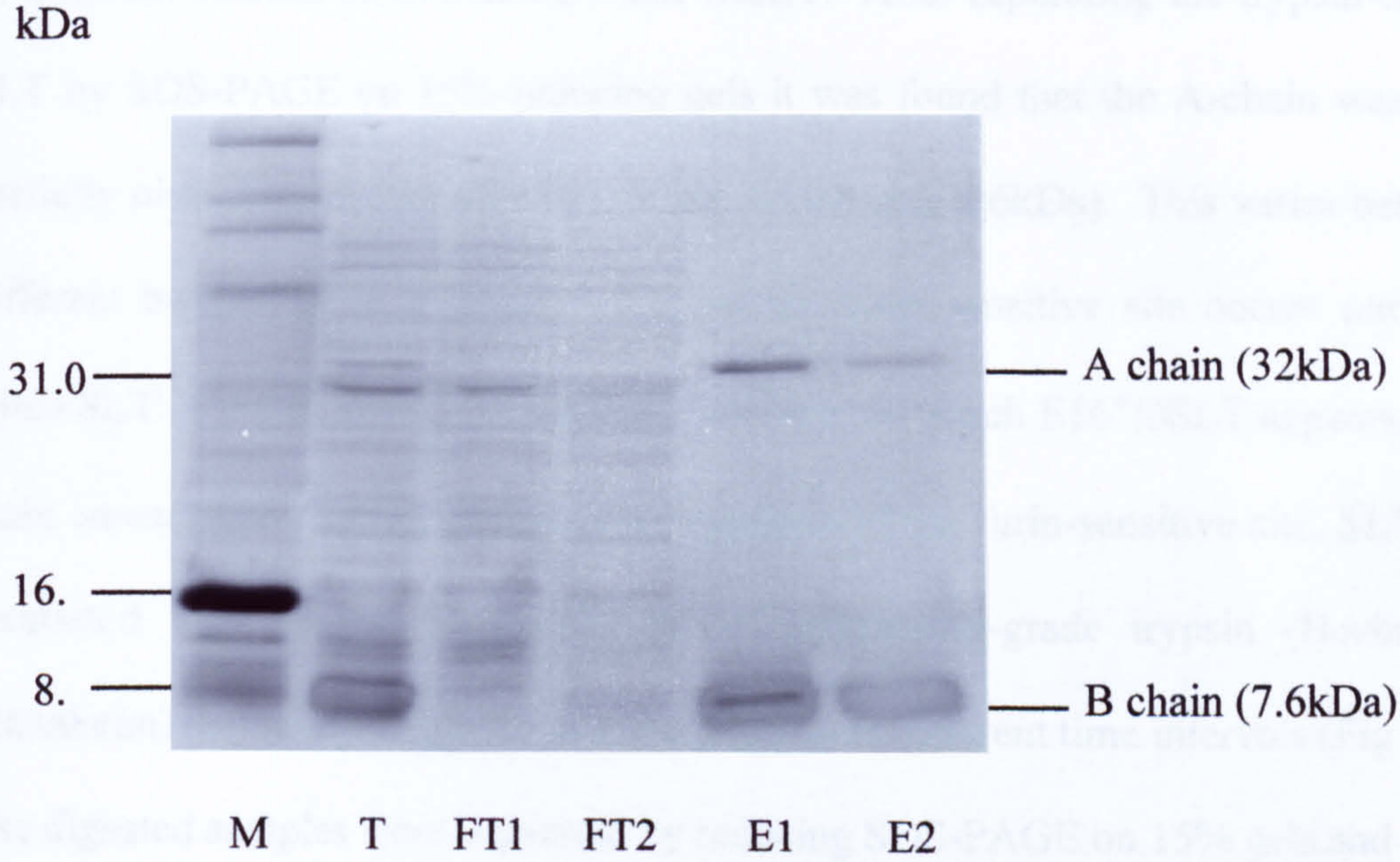


***Figure 4.1 Expression and purification of E167D SLT***

E167D SLT was expressed in IPTG induced *Escherichia coli* TG2 cells harbouring pUC19 containing the SLT1 bicistronic operon for 3 hours. Cells were harvested and osmotically lysed to release assembled E167DSLT oligomers. The resulting high speed supernatant was filter sterilized and applied to a 1ml globotriose-Sepharose affinity column equilibrated in PBS. E167DSLT was subsequently eluted with 6M guanidine hydrochloride, dialysed against PBS and selected samples analysed by reducing 15% SDS-PAGE gels. T refers to a sample of total *E.coli* extract, FT refers to a sample of column flow through, E refers to eluted E167DSLT fractions; SLT A and B chains are labelled (M, molecular weight markers).

ribosome-inactivation assays indicated a degree of discrepancy between the activity of different batches of E167D SLT and wtSLT. After separating the trypsin-treated SLT by SDS-PAGE on 15% reducing gels it was found that the A-chain was only partially nicked resulting in the loss of the A2 subunit (26kDa). This varies between different batches of SLT as processing of the furin sensitive site occurs naturally when SLT is stored at 4°C over a period of time, of which E167DSLT appears to be more susceptible. To ensure complete digestion of the furin-sensitive site, SLT was incubated with various concentrations of sequencing-grade trypsin (Boehringer Mannheim) and analytical grade trypsin (Sigma) at different time intervals (Fig 4.2). The digested samples were separated by reducing SDS-PAGE on 15% gels and silver-stained. Complete cleavage of the furin-sensitive site is visualised by the loss of the full size SLT A-chain (32kDa) and the appearance of the SLT A1 fragment. Figure 4.2 shows that digestion is complete after a 1 hour incubation with 5µg/ml trypsin. If the concentration of trypsin used or the incubation time is reduced, a full size A-chain band can still be visualised on a reducing gel by silver-staining.

## 4.4 *In Vitro* ribosome inactivation assays

The $ID_{50}$ of wtSLT is the concentration of toxin which depurinates 50% of ribosomes. The $ID_{50}$ of wtSLT is typically 100pg/µl, when incubated with rabbit reticulocyte ribosomes (20-30µg) for 30 minutes at 30°C. No depurination of rabbit reticulocyte ribosomes was visualised on aniline gels for E167DSLT over a range of toxin concentration 25ng/µl-0.5ng/µl, over the same range an aniline fragment is seen with wtSLT. In order to make a comparison with wtSLT and the catalytic mutant the toxin range was increased to 75/µl-5ng/µl and the incubation period

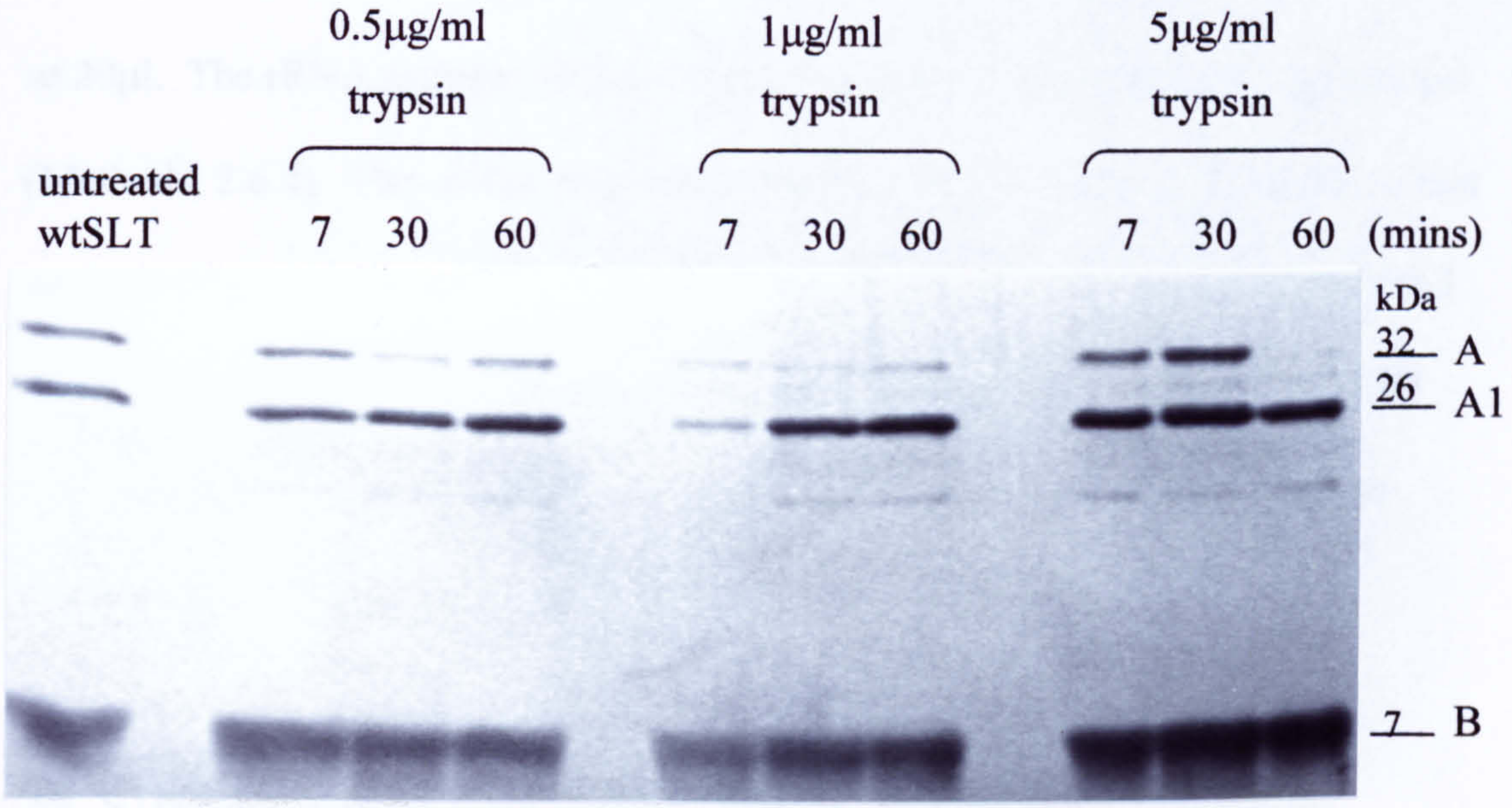


***Figure 4.2 Digestion of wtSLT at 37°C, over various time intervals and concentrations of trypsin***

wtSLT samples (1μg) in 20μl of PBS were incubated at 37°C for 7 minutes, 30 minutes or 1 hour with various concentrations of sequencing grade trypsin (Boehringer Mannheim). The reaction was stopped by the addition of 1μl of 10mg/ml PMSF in isopropanol. The samples were separated on 15% reducing SDS-PAGE gels and silver-stained. SLT A, A1 and B chains are labelled. Complete cleavage of the site is visualised by the loss of the full size SLT A-chain. Digestion is complete after a 1 hour incubation with 5μg/ml Trypsin.

increased to 45 minutes or 1 hour. After 1 hour at 30°C the reticulocyte ribosomes were found to be degraded so a 45-minute incubation period was used to calculate the decrease in activity of E167DSLT compared to wtSLT. Ribosomes were treated with 25ng/μl-25pg/μl of wtSLT and 50ng/μl-50pg/μl of D167SLT in a total volume of 20μl. The rRNA samples were resolved on a denaturing formamide-agarose gel (Methods, 2.6.4). The aniline fragments generated were visualised by northern blot analysis (Fig 4.3). The aniline fragments were then quantified by image-quant and percentage depurination calculated for the samples (Fig 4.4). The $ID_{50}$ of E167D SLT was calculated to be 10000pg/μl, a 100 fold decrease in *in vitro* ribosome depurination activity compared to wtSLT.

## 4.5 Cytotoxicity comparisons of E167D SLT with wtSLT

HeLa-A2 cells were plated into 96-well tissue culture plates and allowed to adhere overnight at 37°C. This was followed by the addition of dilutions of toxin, further incubation and the labelling of cells with $^{35}$S-Methionine (described in Methods, 2.7). The typical $IC_{50}$ of wtSLT (the concentration of toxin at which protein synthesis is 50% that of untreated cells), tested on standard HeLa cells is 0.01 ng/ml and for ricin is 0.1ng/ml. When tested on the stably transfected HLA-A2 HeLa cell line the IC50 was found to be the same for wtSLT but the cells were less susceptible to ricin having an $IC_{50}$ of 5 ng/ml after overnight incubation with ricin compared to an IC50 of 0.4ng/ml for standard HeLa cells in the assay of figure 4.5. These HeLa may be of a different subtype or have altered galactosylation owing to the transfection of HLA-A2 DNA. The $IC_{50}$ of E167D SLT was calculated to be 100ng/ml compared to 0.1ng/ml for wtSLT (for the assay shown in figure 4.6), representing a 1000 fold loss in *in vivo* activity.

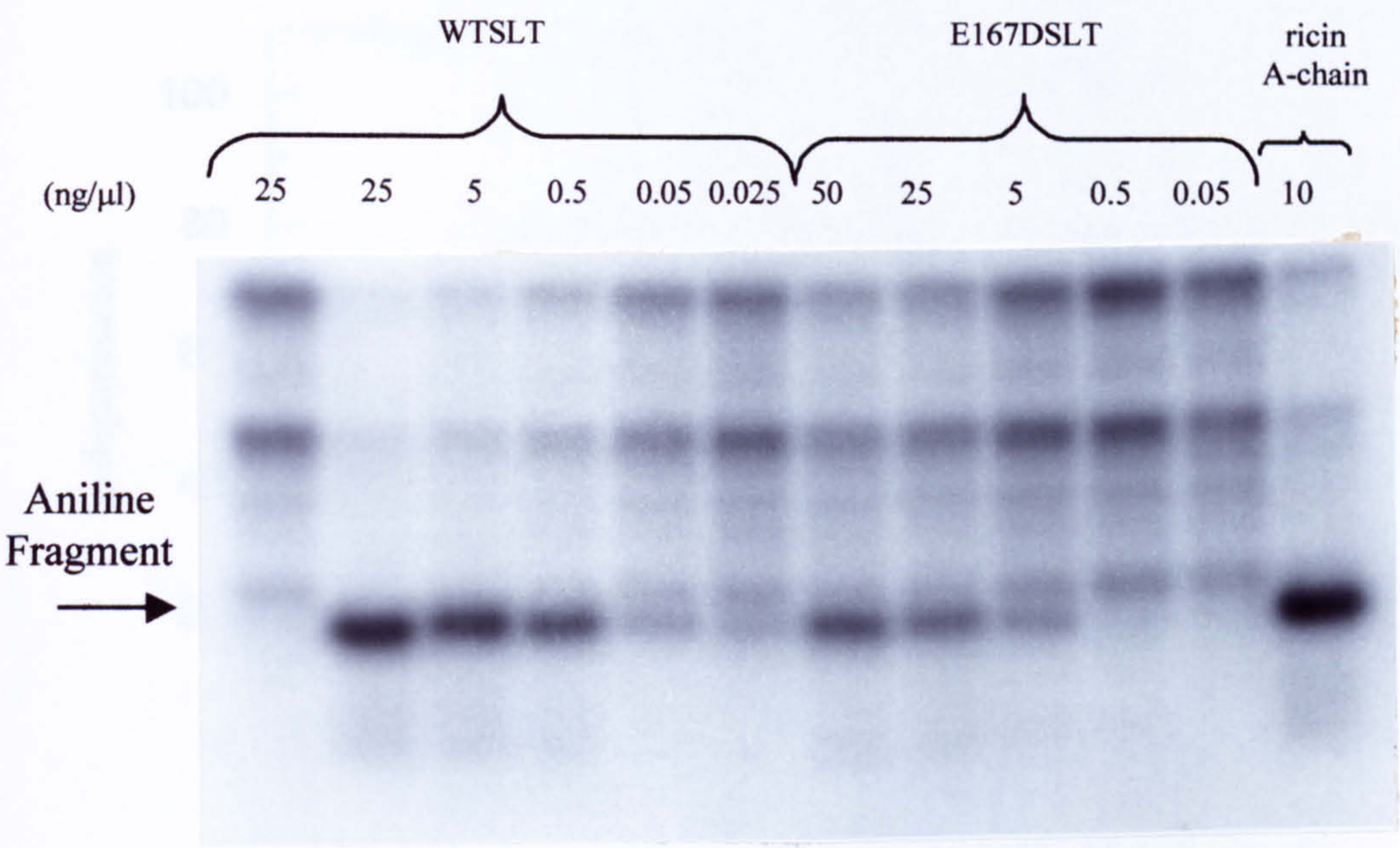


***Fig.4.3 Northern blot analysis of ribosome depurination activity of E167D SLT and wtSLT.***

Rabbit reticulocyte ribosomes (were incubated for 45 minutes with various concentrations of wtSLT and E167DSLT (given in ng/μg) and subsequently treated with acetic-aniline as described in methods. The rRNA samples (2.5μg of each) were resolved on a denaturing formamide-agarose gel and northern blot analysis was used to visualize the 400 ribonucleotide species ('Aniline Fragment') produced by the cleavage of modified rRNA. The aniline fragments were quantified by Image-quant™ and a percentage depurination calculated (Fig4.4). NA refers to rRNA from sample 1 ( 25ng/μl wtSLT) not treated with acetic-aniline.

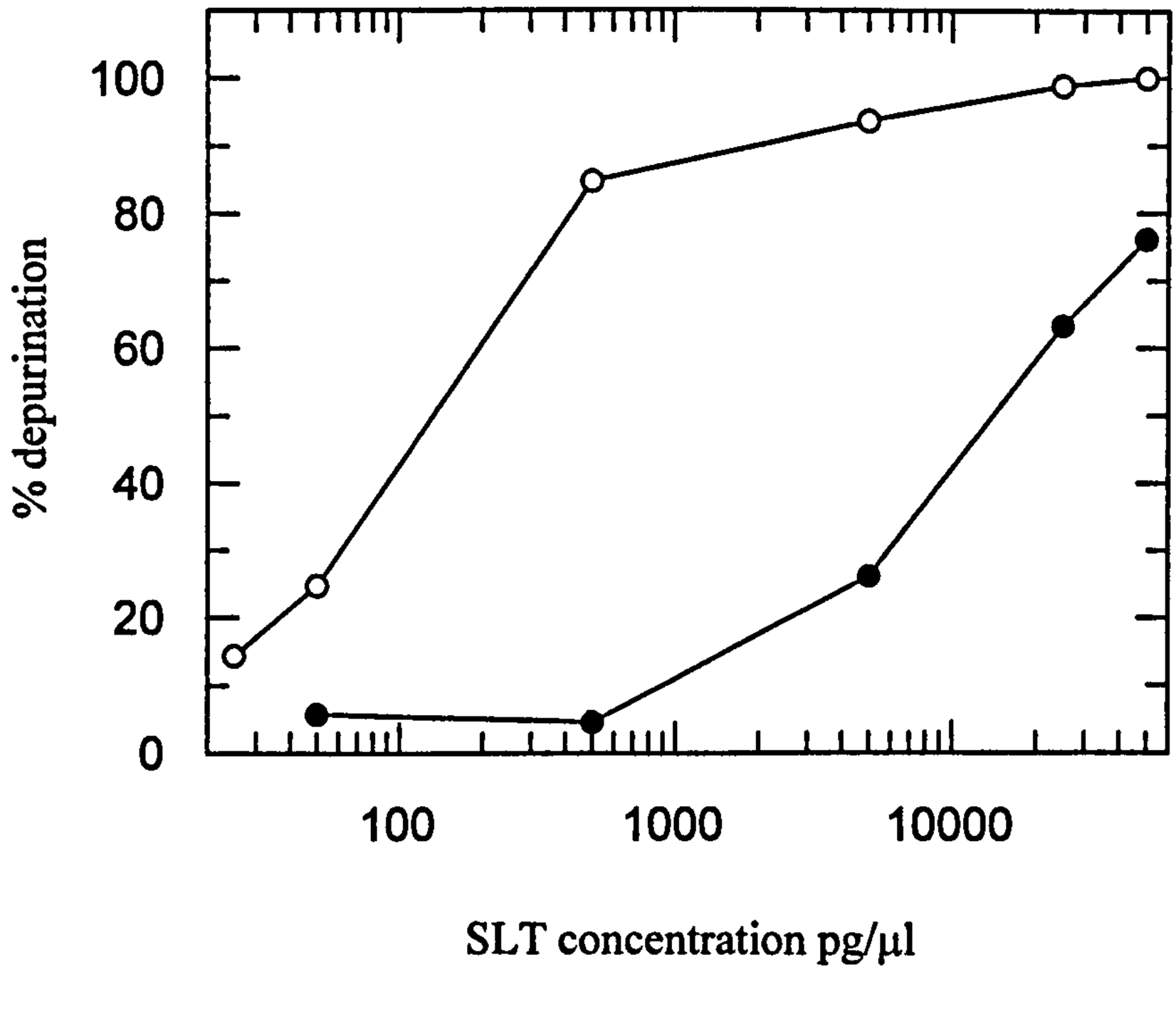


***Fig 4.4 Quantification of the depurination of rabbit reticulocyte ribosomes by wtSLT and E167D SLT.***

Comparison of the percentage depurination of rabbit reticulocyte ribosomes byWTSLT ( o ) and E167DSLT ( ● ). Depurination values were determined by the optical density measurements, using Image Quant, of aniline fragments and 28S ribosomes from Fig 4.3 (see Methods, 2.6.3 for calculation).

The $ID_{50}$ values, the concentration of toxin where 50% of ribosomes are depurinated, were calculated as: WTSLT=100pg/µl  E167DSLT=10000pg/µl

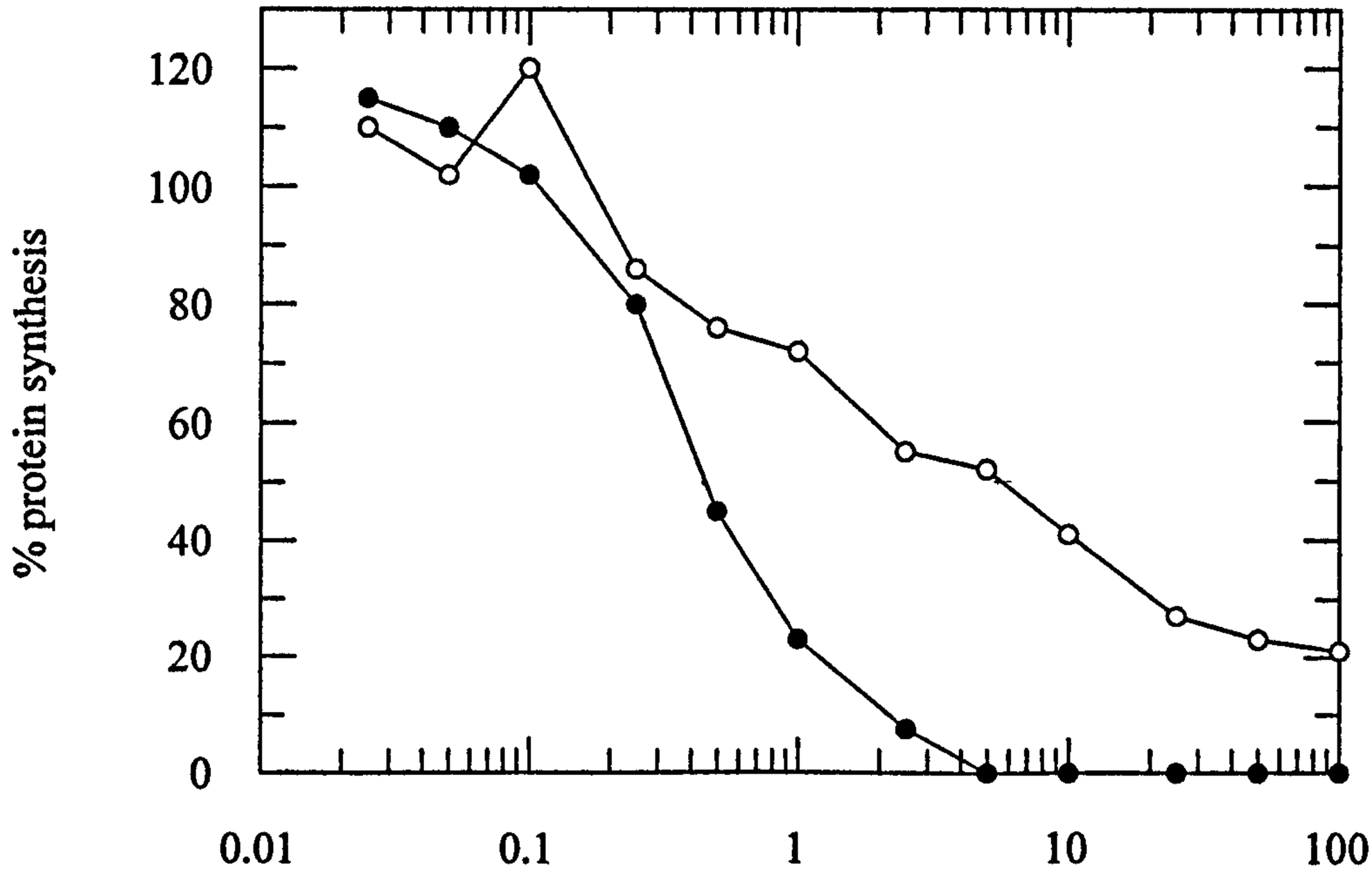


*Fig 4.5 Cytotoxicity of ricin on HeLa cells and HLA-A2 transformed HeLa cells*

Cells were incubated with various concentrations of ricin for 6 hours at 37°C before [$^{35}$S]-Methionine labelling and protein precipitation with 5% TCA. Protein synthesis was measured by the incorporation of [$^{35}$S]-Met into protein and a percentage calculated in relation to toxin-free cells. HeLa cells ● , HLA-A2 transformed HeLa cells ○ .

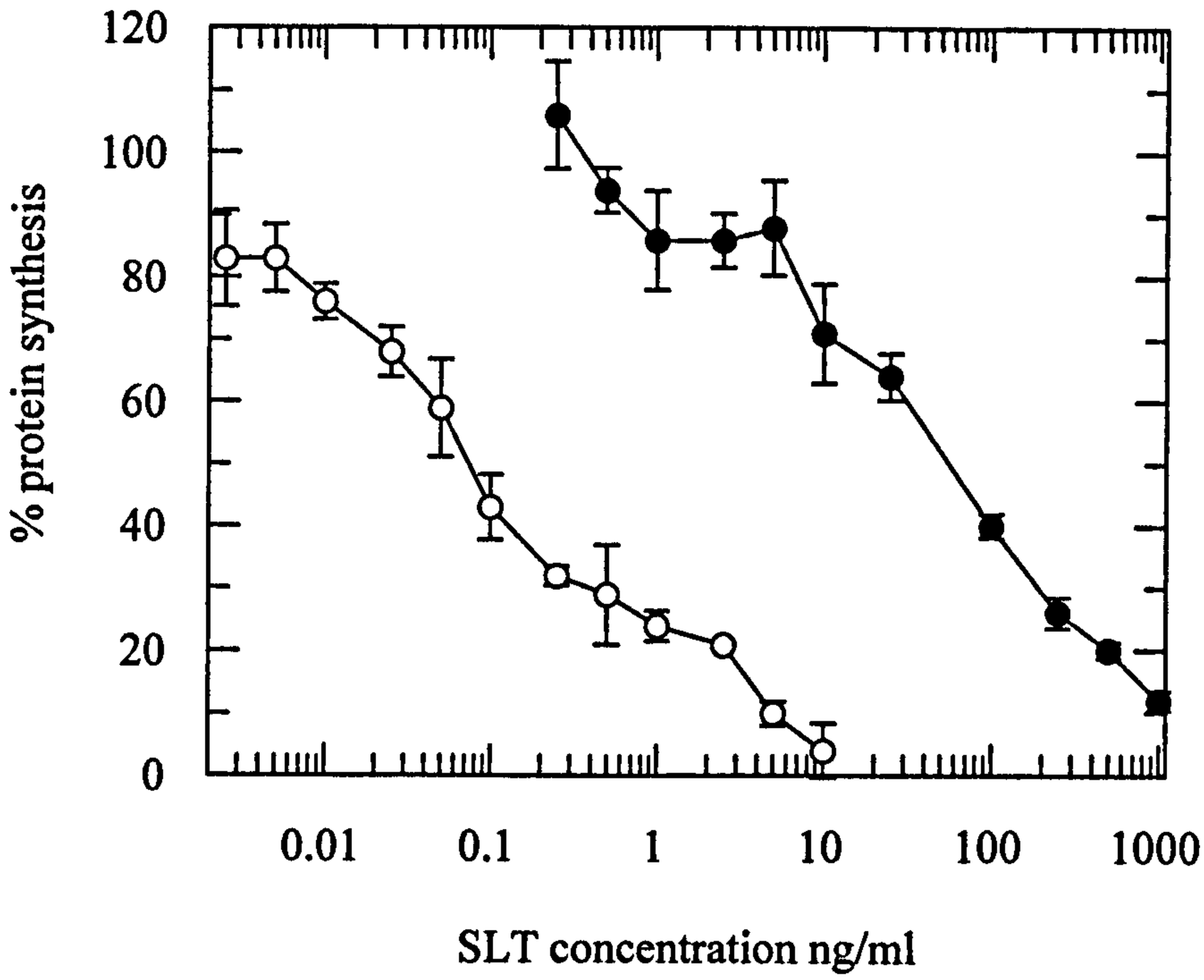


***Figure 4.6 Cytotoxicity of E167D SLT compared to wtSLT***

Cytotoxicity of wtSLT( o ) and E167 DSLT ( ● ) towards HeLa-A2 cells. Cells were incubated with various concentrations of SLT proteins, in quadruplicate, for 16 hours at 37°C before adding [$^{35}$S]-Methionine (1μCi/well) and incubating for a further 2 hours. Cell proteins were precipitated by washing with 5% trichloroacetic acid and radioactivity measured by liquid scintillation counting. Protein synthesis was measured by the incorporation of [$^{35}$S]-Methionine into protein and a percentage calculated in relation to toxin-free control cells. Values shown are the means of quadruplicate determinations and the error bars represent one standard deviation from the mean.

## 4.6 Extraction of E167DSLT treated HeLa ribosomes

To confirm that E167D SLT is able to be endocytosed by HeLa-A2 cells, given its low level of cytotoxicity, ribosomes were isolated from toxin treated HeLa-A2 cells using a guanidine hydrochloride method that instantly denatures SLT during cell lysis. Ribosomes were examined for SLT-specific modification by performing aniline assays (Fig4.7).

## 4.7 Expression of SLT-Ma fusion proteins

The Ma peptide fusion proteins, in both native and E167DSLT backgrounds, were expressed and purified using a protocol as for wtSLT (Methods, 2.2) (Figure4.8). The presence of the influenza matrix peptide in both fusions decreased the level of expression 2-3 fold. Expression at 30°C, which lowers the rate of protein folding and often increases the level of expression, did not alter the amount of SLT-Ma produced suggesting the problem may be one of protein stability. Expression in minimal medium was also tried in an attempt to permit a short burst of SLT fusion production. Low levels of lactose are present in rich LB medium resulting in premature induction of transcription from the *lac*Z promoter and early production of SLT. The use of minimal medium means that SLT is only expressed when transcription is switched on by the deliberate introduction of the gratuitous inducer IPTG once the cells have reached an optical density of 0.6 at 600nm. This strict control of SLT-Ma expression did not alter the amount of Ma fusion proteins produced.

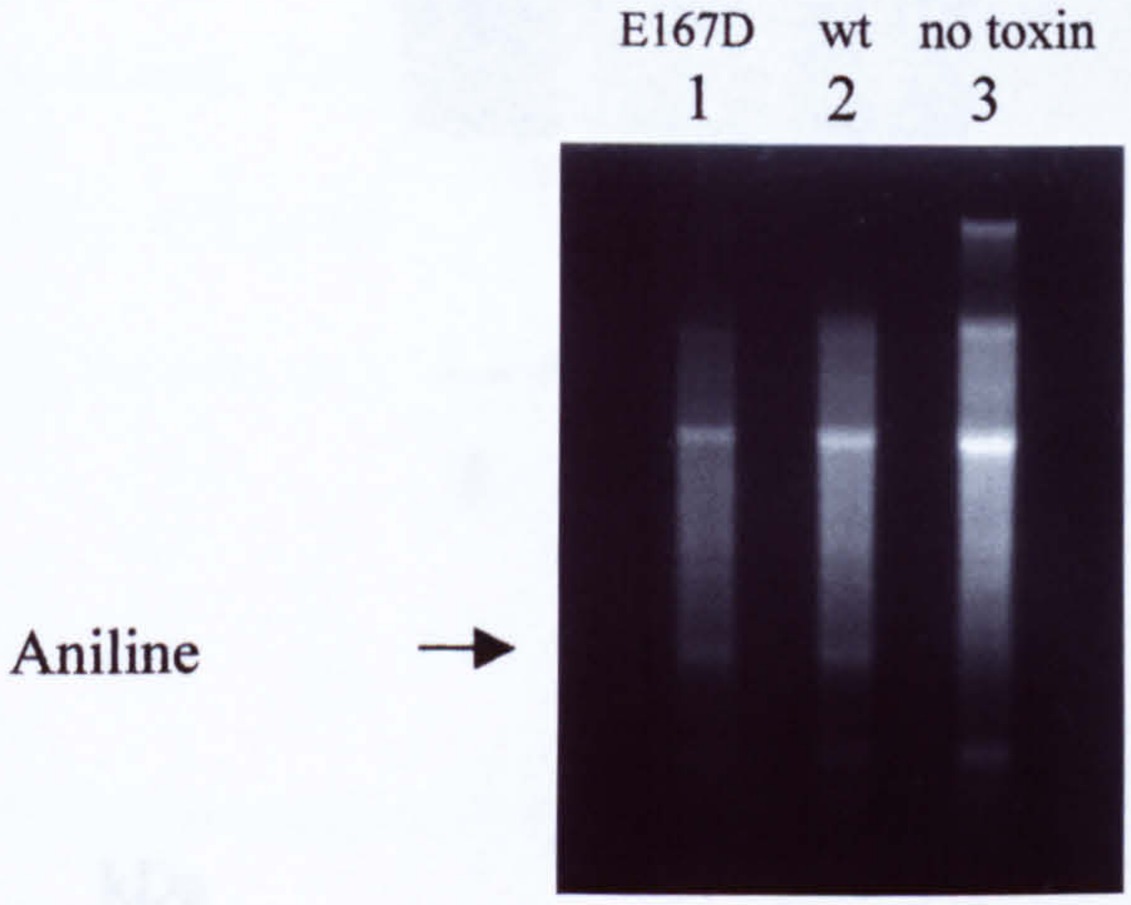


***Figure 4.7 Denaturing gel analysis of aniline treated rRNA from intoxicated HeLa-A2 cells.***

HeLa-A2 cells were incubated with 0.05ng/ml wtSLT (1), 100ng.ml E167D SLT (2) or without toxin (3) at 37°C overnight. In all cases cells were dissolved in 6M guanidine hydrochloride, 20mM Mes pH7, 20mM EDTA, 50mM β-mercaptoethanol for 5 minutes at room temperature and the RNA precipitated, treated with DNase and reprecipitated as described in methods. Extracted RNA was subjected to acetic-aniline treatment as previously described and the rRNA resolved on denaturing formamide-agarose gels.

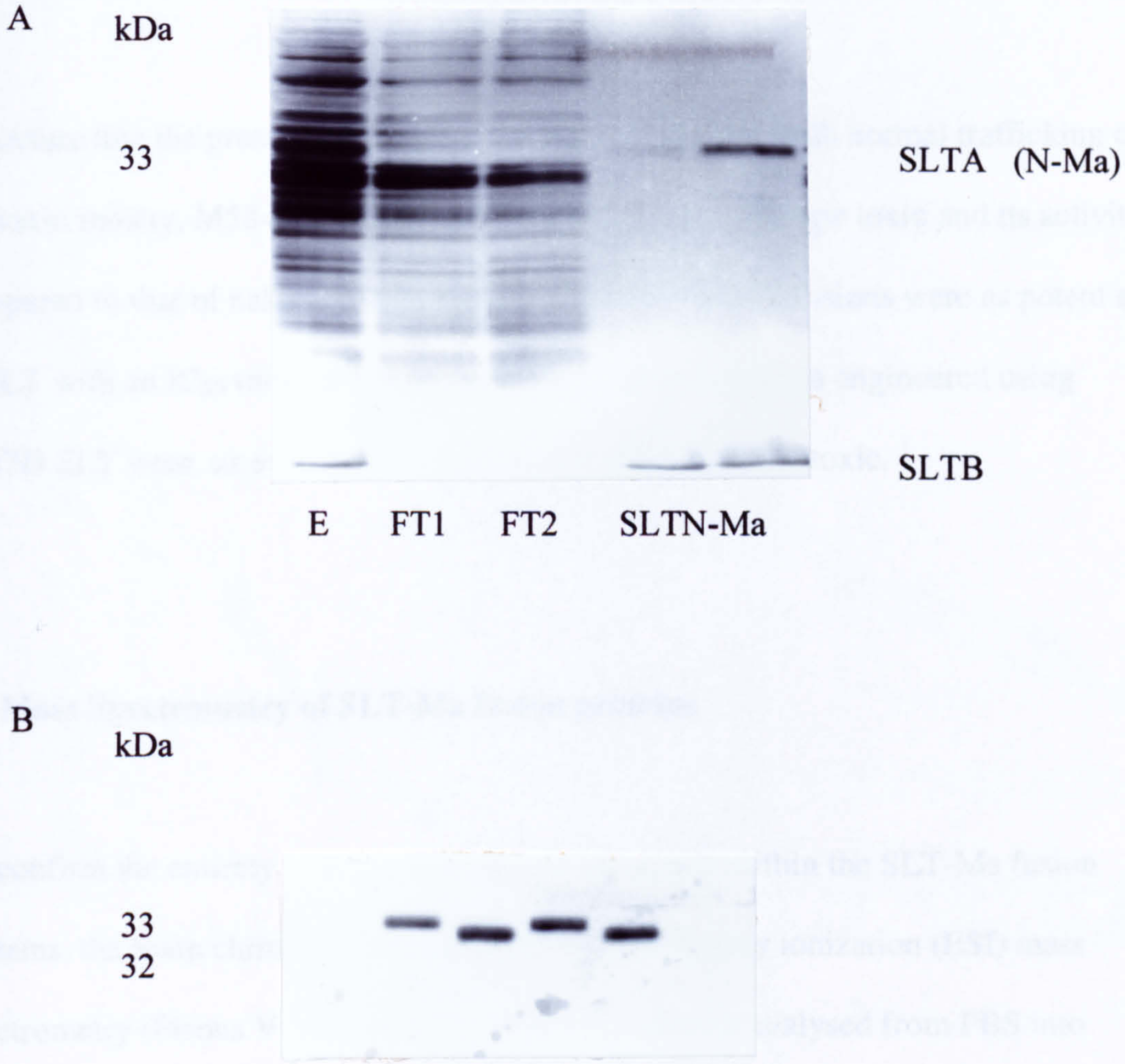


***Figure 4.8 SDS-PAGE of purified SLT-Ma fusion proteins***

A)Recombinant SLT fusions were expressed on IPTG induction of *Escherichia coli* TG2 cells harbouring pUC19 containing the SLT1 bicistronic operon for 3 hours. Cells were harvested and osmotically lysed to release assembled E167D SLT oligomers. The resulting high speed supernatant was filter sterilized and applied to a 1ml globotriose-Sepharose affinity column equilibrated in PBS. SLT-Ma was subsequently eluted with 6M guanidine hydrochloride, dialysed against PBS and selected samples analysed by reducing 15% SDS-PAGE. T refers to a sample of total *E.coli* extract, FT refers to a sample of column flow through, E refers to eluted E167DSLT fractions; SLT A, A1 and B chains are labelled. B) Reducing SDS-PAGE to compare the apparent molecular weights of SLT N-Ma and SLT C-Ma A-chains with native SLT A-chain.

## 4.8 Cytotoxicity of SLT-Ma fusion proteins

To ensure that the presence of the peptide did not interfere with normal trafficking of the toxin moiety, M58-66 was genetically fused to the wild type toxin and its activity compared to that of naked wtSLT (Figure 4.9). The wtSLT fusions were as potent as wtSLT with an $IC_{50}$ value of 0.01ng/ml. The peptide chimeras engineered using E167D SLT were, as expected, approximately 1000 fold less toxic.

## 4.9 Mass Spectrometry of SLT-Ma fusion proteins

To confirm the entirety of the influenza Matrix peptide within the SLT-Ma fusion proteins, the toxin chimeras were analysed by electrospray ionization (ESI) mass spectrometry (Fisons VG Quattro-II). The samples were dialysed from PBS into 2mM ammonium bicarbonate and their mass determined . The predicted molecular mass of SLT A and B chain is 32199.47 and 7688.66 Da respectively The predicted molecular mass of the peptide containing A chains is 33148.58 Da. The presence of the full influenza Matrix nonamer in both constructs was confirmed with molecular masses of 33148.47 +/- 0.31 and 33148.08 +/- 2.83 Da for SLT N-Ma and C-Ma respectively when the fusion proteins were purified in the presence of a protease inhibitor cocktail (Boehringer Mannheim). Degradation products were observed when toxin was purified in the absence of protease inhibitors with a value of 32543.27 +/- 0.06.for SLT C-Ma and 32117.86 +/-1.07 for SLT N-Ma. This loss in mass could not be accounted for and did not represent residues lost from the Ma peptide.

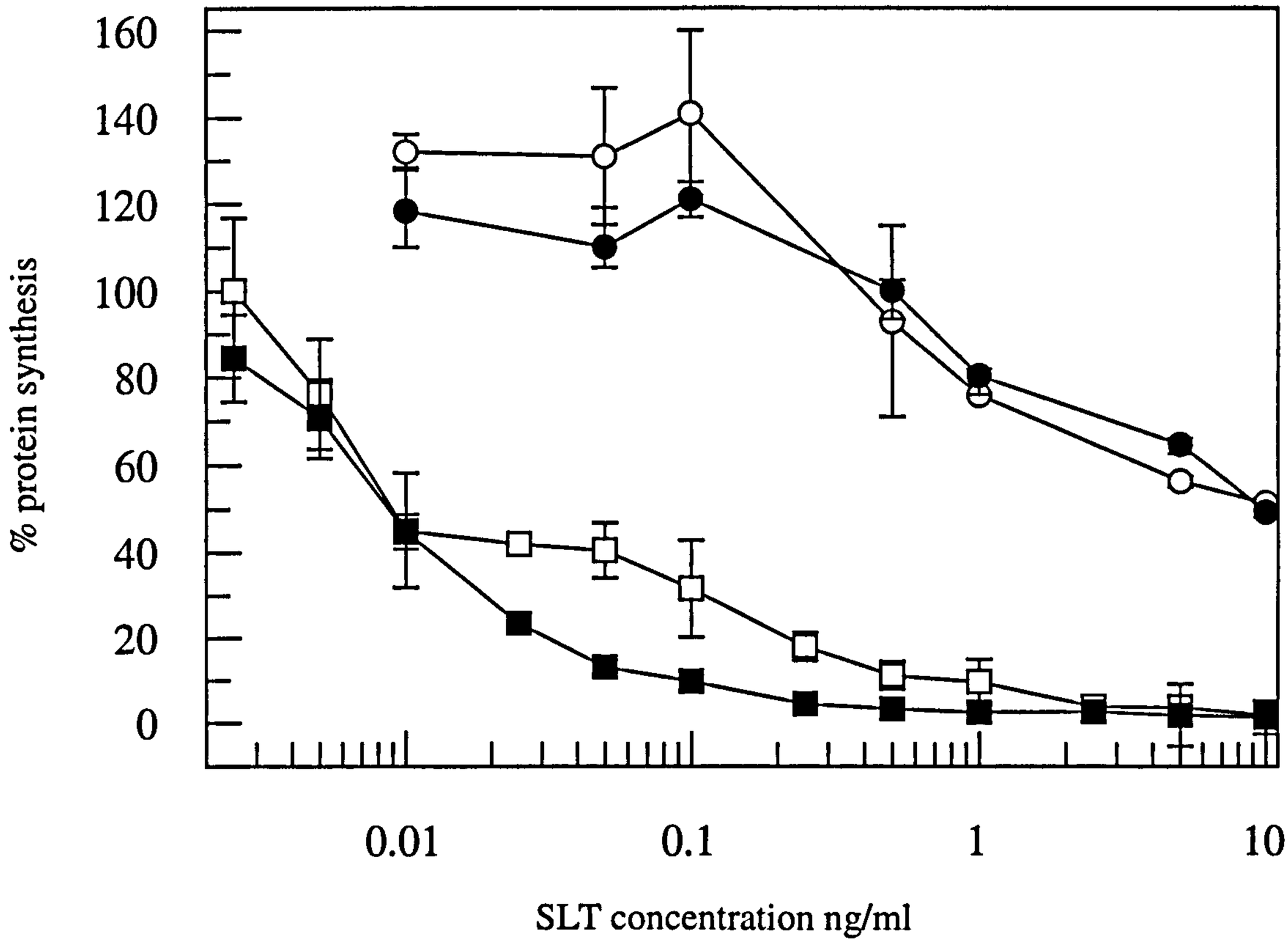


***Figure 4.9 Cytotoxicity of wild-type and E167D SLT-Ma chimeras to HeLa-A2cells***

Cytotoxicity comparison of wild-type and E167D SLT-Ma chimeras against HeLa-A2 cells. Toxins are represented by: wtSLT N-Ma ( ■ ), wtSLT C-Ma ( □ ), E167DSLT N-Ma ( ● ) and E167DSLT C-Ma ( o ). Cells were incubated with various concentrations of SLT proteins, in quadruplicate, for 16 hours at 37°C before pulse labelling with [$^{35}$S]-Methionine, cell lysis and scintillation counting (as described in Methods). Protein synthesis was measured by the incorporation of [$^{35}$S]-Met into protein and a percentage calculated in relation to toxin-free control cells.

# CHAPTER 5

# THE DELIVERY OF INFLUENZA MATRIX PEPTIDE INTO THE MHC CLASS 1 PATHWAY BY E167D SLT

# Chapter 5

# The delivery of influenza matrix peptide into the MHC class 1 pathway by E167D SLT.

## 5.1 Introduction

The *in vitro* ability of the engineered SLT fusion proteins to deliver influenza matrix peptide to MHC class 1 molecules was tested by pulsing HeLa-A2 target cells with toxin and then mixing with Matrix 58-66-matched CTL. Sensitisation to lysis by the SLT fusion proteins was quantified by loading the target cells with radioactive $^{51}$Chromium and measuring its release in sensitised cells. The expression of HLA-A2 MHC class 1 molecules by the stably transfected HeLa cells was confirmed by FACS analysis. Appropriate controls were carried out to demonstrate that the HeLa-A2 cells were capable of processing and presenting intracellular antigens. To confirm that intracellular proteases rather than serum proteases generated the M56-66 epitope, a cell-line resistant to SLT was used as alternative target cells.

The mode of transport and processing of the SLT fusion proteins were also studied by pre-treating HeLa-A2 cells with brefeldin-A or lactacystin, before challenging with the toxin constructs. The cellular affects of these agents are described in the Introduction (sections 1.3.2.4 and 1.6.1). HeLa cells were found to be deficient in processing epitopes for presentation and the MHC class-1 processing machinery was enhanced by pre-treatment of HeLa cells with interferon-γ. Over 200 genes are presently known to be upregulated by IFN-γ, some of these have direct effects on the MHC class 1 processing pathway (detailed in Introduction, section 1.6.6). Others may generally increase the overall trafficking in cells, potentially having an affect on

the cytotoxicity of toxins taking advantage of a retrograde transport pathway from endosomes via the trans-Golgi network to the ER.

## 5.2 HeLa-A2 transfected cells express HLA-A2 MHC class 1 molecules.

To confirm that the HeLa cells transfected with HLA-A2 DNA were expressing A2 MHC class-1 molecules, FACS analysis was carried out on the cells. An A2-positive B cell-line and standard HeLa cells were used as positive and negative controls respectively. Cells were stained with an HLA-A2 mouse monoclonal antibody and a FAB-specific FITC secondary antibody. A muscle-specific primary antibody was used as a control for non-specific staining and secondary antibody-only stains also carried out (Figure 5.1). FACS analysis confirmed that the HeLa-A2 cells were expressing HLA-A2 class 1 molecules and showed a 10-fold increase in fluorescence compared to standard HeLa cells.

## 5.3 Ability of SLT fusion proteins to deliver exogenous antigen into the MHC class 1 presentation pathway.

To demonstrate that HeLa-A2 cells were capable of processing and presenting intracellular antigens, two positive controls were performed. HeLa-A2 cells were infected with vaccinia virus encoding full length influenza Matrix protein at the same time as $^{51}$Cr-labelling of the cells. In other assays HeLa-A2s were mixed with free Ma peptide (2μM) when plated out with CTLs.

*Figure 5.1 Flow cytometry analysis of HLA-A2 transfected HeLa cells*

Cells were stained with either an HLA-A2 specific (BB7.2) or a muscle specific mouse monoclonal antibody for 1 hour before staining with a goat anti-mouse FAB-specific FITC-conjugated secondary antibody for 1 hour. Cells were fixed in 1% paraformaldehyde before FACS analysis. A) Muscle-specific antibody stain of HeLa-A2 ( — )and non-transfected ( ---- ) HeLa cells. B) FITC- conjugated secondary only antibody stain of HeLA-A2 cells ( — ) and an A2-positive B cells line (– - ·). C) HeLa-A2 (— ), HeLa (--- ) and A2-positive B cells (– - ·) stained with an HLA-A2 specific antibody. D) Comparison of HeLa-A2 cells stained with non-specific primary (▪▪▪▪ ) and secondary only (▪▪▪▪▪▪▪ ) controls with those stained with BB7.2 ( — )

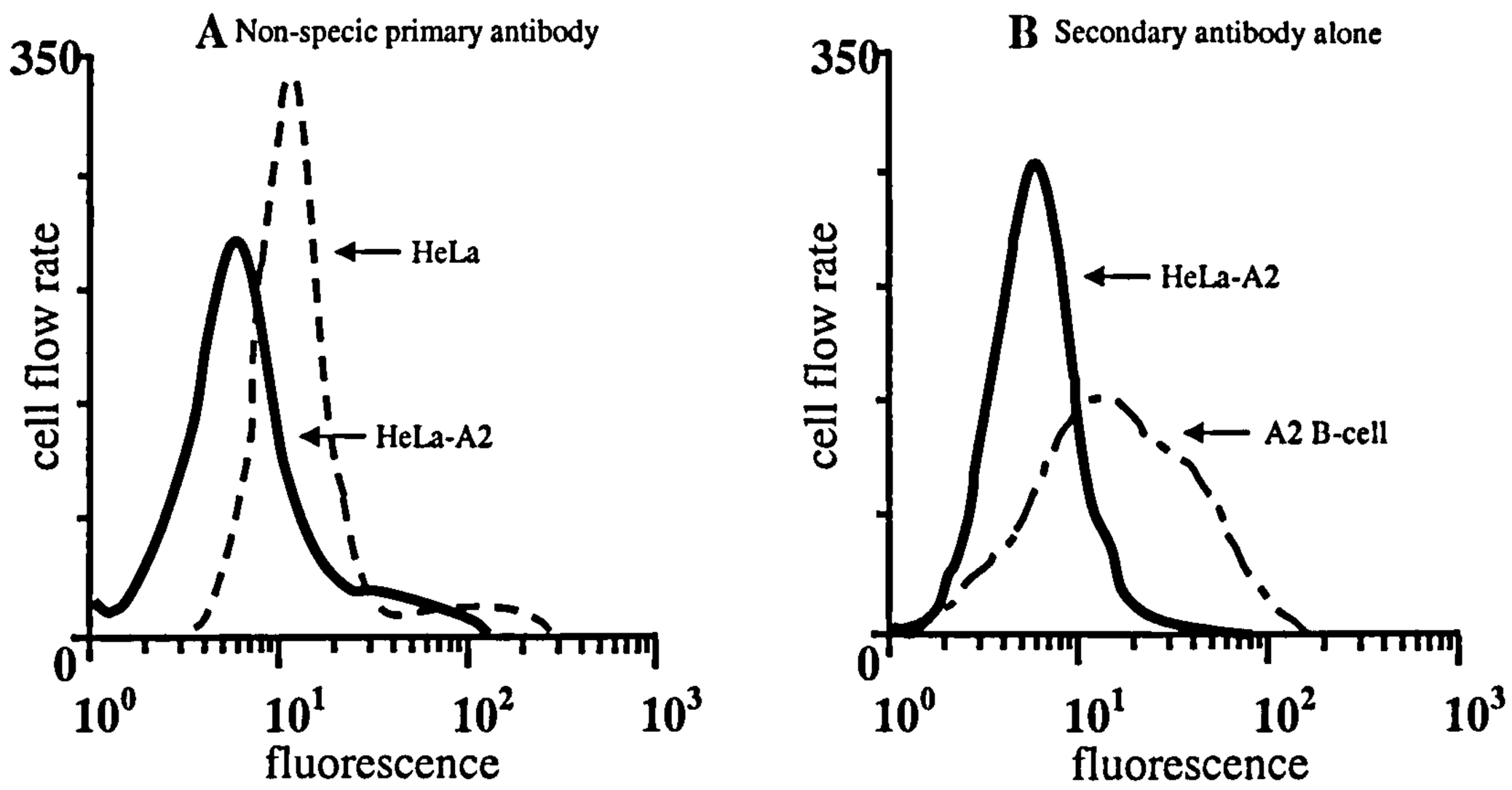
A Non-specic primary antibody
350
cell flow rate
HeLa
HeLa-A2
0
$10^0$
$10^1$
$10^2$
$10^3$
fluorescence
B Secondary antibody alone
350
cell flow rate
HeLa-A2
A2 B-cell
0
$10^0$
$10^1$
$10^2$
$10^3$
fluorescence

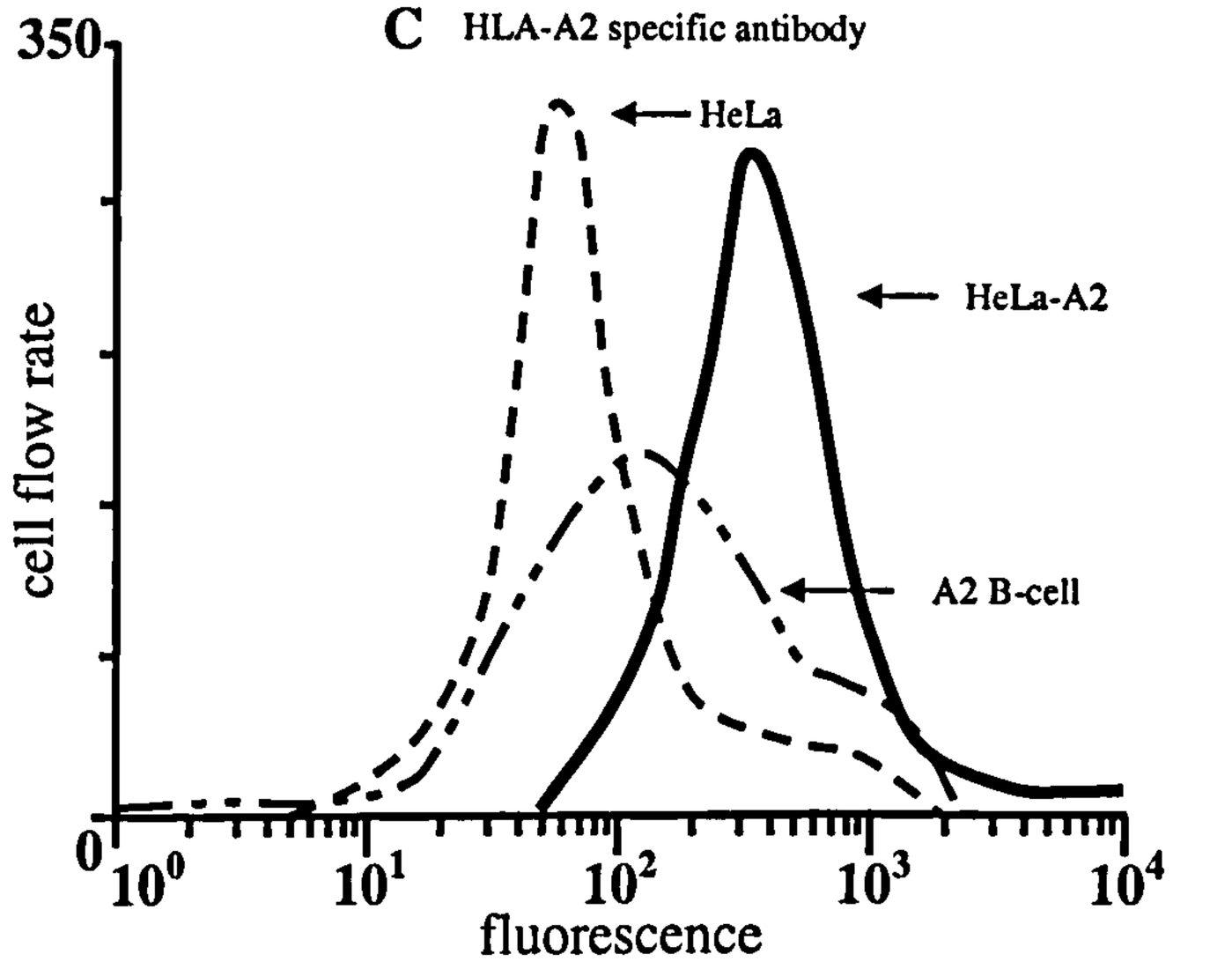
C HLA-A2 specific antibody
350
cell flow rate
HeLa
HeLa-A2
A2 B-cell
0
$10^0$
$10^1$
$10^2$
$10^3$
$10^4$
fluorescence

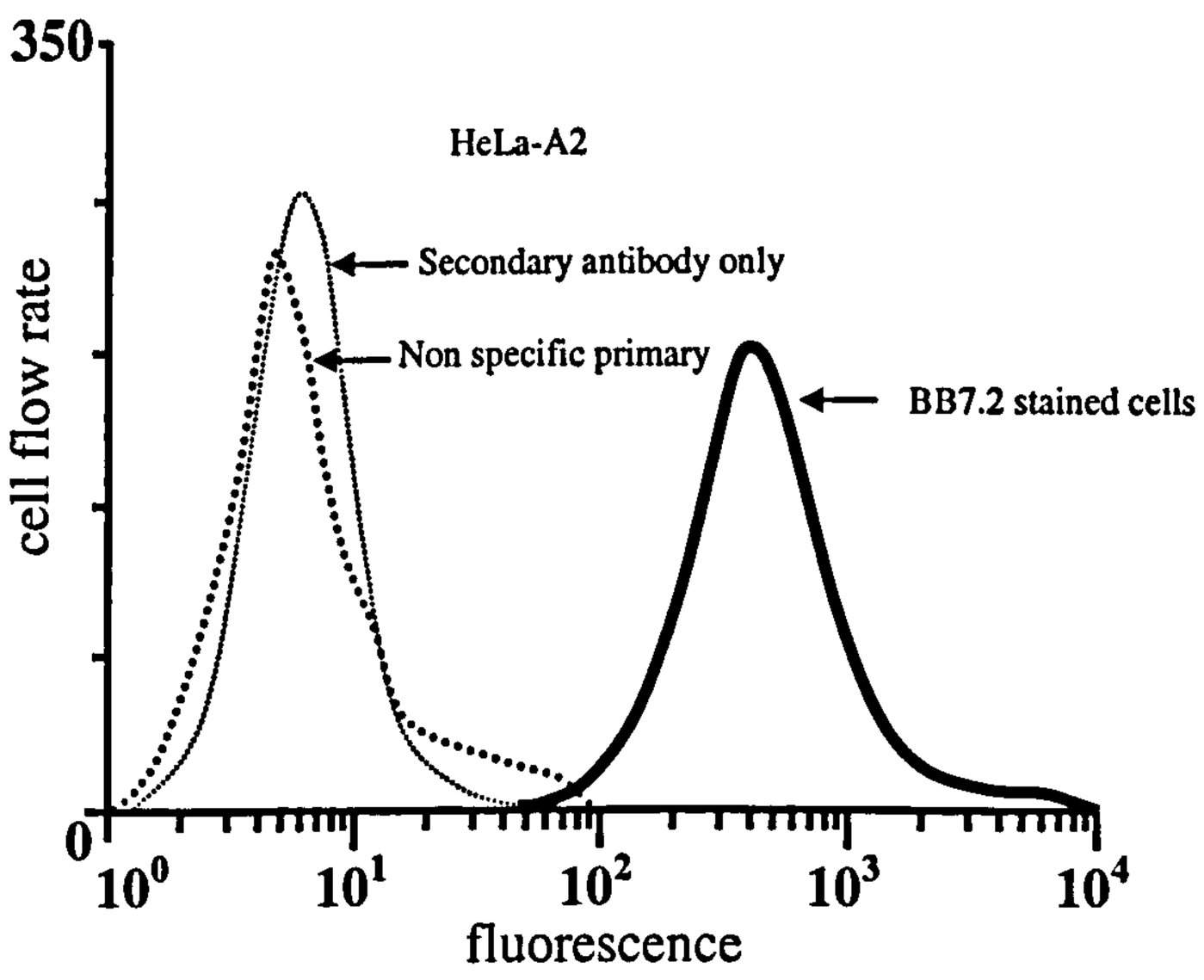
350
cell flow rate
HeLa-A2
Secondary antibody only
Non specific primary
BB7.2 stained cells
0
$10^0$
$10^1$
$10^2$
$10^3$
$10^4$
fluorescence

When HeLa-A2 cells are challenged overnight with E167D SLT, protein synthesis starts to decrease at 5-10ng/ml toxin. At 10ng/ml on average, protein synthesis occurs at 70% that of untreated control cells. This concentration was taken as the maximum amount of toxin that could be used to treat the cells overnight before cells started to decrease in numbers and couldn't be used in subsequent CTL assays. HeLa-A2 cells were challenged with a range of SLTN-Ma and SLTC-Ma concentrations (1ng/ml-10ng/ml) and incubated at 37°C overnight. Cells were washed free of surface bound toxins by washing twice in PBS (10mls) and used in CTL lysis assays (Methods, 2.8). CTL-specific lysis was calculated as a percentage of cell lysis resulting from $^{51}$Cr-loaded HeLa-A2 cells mixed with CTLs and HeLa-A2 cells mixed with 5% triton (100% cell lysis). Background $^{51}$Cr-release was taken into account by subtracting the cell lysis from $^{51}$Cr-loaded HeLa-A2 cells incubated in PBS. No CTL-specific lysis was observed after the addition of SLTN-Ma and SLTC-Ma up to an overnight incubation concentration of 10ng/ml. Over several independent experiments, the typical cell lysis observed for cells infected with VacM1 or mixed with exogenous Ma was between 5-10% (Fig.5.2). CTL-specific lysis increased when HeLa-A2 cells were infected with VacM1 the day prior to use in CTL assays and allowed to express influenza Matrix protein overnight.

To enhance CTL-specific lysis, HeLa-A2 cells were treated with interferon-γ (100units/ml) for 48 hours prior to toxin incubation and use in CTL assays. The toxin concentration applied to cells was also increased to 20ng/ml as incubation of HeLa-A2 cells overnight with 10ng/ml E167DSLT-Ma fusions had not diminished the number of live cells required to carry out the CTL assays.

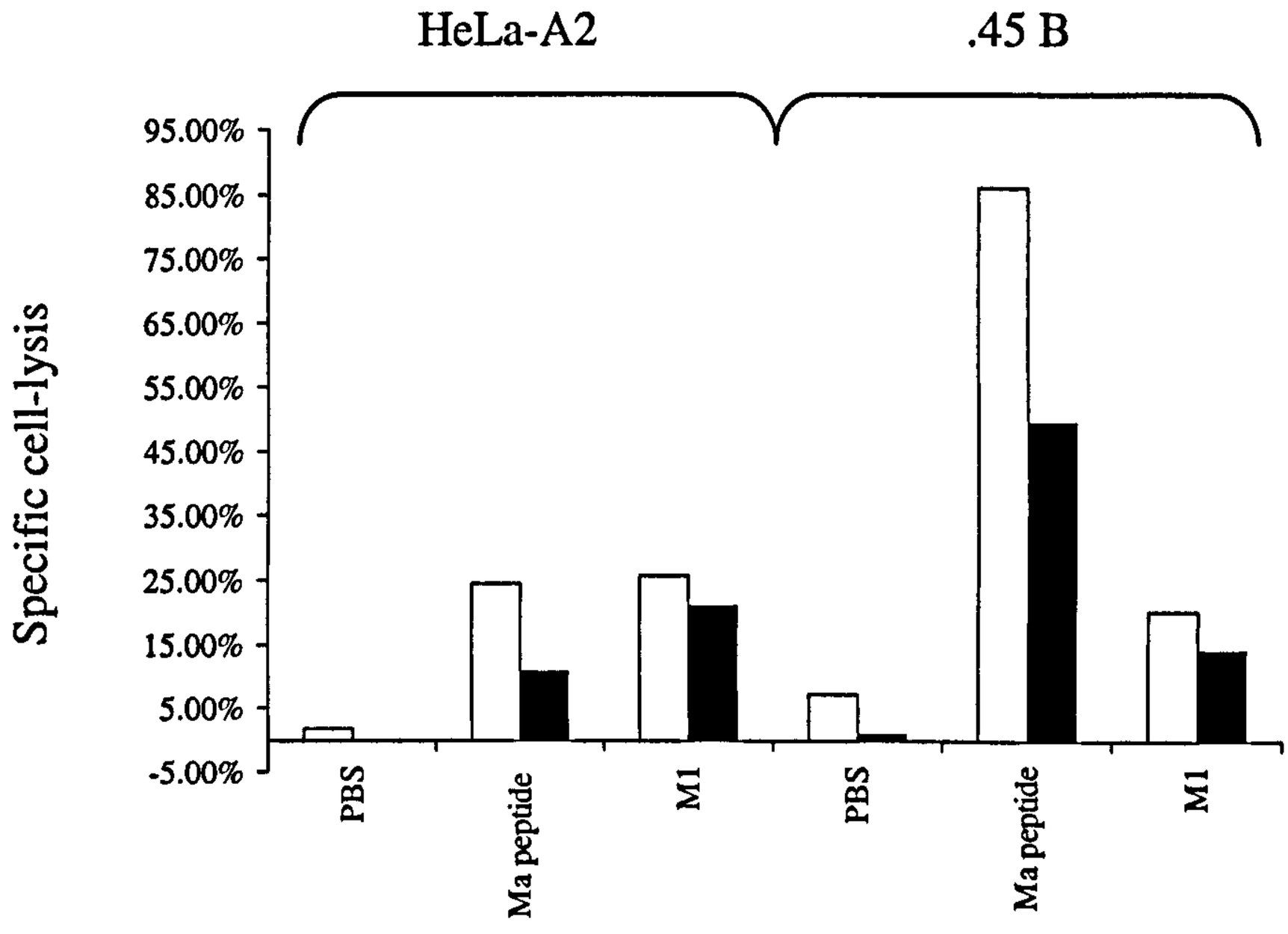


***Figure 5.2 Lysis of chromium-labelled HeLa-A2 cells by Matrix 58-66 specific CTL***

$^{51}$ Cr-loaded HeLa-A2 and .45 B cells were treated with M1 vaccinia virus, Matrix 58-66 peptide or PBS and plated with CTLs at effector/target ratios of 5:1 (white bars) and 2:1 (black bars). Cells were then incubated for 4 hours at 37°C before $^{51}$Cr-release counting (Methods, section 2.8). This represents 1 of 5 equivalent sets of data.

Specific cell lysis of interferon-γ treated HeLa-A2 cells was enhanced 3-6 fold in cells expressing full length influenza Matrix protein and 2-fold in interferon-γ treated HeLa-A2 cells where exogenous Ma peptide was applied. Significantly, specific CTL lysis of interferon-γ treated HeLa-A2 cells was observed when target cells had been treated with SLTN-Ma. In contrast, no cell lysis was observed when SLTC-Ma was applied to HeLa-A2 cells, even though the SLT fusion could be internalised by HeLa-A2 cells (refer to Figure 4.9). Results of 7 independent experiments revealed similar effects, one typical set of results is shown in Figure 5.3. Statistical analysis comparing IFN-γ-treated HeLa-A2 cells and untreated cells, incubated with SLTN-Ma revealed a significant difference in cell lysis, with a P value of $< 0.0001$ (calculated using a paired t-test). These results were consistent with a IFN-γ-dependent upregulation of the class 1 processing and presentation pathway.

### 5.4 The effect of interferon-γ treatment on HeLa-A2 cells

Expression of the MHC-encoded proteasomal subunits, LMP2 and LMP7, was significantly enhanced after incubation of HeLa cells with IFN-γ as shown by western blotting using anti-LMP2 and anti-LMP7 mouse monoclonal antibodies (Figure 5.4). FACS analysis of IFN-γ treated HeLA-A2 cells also confirmed that MHC class 1 molecules are generally upregulated by IFN-γ (Figure 5.5).

***Figure 5.3 HeLa-A2 cells incubated with SLT N-Ma are sensitised for lysis by Matrix 58-66 specific CTL***

HeLa-A2 cells were incubated with E167DSLT-Ma chimeras (20ng/ml) overnight, washed and labelled with $^{51}$ Chromium. Cells were then plated with CTLs at 5:1 (black bars) and 2:1 (white bars) effector:target ratios and incubated for 4 hours at 37°C before $^{51}$ Cr-release counting. HeLa-A2 cells were treated with IFN-γ (100U/ml) for 48 hours before the incubation with toxin. HeLa-A2 cells were infected for 90 minutes with 5 plaque forming units (pfu)/cell of vaccinia virus encoding influenza Matrix (M1). Cells were then washed and allowed to express influenza Matrix protein overnight prior to $^{51}$ Cr-labelling.

A)

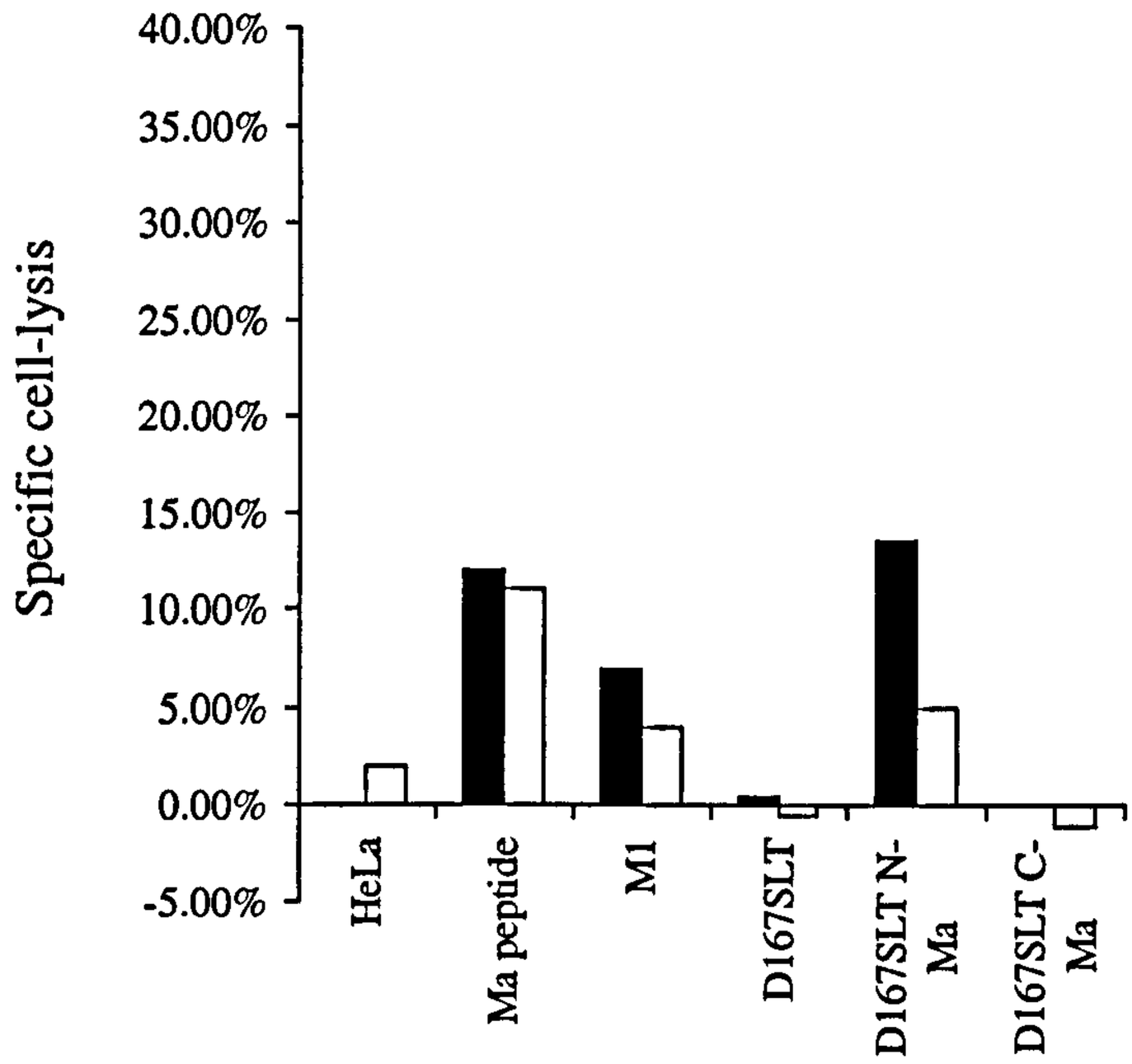


B) + Interferon-γ

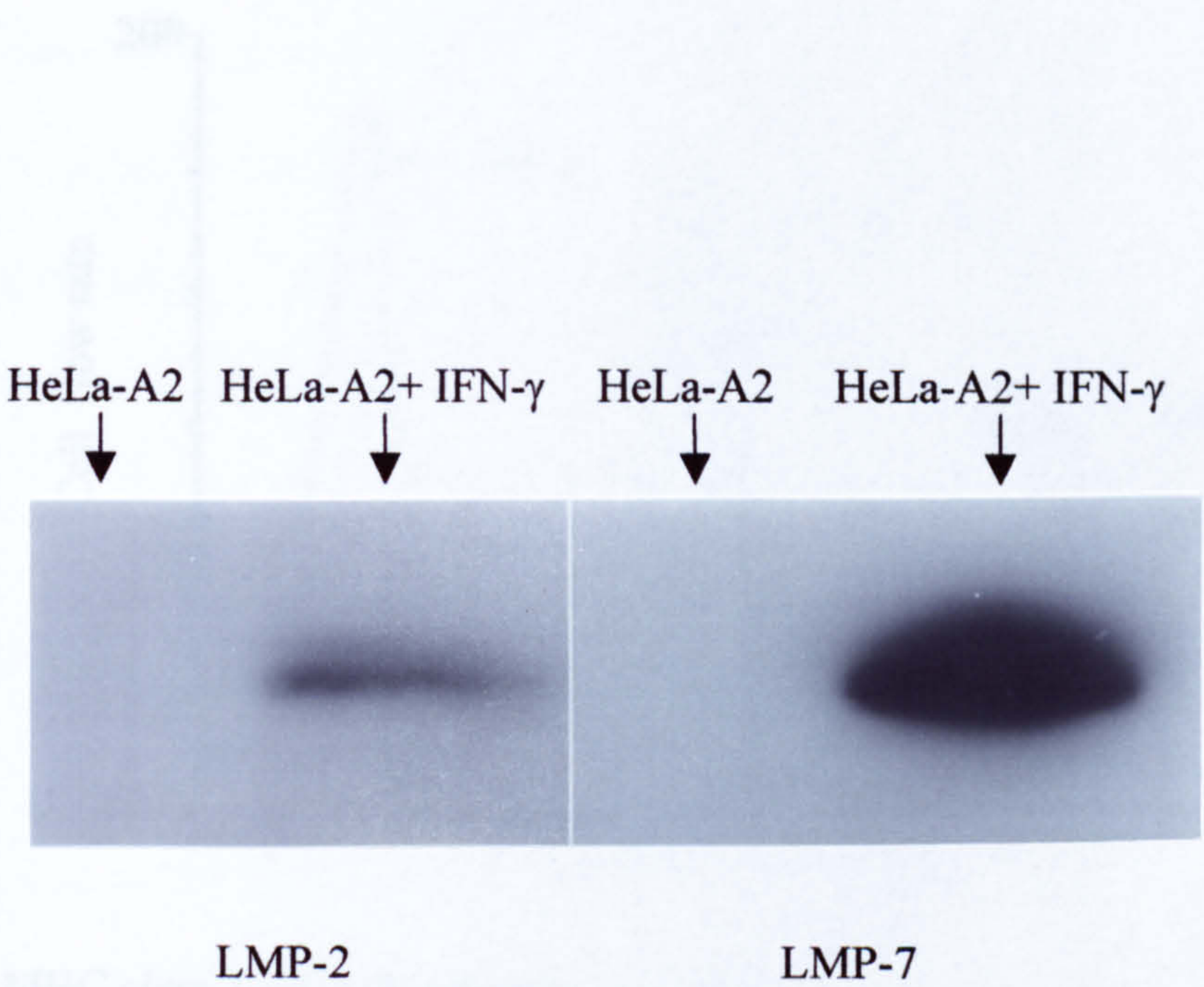


***Figure 5.4 Western blot of interferon-γ treated/untreated HeLa-A2 cells against LMP2 and LMP7 proteasomal subunits***

HeLa-A2 cells were pre-treated with interferon-γ for 48 hours. Total proteins were resolved by SDS-PAGE along with untreated HeLa-A2 cells and subjected to Western blot analysis. Bands were visualised by the use of LMP-2 and LMP-7 specific antibodies and a HRP-conjugated secondary antibody.

**A** HLA.A2 specific primary antibody

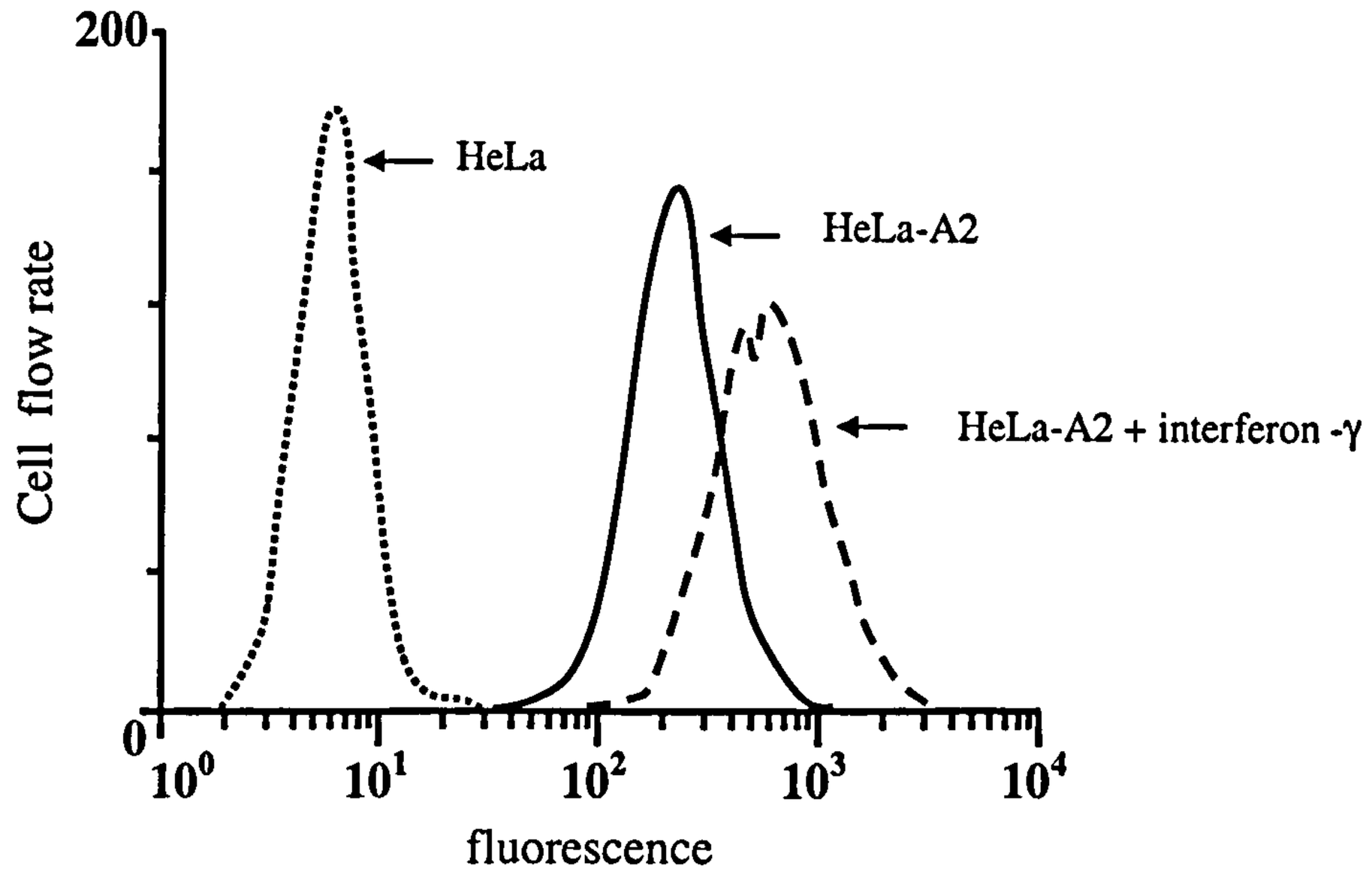


**B** MHC class 1molecules primary antibody

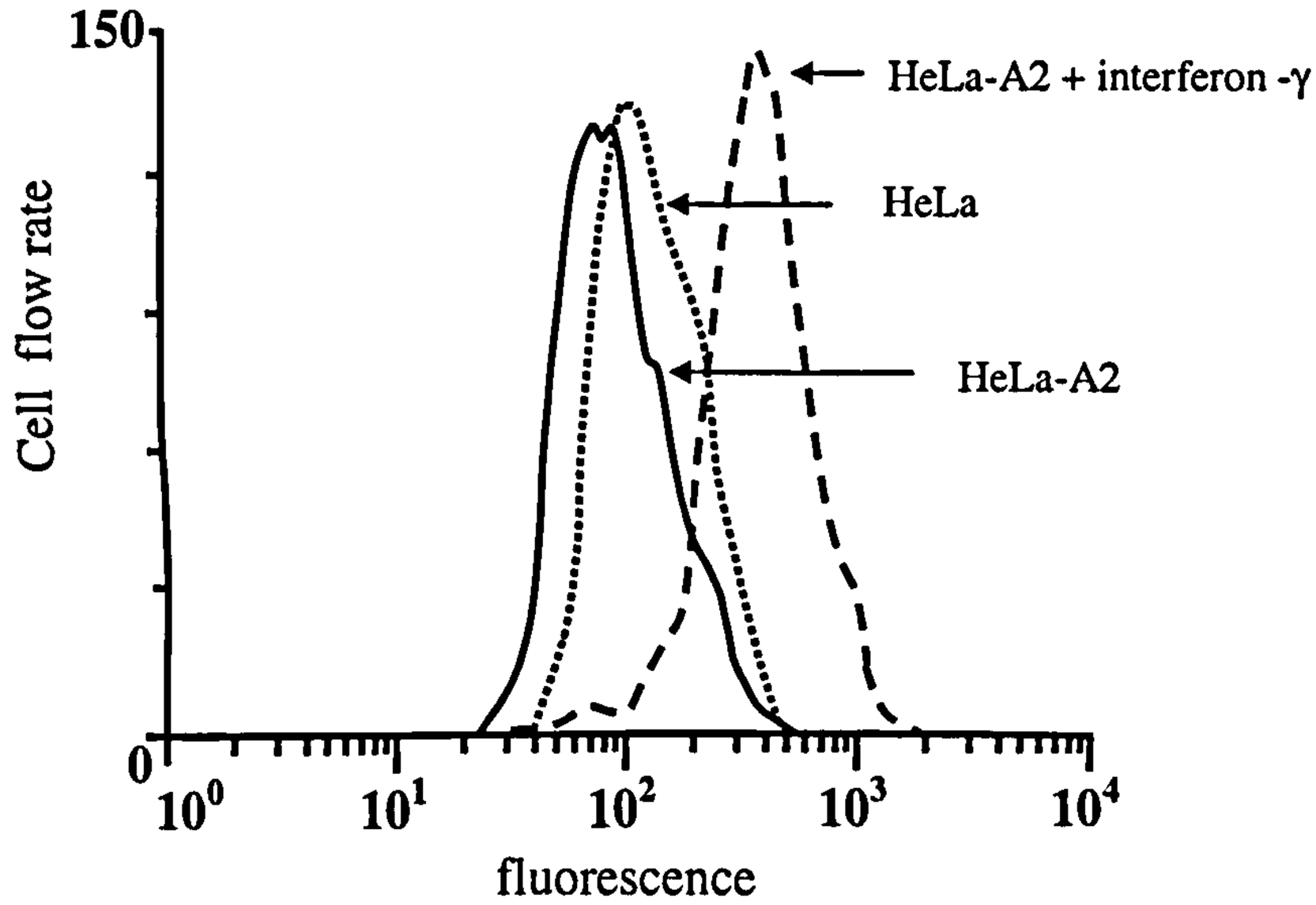


***Figure 5.5 Flow cytometry analysis of HeLa-A2 cells upregulated by interferon-γ.***

HeLa-A2 cells were pre-treated with interferon-γ for 48 hours before staining with HLA.A2 (**A**) or MHC class 1 (**B**) antibodies and a FITC-conjugated secondary antibody. Standard HeLa cells (HLA.A2 negative) were also stained.

## 5.5 Interferon-γ treatment of HeLa-A2 cells increases their sensitivity to wtSLT

HeLa-A2 cells were treated with IFN-γ (100U/ml) for 48 hours before their sensitivity to wtSLTN-Ma was compared to that of untreated cells. WtSLTN-Ma cytotoxicity increased 3-fold in HeLa-A2 cells treated with IFN-γ (Figure 5.6). This is likely to be due to a overall enhancement of trafficking in the cell, upregulated by Interferon-γ .

## 5.6 The M58-66 epitope must be internalised to sensitise target cells for lysis

To confirm that the M58-66 epitope was generated by intracellular proteases rather than serum proteases, the melanoma line Skmel-29, which is naturally resistant to SLT (Figure 5.7) was used to provide target cells. The results of these experiments are shown in Figure 5.8. Skmel-29, whilst sensitised for lysis when free A2-MAGE-3 peptide 271-279 was applied, were not sensitised for lysis by the addition of SLTN-Ma (Figure 5.8a).

In addition brefeldin-A blocked CTL specific lysis of HeLa-A2 treated with SLTN-Ma and HeLa-A2 cells infected with M1 vaccinia virus (Figure 5.8b). It is known that brefeldin-A treated cells are resistant to wtSLT as the toxin is unable to pass through the Golgi network. This was also shown to be the case for wtSLTN-Ma (Figure 5.7), implying that the presence of the peptide does not affect toxin routing.

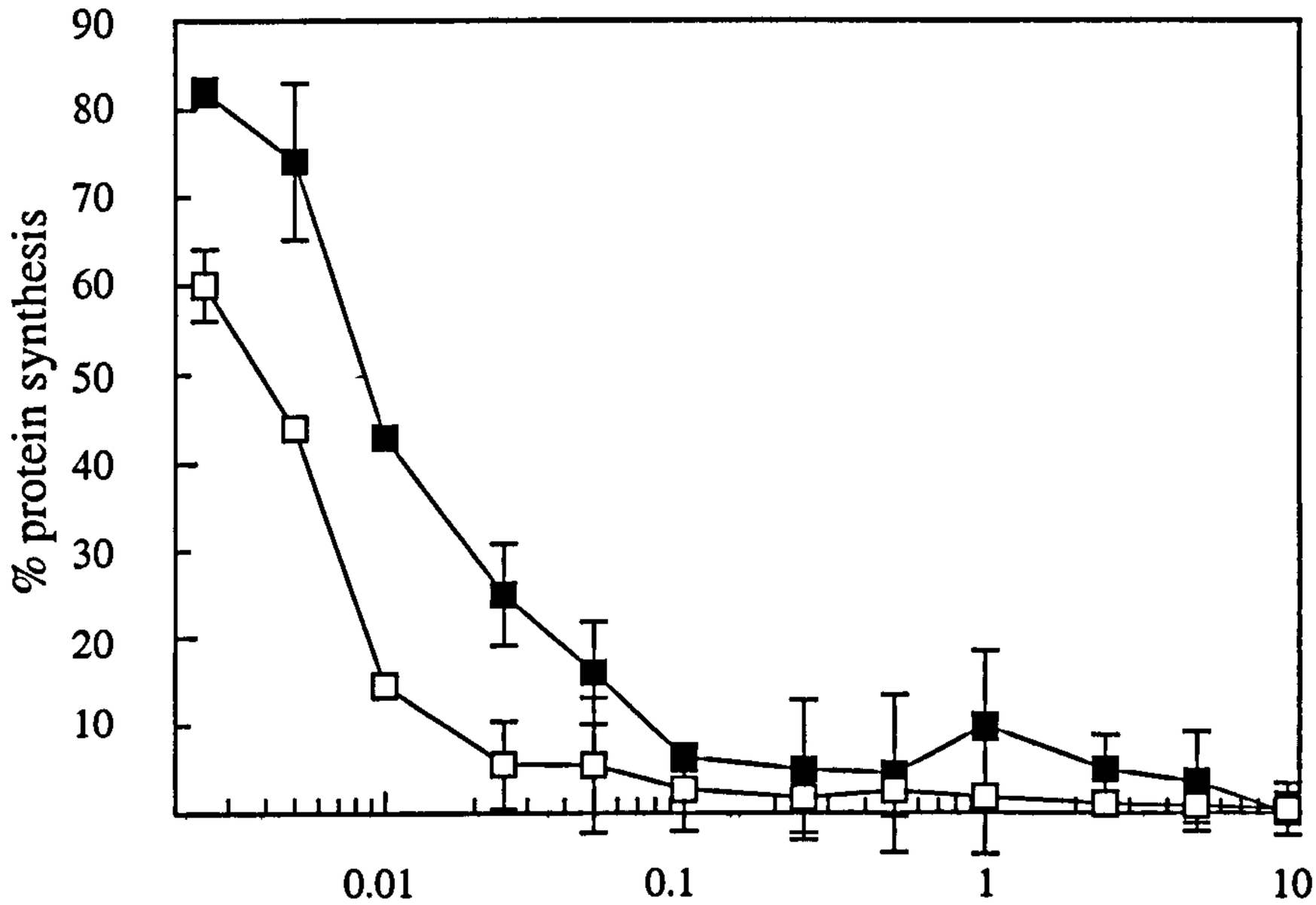


***Figure 5.6 Cytotoxicity of wtSLTN-Ma to interferon-γ treated HeLa-A2 cells***

HeLa-A2 cells were pre-treated with 100U/ml interferon-γ for 48 hours before incubation with various concentrations of wtSLTN-Ma and pulse-labelling with [$^{35}$S]-Met. Interferon-γ treated cells (□) are shown compared to untreated cells (■)

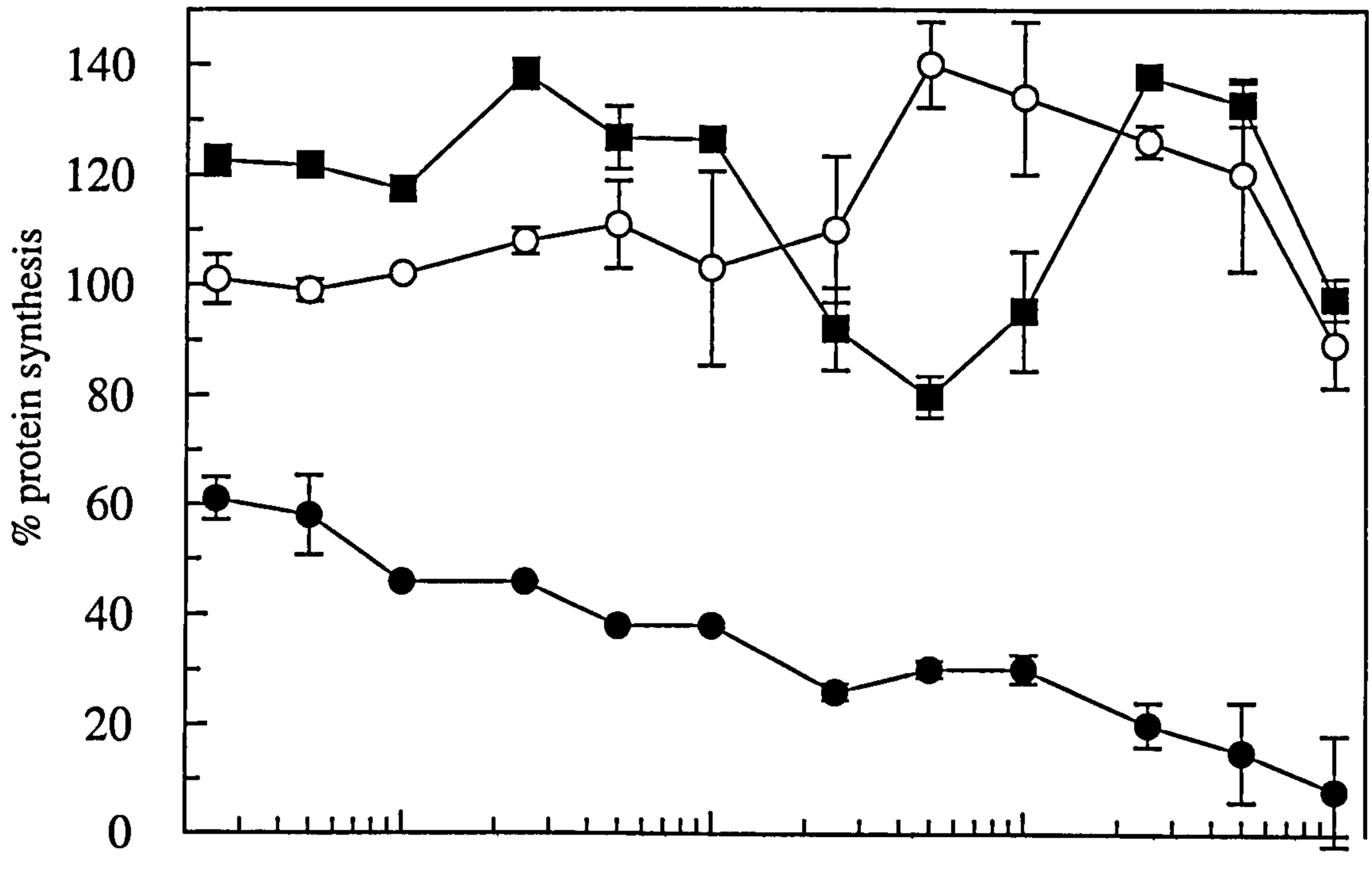


***Figure 5.7 Susceptibility of brefeldin-A treated HeLa-A2 cells (○)and untreated HeLa-A2 cells (●) to wtSLT- NMa.***

Cells were incubated with 5µg/ml brefeldin A (BFA) or PBS for 1 hour prior to toxin addition. BFA was maintained throughout the assay at 2.5µg/ml. Cells were incubated with various wtSLTN-Ma concentrations for 16 hours at 37°C before pulse labelling with [$^{35}$S]-Met as described in Methods. The melanoma line Skmel-29 (■), which is naturally resistant to wt SLT is also shown.

***Figure 5.8 The ability of SLT- resistant Skmel-29 cells to be sensitised for lysis and the effect of BFA and lactacystin on CTL-specific lysis of SLTN-Ma treated HeLa-A2 cells.***

**A)** SKmel-29 cells were incubated with SLTN- Ma toxin under the same conditions as HeLa-A2 cells (Figure5.5). The ability of Skmel-29 cells to be sensitised for CTL-specific lysis was determined using the A2 MAGE-3 peptide 271-279 (10μM for 1 hour). Cells were incubated with Matrix 58-66 specific CTL or 271-279 MAGE-3 specific CTL at effector/target ratios of 27:1 (black bars) and 9:1 (white bars). **B)** HeLa-A2 cells were treated with interferon-γ and incubated with either SLT N-Ma or M1 vaccinia. Cells were incubated with BFA (5μg/ml) or PBS for 1 hour before addition of SLT N-Ma or M1 vaccinia. BFA was maintained at this concentration throughout the assay. **C)** Cells were treated with lactacystin (100μM) for 1 hr and then incubated with SLT N-Ma overnight in a final concentration of 1μM Lactacystin. The Lactacystin was washed off the cells with the toxin prior to $^{51}$Cr-labelling.

A)

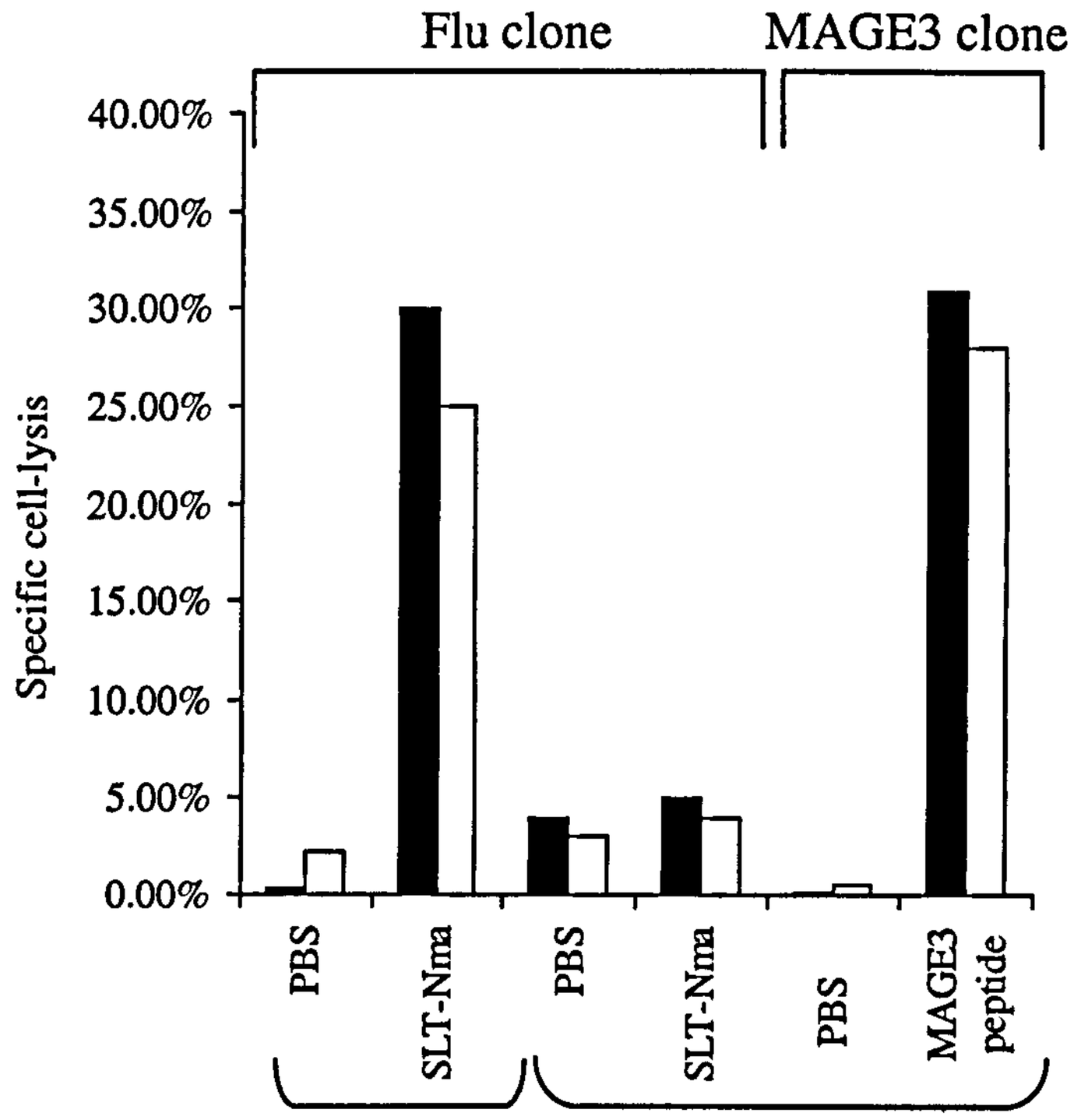
Flu clone
MAGE3 clone
40.00%
35.00%
30.00%
25.00%
20.00%
15.00%
10.00%
5.00%
0.00%
Specific cell-lysis
PBS
SLT-Nma
PBS
SLT-Nma
PBS
MAGE3 peptide
HeLa-A2
SK-mel-29

B)

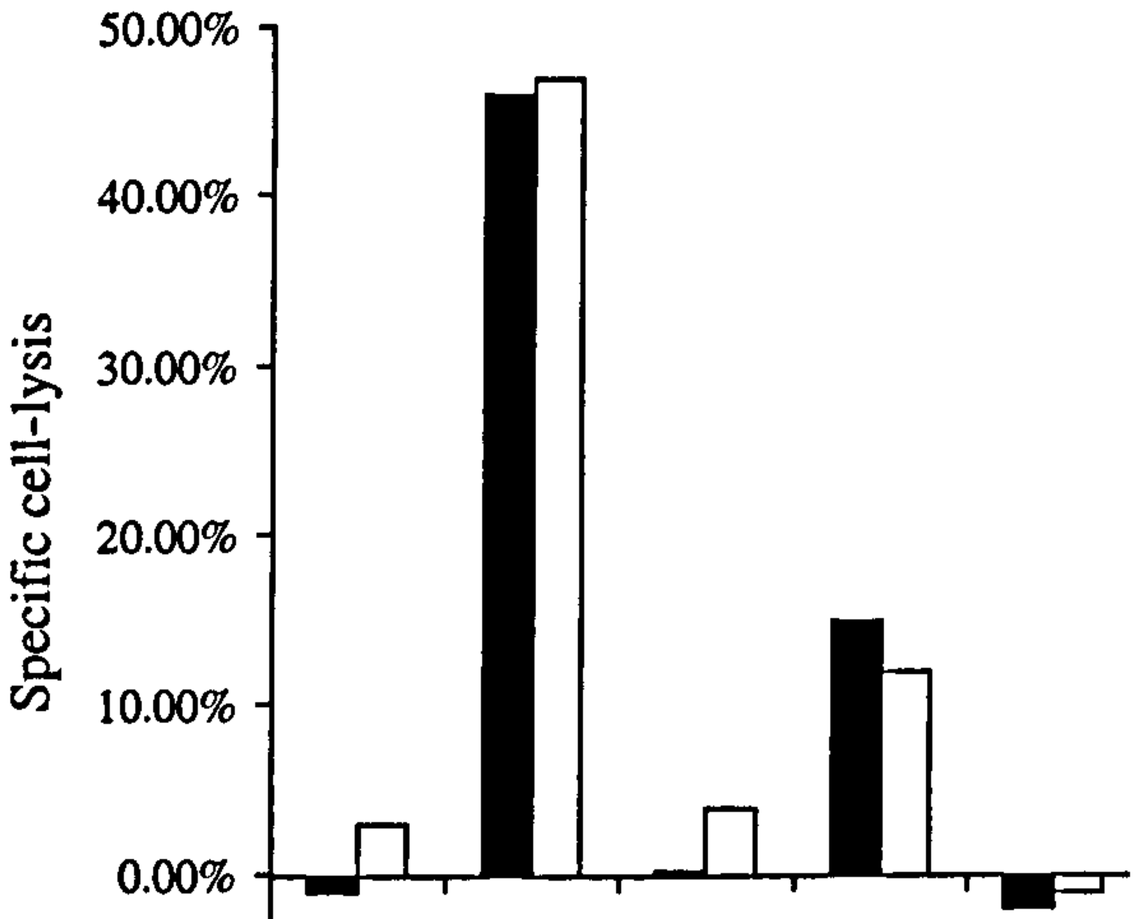
50.00%
40.00%
30.00%
20.00%
10.00%
0.00%
-10.00%
Specific cell-lysis
PBS
M1
M1+BFA
SLTN-Ma
SLTN-Ma +BFA

C)

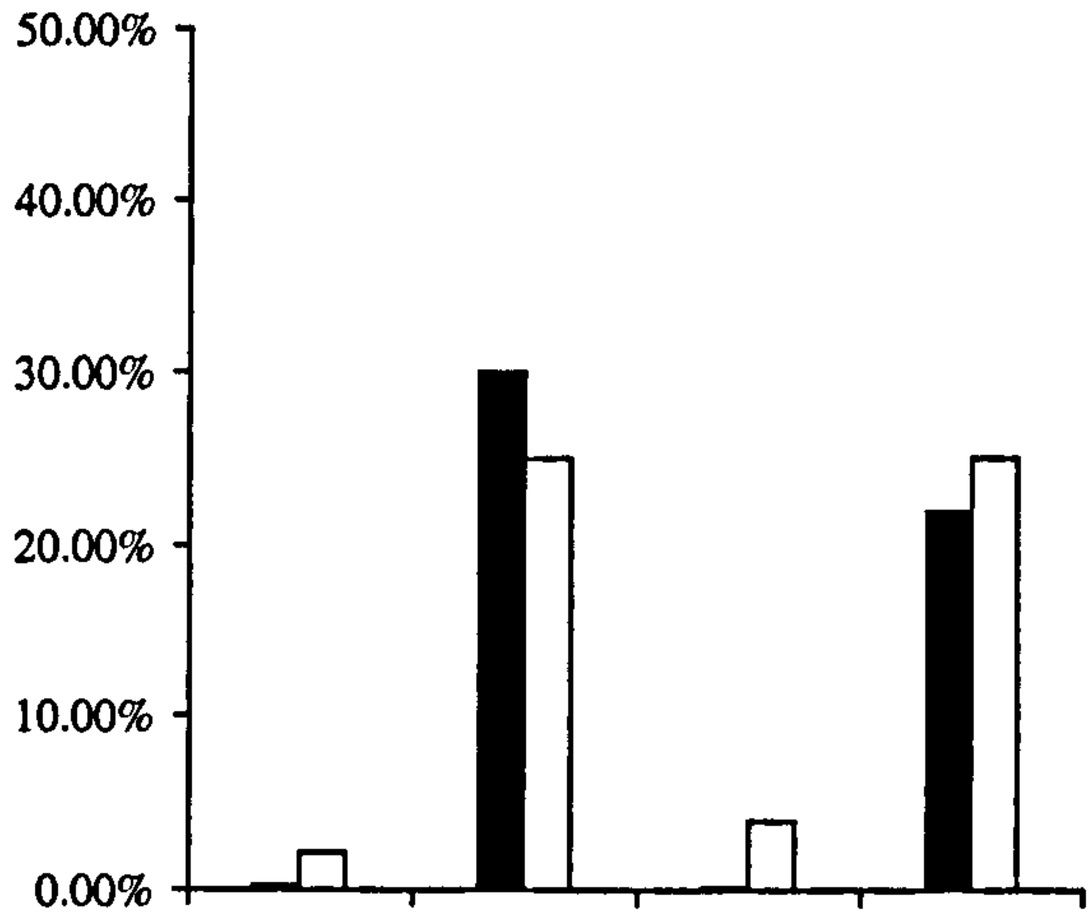
50.00%
40.00%
30.00%
20.00%
10.00%
0.00%
PBS
SLTN-Ma
PBS
SLTN-Ma +Lac

# CHAPTER 6

# THE CONSTRUCTION OF EXPRESSION PLASMIDS FOR RTA ACTIVE-SITE MUTANTS AND RTA-PEPTIDE FUSION PROTEINS

# Chapter 6

# The construction of expression plasmids for RTA active-site mutants and RTA-peptide fusion proteins.

## 6.1 Introduction

Protein toxins such as ricin and SLT must first bind cell surface receptors in order to be endocytosed and exert their toxic effect on cells. Ricin binds to both glycolipids and glycoproteins with terminal galactose, thus a large number of toxin molecules (3 x $10^7$ molecules per HeLa cell) are able to bind the majority of cells. Shiga toxin and Shiga-like toxin-1 (SLT-1) bind to a limited number of receptors at the cell surface ($10^6$ receptors per cell in sensitive HeLa cells) and are only able to bind members of the globo-glycolipid family, primarily to globotriose ($Gb_3$)-ceramides. In addition, these receptors are found in only certain tissue types, such as kidney endothelial cells, although the affinity of Shiga-toxin and SLT for these cell types is very high. An advantage of creating ricin fusion proteins is the potential to deliver peptide to all cells, including professional antigen presenting cells, such as dendritic cells.

Previous studies have shown that the active-site mutant E177D ricin A-chain (RTA) which is functionally equivalent to that of E167D SLT reduces catalytic activity 80-fold when assessed by an assay based on protein synthesis inhibition (Schlossman *et al.*, 1989). More recent studies have shown that the active-site mutant R180H-RTA reduces the cytotoxicity of R180H- ricin applied to Vero cells by 1000-fold (Day *et al.*, 1996).

Ideally, a peptide delivery system should be non-toxic. This can be achieved using SLT by fusing peptides to the SLT B-chain and expressing the B-chain chimera alone (Lee *et al.*, 1998) but this is impossible with ricin as the B-chain is unstable when expressed without ricin A-chain.

The catalytic mutations E177D and R180H of RTA were combined in an attempt to produce a catalytically inactive mutant ricin. Influenza Matrix peptide 58-66 (Ma) and influenza Nucleoprotein 366-374 (NP) were placed at the N-terminus of RTA. NP was also placed within an external loop (residue 113-114), accessible by a *Cla*I site.

## 6.2 Construction of active-site RTA expression plasmids.

Mutagenic PCR was performed on the RTA expression plasmid, pUTA (Ready *et al.*, 1991). Separated primers were designed containing the base changes for E177D and R180H on separate primers. The entire pUTA plasmid was amplified using these primers by inverse PCR (i PCR). Details of these PCR reactions are shown in Figure 6.1. The plasmid was amplified by 30 cycles of PCR (94°C for 30 s, 55°C for 1 min and 72°C for 3½ min) then a further extension period at 72°C for 7 minutes. Fragments were gel purified and phosphorylated by incubation with T4 polynucleotide kinase (Gibco BRL), following the manufacturer's instructions. The plasmid was then ligated using T4 DNA ligase (Gibco BRL) and used to transform competent *E.coli* TG2 cells (Methods, 2.3.1).

***Figure 6.1 Mutagenesis of pUTA performed by inverse PCR***

***A*** *Insertion of E177D or R180H mutations (shown in bold) within RTA*

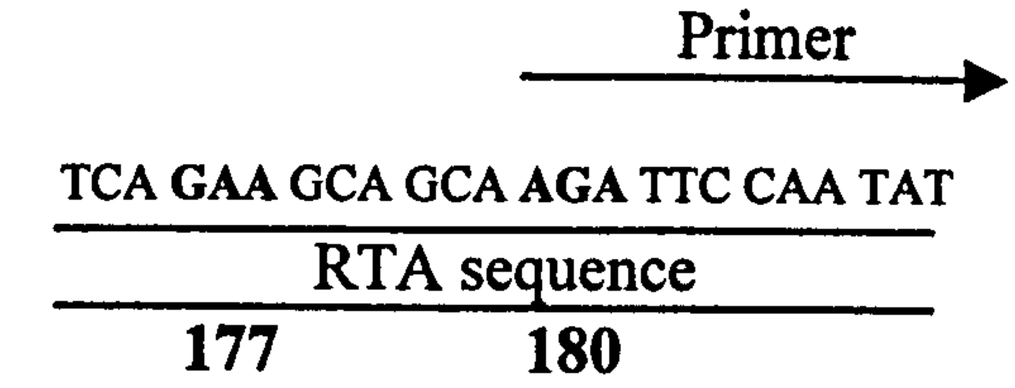


| | |
|---|---|
| <u>D177-RTA (primer 1)</u> | 5' TGC TGC **ATC** TGA AAT CAT TTG G 3' |
| E177-RTA (primer 1) | 5' TGC TGC TTC TGA AAT CAT TTG G 3' |
| <u>H180-RTA (primer 2)</u> | 5' **CAT** TTC CAA TAT ATT GAG GG 3' |
| R180-RTA (primer 2) | 5' AGA TTC CAA TAT ATT GAG GG 3' |

***B*** *Construction of RTAClaI-NP chimera by inverse-PCR*

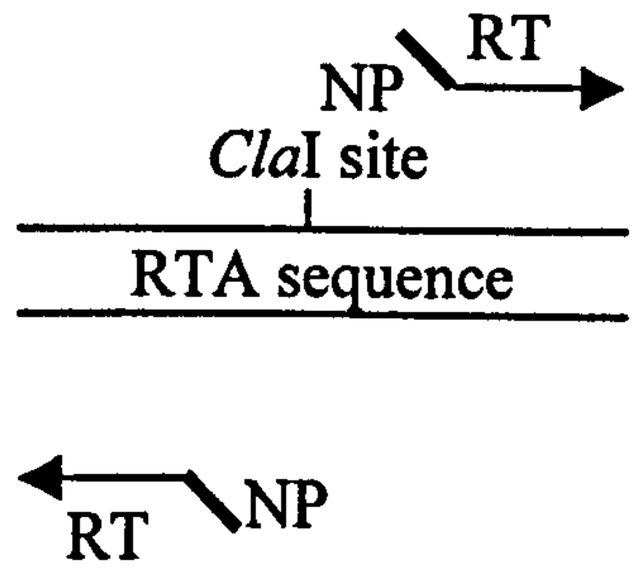


| | |
|---|---|
| <u>RTA-NP1</u> | 5' **T CTC GTT GCT CGC** ATT TTG AAC ATC AGT GAA AAG 3' |
| (antisense, letters in bold coding for the first 13 bases of the NP peptide) | |
| <u>RTA-NP2</u> | 5' **AT ATG GAC GCC ATG** CGA TAT ACA TTC GCC TTT 3' |
| (sense, letters in bold coding for the last 14 bases of the NP peptide) | |

## 6.3 Construction of ricin-Ma and ricin-NP expression plasmids.

DNA coding for the influenza Matrix peptide 58-66 (GILGFVFTL) was genetically fused to the N-terminus of E177D R180H RTA by mutagenic PCR. A construct placing influenza Nucleoprotein 366-374 (ASNENMDAM) in the same position was also made. A similar PCR approach was used as for the construction of SLT-Ma plasmids. The PCR strategy is shown in Figure 6.2 and Figure 6.3. NP was also placed within a *Cla* I site (residue 113-114) by inverse PCR (Fig 6.1) such that the restriction-site was destroyed and could be used as a marker (by digesting potential candidates with *Cla*I) for incorporation of the NP sequence. Reaction conditions for the construction of these fusion proteins are given below (table 6.1).

| | hot start<br>94°C | denaturing<br>94°C | annealing<br>variable | extension *<br>72°C |
|---|---|---|---|---|
| RTAN-NP<br>Reaction 1 | | 30 s | 1 min<br>60°C | 1 min |
| RTAN-NP<br>Reaction 2 | | 30 s | 1 min<br>60°C | 1 min |
| RTAN-NP<br>Reaction 3 | 1 min | 30 s | 1 min<br>45°C | 1 min |
| | (add primers) | 30 s | 1 min<br>55°C | 1 ½ min |
| RTAN-Ma<br>Reaction 1 | | 30 s | 1 min<br>65°C | 1 min |
| RTAN-Ma<br>Reaction 2 | | 30 s | 1 min<br>65°C | 1 min |
| RTAN-Ma<br>Reaction 3 | 1 min | 30 s | 1 min<br>45°C | 1 min |
| | (add primers) | 30 s | 1 min<br>55°C | 1 ½ min |

Table 6.1 ***PCR conditions for the construction of pRTAN-NP and pRTAN-Ma..***

PCR reactions were typically carried out in a total volume of 50µl or 100µl (see Methods, 2.2.7) using a Hybaid thermocycler. The products of reactions 1 and 2 (amplified by 30 cycles of PCR) were gel purified (see section 2.3.1) and approximately 1 ng of each DNA used in reaction 3. Reaction 3 consisted of 10 cycles of PCR in the presence of PWO (0.5µl) alone followed by the addition of M13 vector primers and extra PWO (0.5µl) for 30 cycles.

*Figure 6.2 Construction of RTAN-Ma by 2-stage mutagenic PCR*

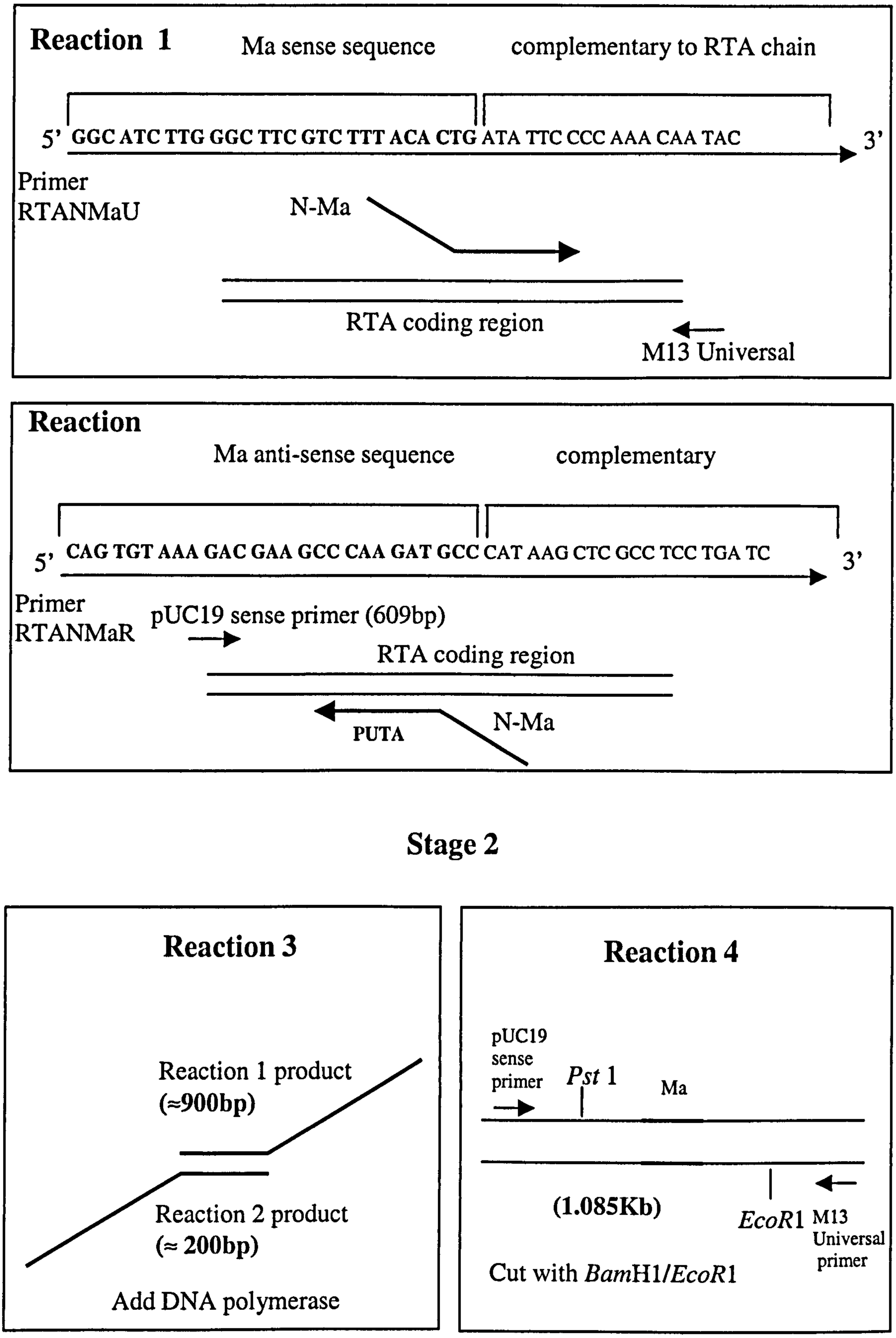

*Figure 6.3 Construction of RTAN-NP by 2-stage mutagenic PCR.*

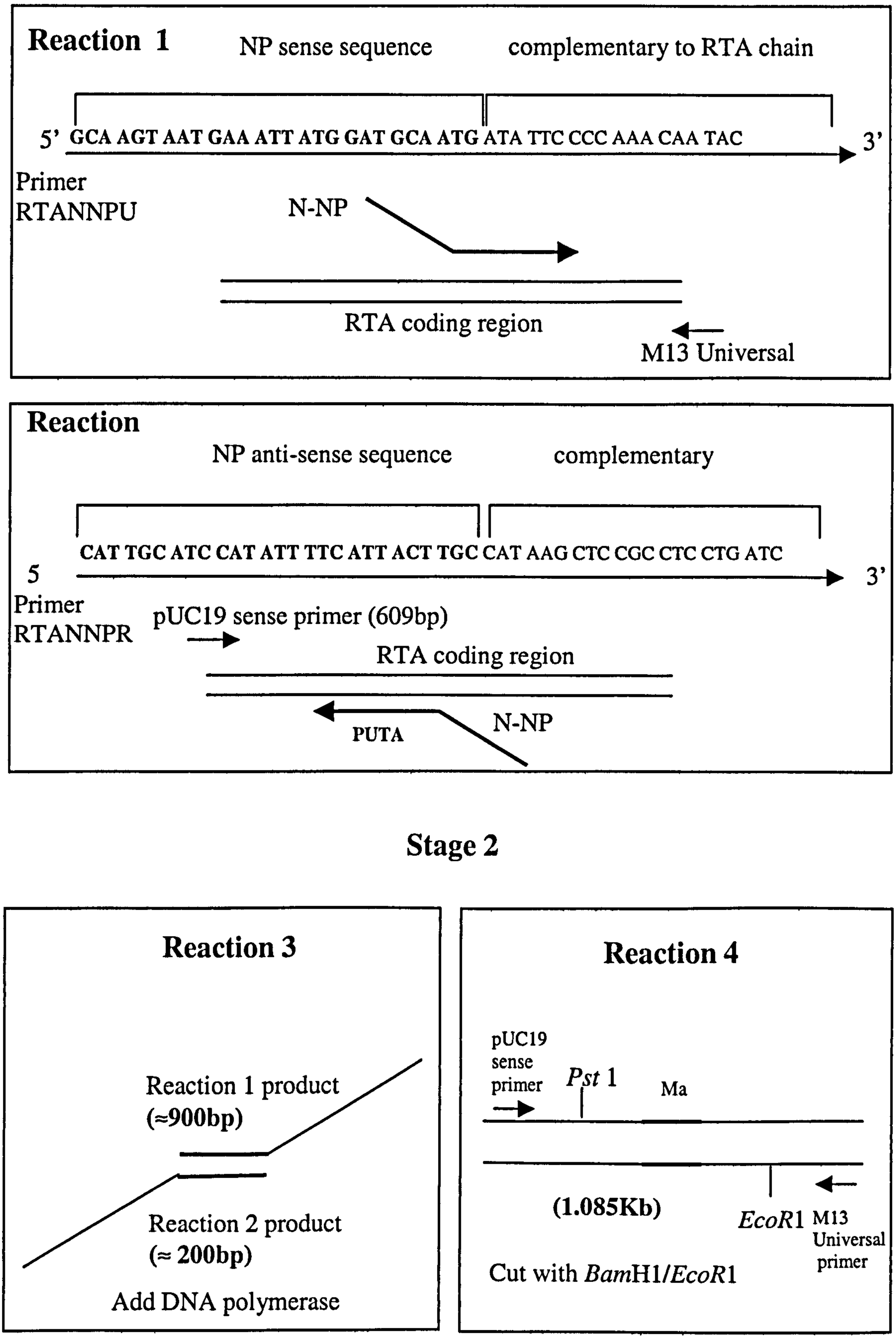

# CHAPTER 7

# THE ACTIVITY ASSESSMENT OF E177D R180H RICIN AND CONSTRUCTION OF RICIN FUSION PROTEINS.

# Chapter 7

# The activity assessment of E177D R180H ricin and construction of ricin fusion proteins.

## 7.1 Introduction

All the RTA constructs were expressed from the high-level RTA expression vector pUTA (Ready *et al.*, 1991) which consists of the RTA coding sequence fused to a Shine-Dalgarno linker sequence and the *lac Z* promoter from plasmid pUC18. Hence expression can be driven by the *lac Z* promoter. Wild-type RTA is normally purified by cation exchange using carboxymethyl (CM)-Sepharose equilibrated in 5mM sodium phosphate (pH6.5), since RTA is positively charged below its pI of pH7.5. The addition of a nonamer to RTA may potentially change the pI of the protein and alter the binding characteristics of the protein to CM-Sepharose. The peptide may carry a charge itself or affect the pI of RTA by preventing the correct folding of the protein. For this reason a range of buffers at various pHs were used to purify the RTA fusion proteins by cation and anion exchange chromatography.

## 7.2 Preparation of E177D R180H ricin

E177D R180H RTA was expressed in *E.coli* and purified on a CM-Sepharose column, equilibrated in 5mM sodium phosphate pH6.5. The loaded column was washed in 50-100ml 0.1M sodium chloride and E177D R180H RTA was eluted over a 0.1M-0.5M sodium chloride gradient in a total volume of 500ml. Mutant E177D R180H RTA peak fractions were typically collected between 160-210ml, a salt gradient range of 0.17-0.18M sodium chloride, eluting in the same pattern as wild-

type RTA (Figure 7.1). Typically less than 0.5 mg of RTA was obtained from a 500ml culture, approximately 30-fold less than wild-type RTA. As a test of solubility E177D R180H RTA was subjected to ultracentrifugation at 412,000 xg (100 000 rpm) in a Beckman TL-100 ultracentrifuge (using a TL-100 rotor) for 20 minutes. The protein remained in the supernatant and was therefore deemed soluble, but after 3-4 weeks stored at 4°C the RTA had started to precipitate, indicating that the double mutant was more unstable than native RTA.

## 7.3 *In vitro* ribosome inactivation assays

The *in vitro* ribosome depurination activity of E177D R180H was assessed by aniline-cleavage assays (Methods, 2.6.3). Rabbit reticulocyte ribosomes were treated with RTA and mutant RTA from a range of 5 pg/µl to 375 ng/µl for 30 minutes at 30°C. A typical formamide-agarose gel of the acetic-aniline treated rRNA samples is shown in Figure 7.2. Whilst an aniline fragment is clearly visible down to 25pg/µl (0.5ng total protein) wild-type RTA, an aniline fragment only appears at 25ng/µl (0.5µg total protein) E177D R180H RTA. From this visualisation, the catalytic activity of the double mutant can be estimated to be at least a 1000-fold down from wild-type RTA.

## 7.4 Cytotoxicity comparison of E177D R180H ricin with native ricin

E177D R180H RTA and wild-type RTA were reassociated with ricin B-chain as described in methods (section 2.5.3) and the concentration of ricin calculated by

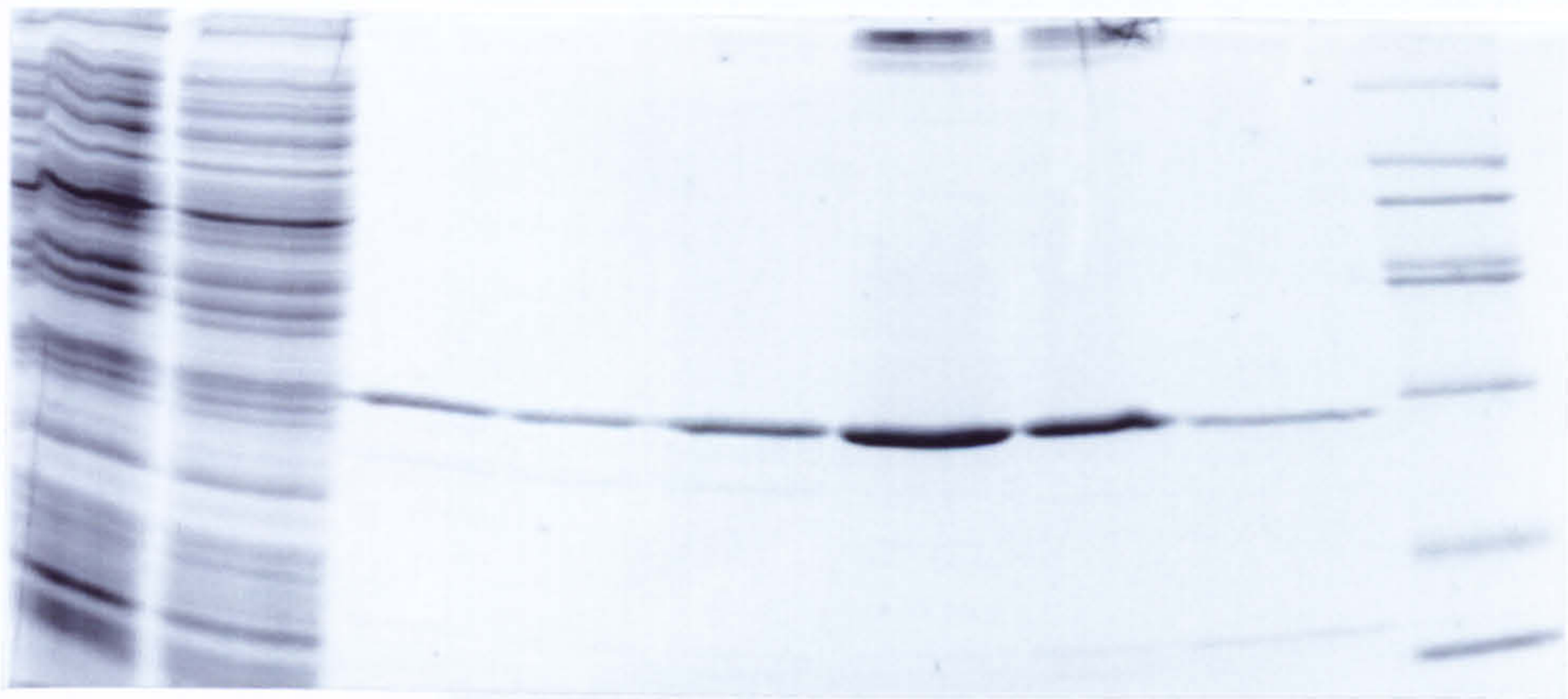


***Figure 7.1 Expression and purification of E177D R180H RTA***

An overnight culture of *E.coli* TG2 harbouring pUTA:E177D R180H plasmid was used to inoculate 500ml of 2TY media. Expression of RTA was induced by the addition of 0.05mM IPTG. Cells were harvested by centrifugation, resuspended in 5mM sodium phosphate (pH6.5) buffer and broken by sonication. Following centrifugation to remove cell debris, the supernatant was loaded onto a 100ml carboxymethyl-Sepharose (Pharmacia) column equilibrated in the same buffer. Unbound protein was washed with 1500ml 5mM sodium phosphate (pH6.5) followed by a further 200ml of buffer containing 100mM sodium chloride. E177D R180H RTA was eluted with a linear 500ml 0.1-0.3M sodium chloride gradient, collection of 10ml E177D R180H RTA fractions starting at ≈0.17M sodium chloride. A high molecular weight protein was occasionally visualised in the RTA fractions which had no effect on the reassociation of RTA with ricin B-chain. Pre refers to a sample of pre-column sonicated *E.coli* supernatant , FT refers to a sample of column flow through, E14-E19 refers to eluted fractions of E177D R180H RTA (M, molecular weight markers).

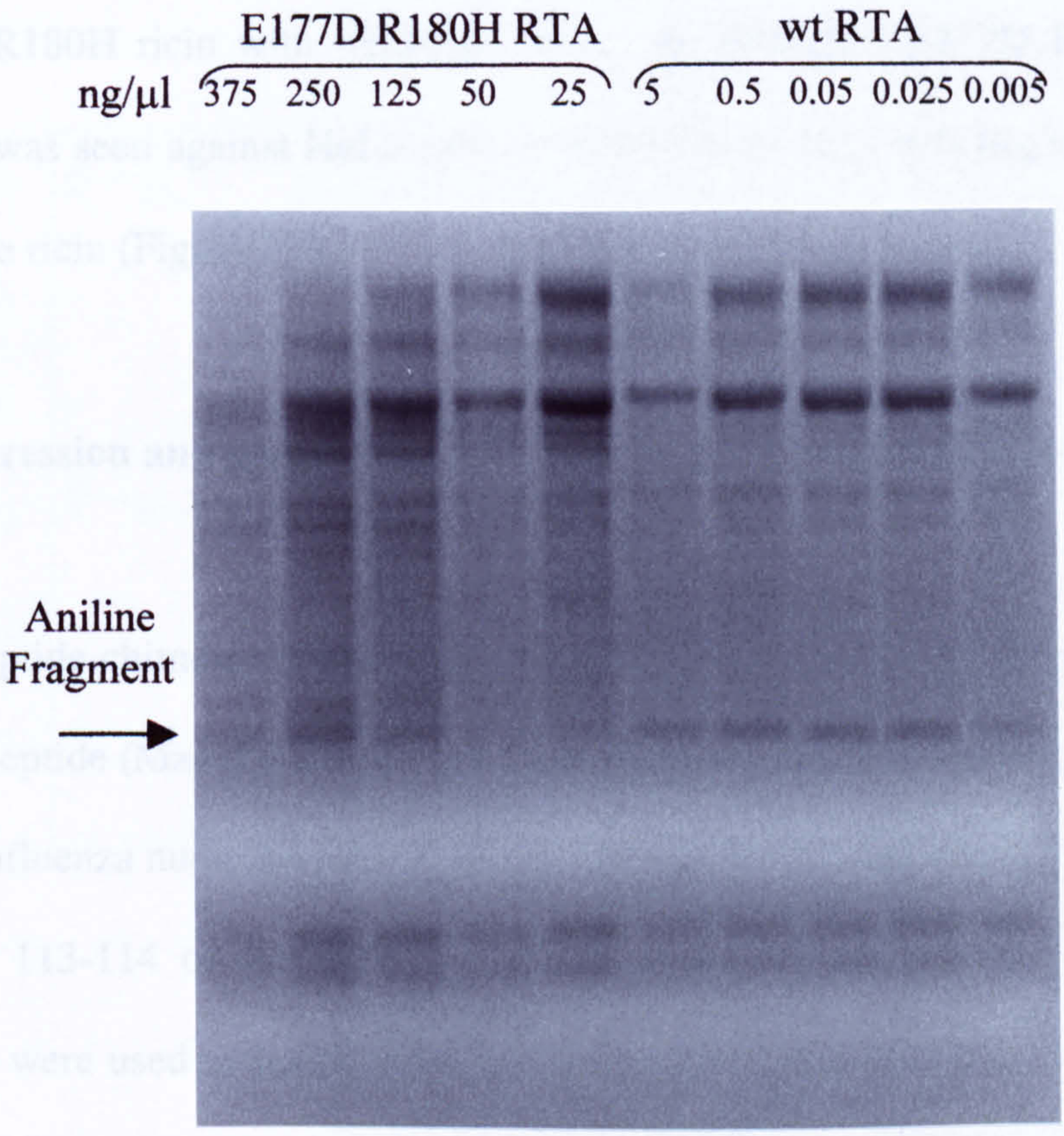


***Figure 7.2 Northern blot analysis of ribosome depurination activity of E177D R180H RTA and wtRTA.***

Rabbit reticulocyte ribosomes (20μg) were incubated for 30 minutes with various concentrations of wtRTA and E177D R180H RTA (given in ng/μl) and subsequently treated with acetic-aniline (as described in Methods). The rRNA samples (2.5μg of each) were resolved on a denaturing formamide-agarose gel.

comparing the optical density of RTA bands separated by SDS-PAGE with known RTA concentrations. Cytotoxicity assays were carried out (Methods, 2.7) comparing E177D R180H ricin with wild-type ricin. At 100ng/ml E177D R180H ricin, no activity was seen against HeLa cells compared to an $IC_{50}$ of 0.1ng/ml calculated for wild-type ricin (Figure 7.3).

## 7.5 Expression and purification of E177D R180H ricin fusion proteins

Ricin-peptide chimeras were expressed using the same protocol as ricin. Influenza Matrix peptide (Ma) or influenza nucleoprotein (NP) was placed at the N-terminus of RTA. Influenza nucleoprotein (NP) was also placed within an external loop between residues 113-114 of the RTA chain. A range of pH buffers and ion-exchange matrices were used to purify these fusion proteins, detailed in table 7.1. RTAN-Ma was purified under identical conditions to wild-type RTA by applying to CM-Sepharose equilibrated in 5mM sodium phosphate pH6.5. When a sample of protein was centrifuged at 412,000 xg (100 000 rpm) for 20 minutes at 4°C using a TL100 centrifuge and TL100 rotor (Beckman), RTAN-Ma was found to have precipitated, no protein was visualised in the supernatant when resolved by SDS-PAGE and analysed by Western blotting. RTAClaI-NP bound to CM-Sepharose at a lower optimal pH (pH5.8) than wild-type RTA. This can be accounted for by the addition of a negatively charged nonamer. RTAN-NP was unable to bind CM-Sepharose over the pH range pH4-pH8. RTAN-NP bound to the anion-exchange matrix DEAE-Sephacel, along with the majority of *E.coli* proteins present in the expression extract which eluted in the same fractions as RTA. The RTA fractions collected

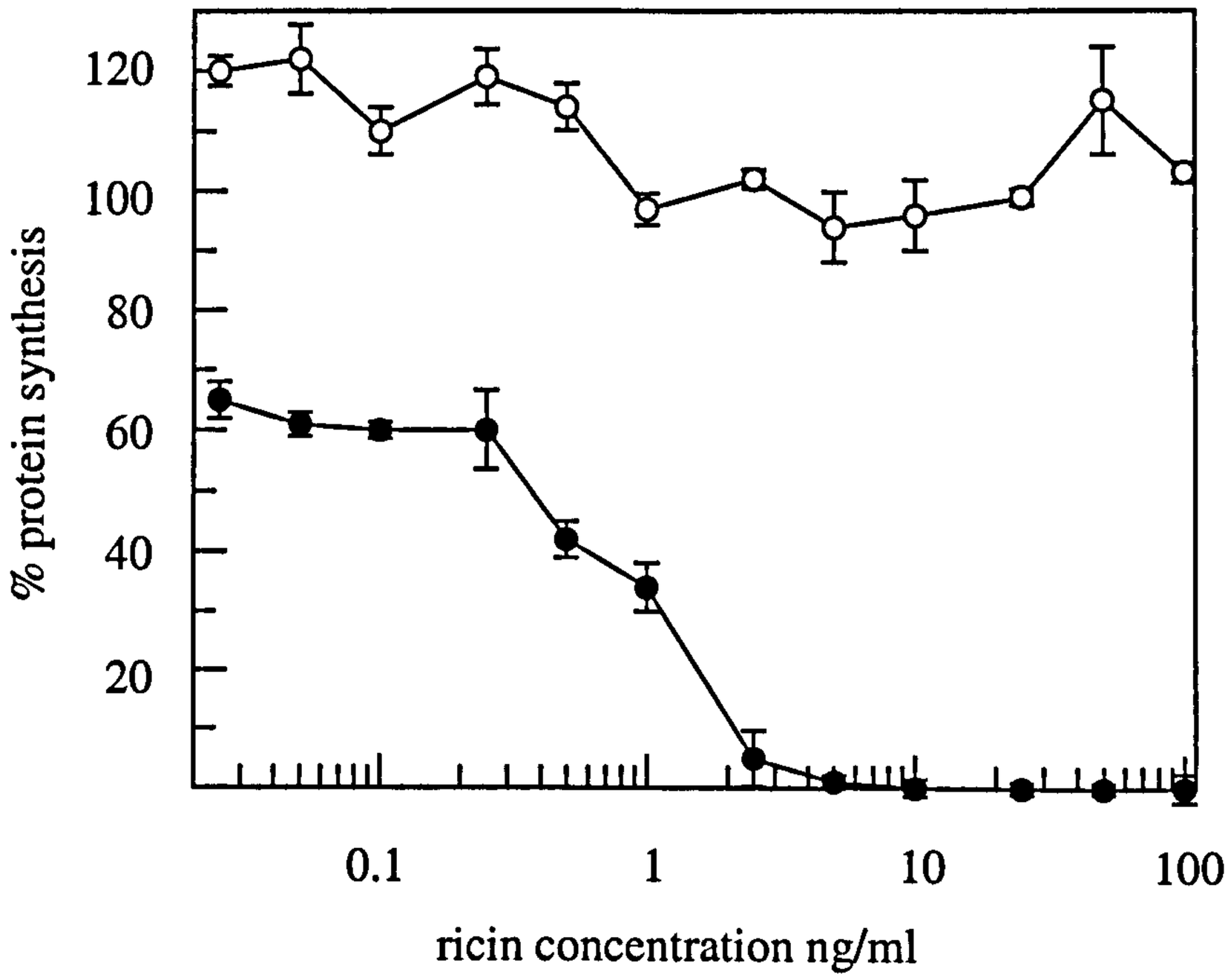


*Figure 7.3 Cytotoxicity of wild-type and E177D R180H ricin to HeLa cells*

Cytotoxicity of ricin ( ● ) and E177D R180H ricin ( o ) towards HeLa cells. Cells were incubated with various concentrations of ricin proteins, in quadruplicate, for 16 hours at 37°C before adding [$^{35}$S]-methionine (1μCi/well) and incubating for a further 2 hours. Cell proteins were precipitated by washing with 5% trichloroacetic acid and radioactivity measured by liquid scintillation counting. Protein synthesis was measured by the incorporation of [$^{35}$S]-Methionine into protein and a percentage calculated in relation to toxin-free control cells.

were resolved by SDS-PAGE and visualised by Western blotting. There was no visible size difference between peptide-containing A-chains and native RTA.

Peak RTA fractions were concentrated and reassociated with ricin B-chain (Methods, 2.5.3). In the case of RTAN-NP, unpurified extract was reassociated with RTB.

| Matrix | CM-Sepharose CL-6B | | | | | DEAE-Sephacel |
|---|---|---|---|---|---|---|
| Buffer (pH) | 10mM acetic acid pH4 | 5mM sodium phosphate pH5.8 | 5mM sodium phosphate pH6 | 5mM sodium phosphate pH6.5 | 5mM sodium phosphate pH8 | 10mM Tris pH8 |
| RTAN-Ma | | X | X | • | X | |
| RTAN-NP | X | X | X | X | X | • |
| RTAClaI-NP | | • (optimal) | • | • | | |

**Table 7.1 Purification conditions tested for E177D R180H RTA fusion proteins**

*E.coli* cells expressing RTA fusion proteins were harvested and resuspended in 30ml of the appropriate buffer and broken by sonication. Following centrifugation to remove cell debris, the supernatant was loaded onto a 100ml column equilibrated in the same buffer. Two types of matrix were tested, CM-Sepharose and DEAE-Sephacel. The carboymethyl (CM) group is a weak cation used in cation exchange for the recovery of positively-charged proteins. The diethylaminoethyl (DEAE) group is used in anion exchange to purify negatively charged proteins. X denotes where purification under the set conditions did not succeed and • denotes the conditions where protein bound and was successfully eluted from the matrix.

## 7.6 Thermal denaturation of E177D R180H RTA

As a measure of stability, E177D R180H RTA and wild-type ricin (1mg/ml) were incubated at 40°C for 5 minutes in a total volume of 50µl of 0.1M MES or 0.1M HEPES at a variety of pH values. Denatured protein samples were pelleted by centrifugation and 20µl aliquots analysed by SDS-PAGE on 15% gels and Western blotting. Figure 7.4 shows that E177D R180H remains soluble after a 5 minute incubation at 40°C over a pH range 5.2-6.5. Wild-type RTA remains soluble at all the pH values tested.

***Figure 7.4 Stability measurements of E177D R180H RTA compared to wt RTA.***

A) *Thermal stability of E177D R180H RTA.* RTA was incubated at 40°C for 5 minutes at varying pH values in either MES or HEPES buffer. Denatured protein samples were pelleted by centrifugation and supernatant aliquots, resolved by SDS-PAGE on 15% gels. Remaining RTA was visualised by western blotting.

B) *Stability of E177D R180H RTA to proteolysis.* The sensitivity of E177D R180H RTA to proteolysis was measured by incubating RTA with 1% trypsin (w/w) over a range of pH values.

**A.** *Thermal stability of E177D R180H RTA at 40°C.*

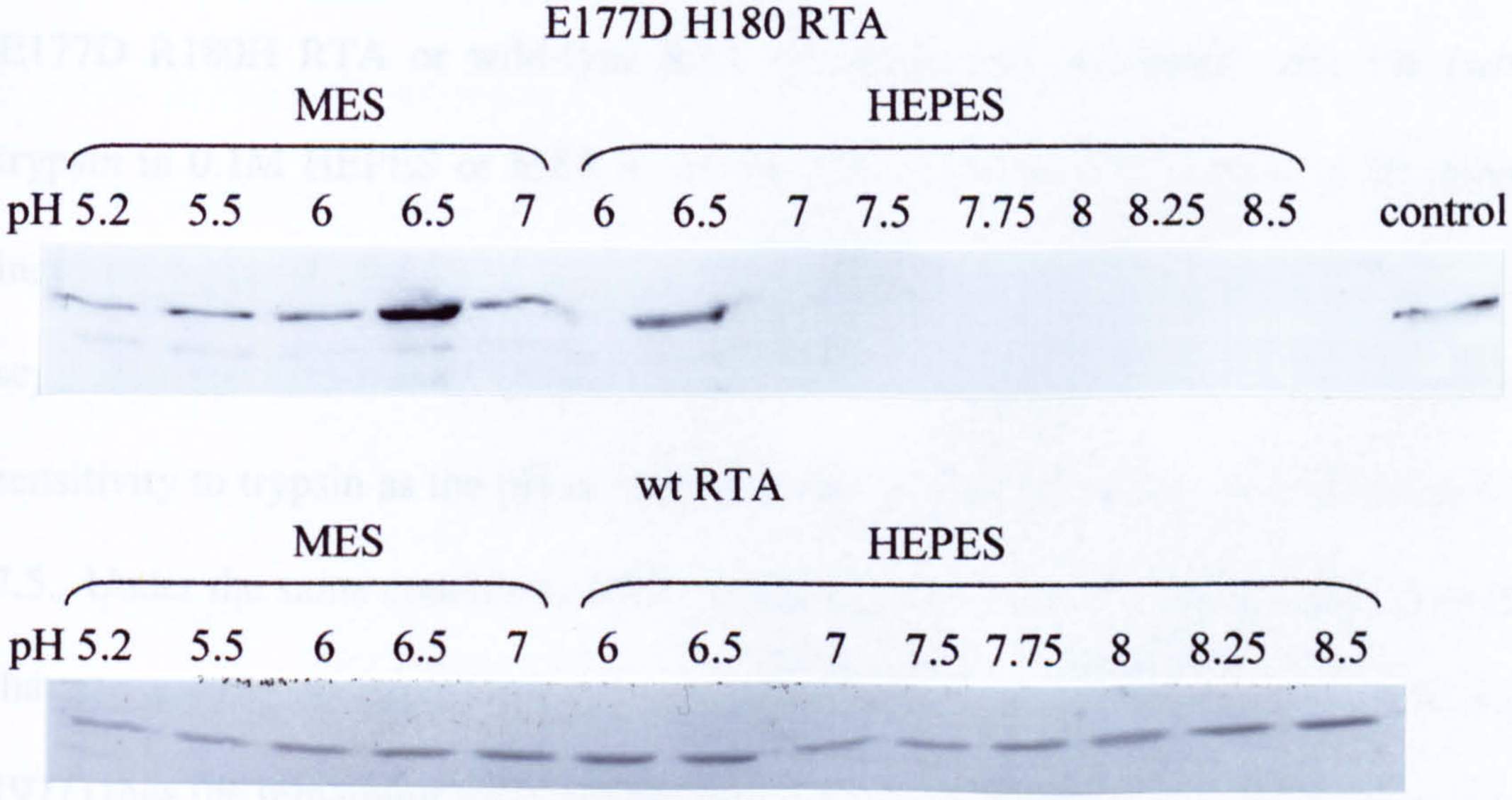


**B.** *Stability of E177D R180H to proteolysis.*

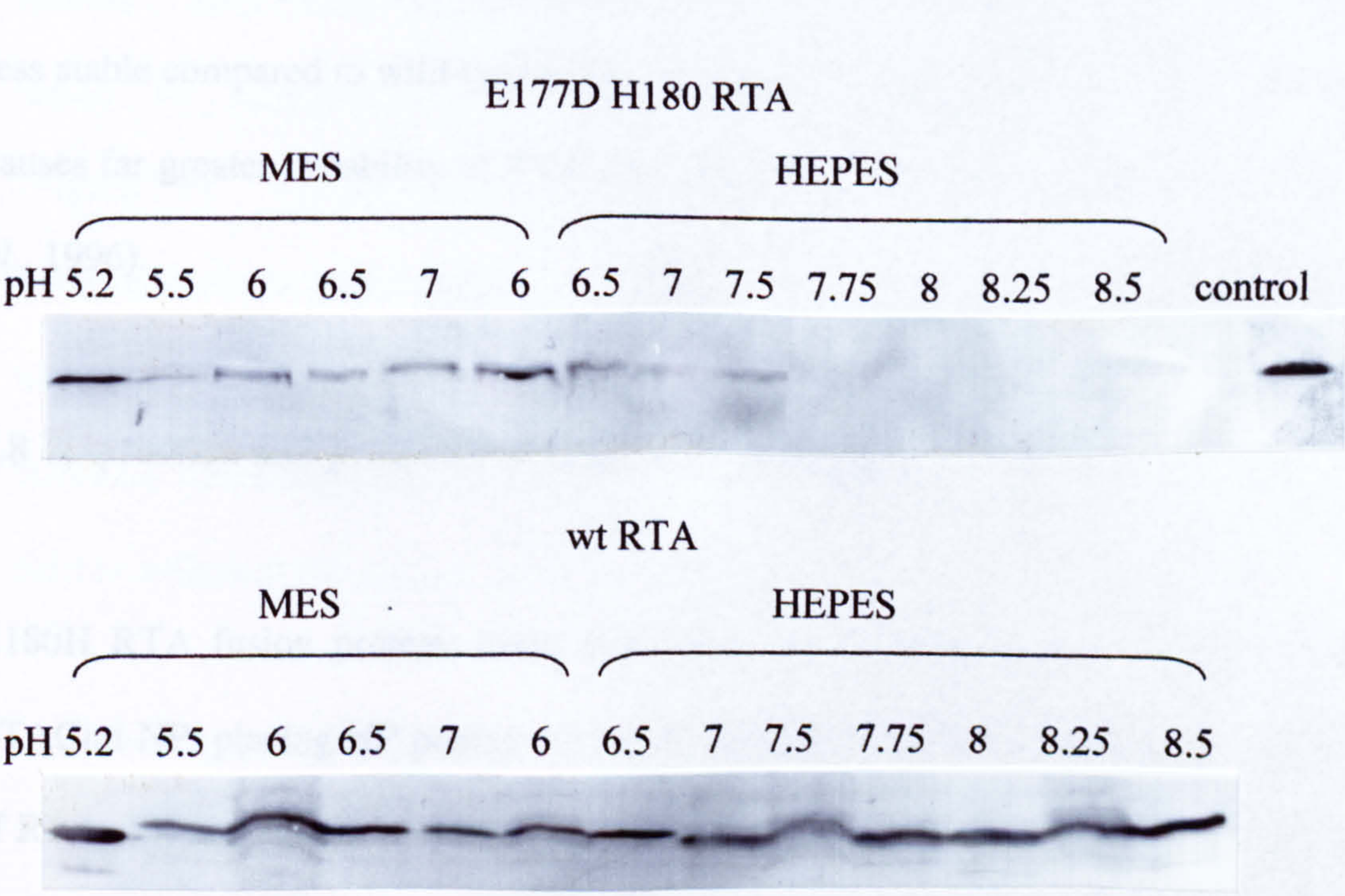

## 7.7 Tryptic digestion of E177D R180H RTA

E177D R180H RTA or wild-type RTA (1mg/ml) was incubated with 1% (w/w) trypsin in 0.1M HEPES or MES at various pH values at 37°C. After a 20 minute incubation period, the samples were boiled for 3 minutes with sample buffer and separated by SDS-PAGE (Figure 7.4). E177D R180H RTA shows increasing sensitivity to trypsin as the pH is increased and is only intact over the pH range 5.2-7.5. Under the same conditions RTA is visualised at all pH values. It must be noted that the activity of trypsin varies over the pH range tested (Spomer and Wooton, 1971) thus the remaining RTA in different pH buffers can not be directly compared.

The thermal and proteolytic stability data show that E177D R180H RTA is much less stable compared to wild-type RTA. As would be expected, the double mutation causes far greater instability of RTA than either of the mutations separately (Day *et al.*, 1996).

## 7.8 Expression and purification of R180H ricin fusion proteins

R180H RTA fusion proteins were expressed and purified as for E177D R180H RTAClaI-NP, placing NP peptide at the N-terminus of RTA or within the *Cla*I site of RTA. Typical yields were 2-4 mg per 500ml culture of each RTA fusion protein and reassociation with ricin B-chain was more efficient than that of the E177D R180H ricin-NP chimeras. Whereas reassociated E177D R180H ricin-NP chimeras could only clearly be visualised by Western blotting, reassociated R180H ricin-NP

bands could be seen by coomassie or silver-stained, non-reducing SDS-PAGE (Figure 7.5). It was possible to estimate the amounts of reassociated ricin fusions by comparing silver stained proteins of reassociated ricin, affinity purified on immobilised lactose prior to reducing SDS-PAGE, with known amounts of native RTA. Using these estimates of toxin concentrations, the cytotoxicity of the R180H ricin-NP toxins was calculated to be between 100-500 fold less than that of wild-type ricin (Figure 7.5). Day *et al.*, (1996) have reported a loss in activity of up to a 1000-fold with R180H ricin compared to wild-type ricin.

## 7.9 Ability of ricin fusion proteins to deliver exogenous antigen into the MHC class 1 presentation pathway.

R180H ricin-NP fusion proteins were incubated overnight with ricin-sensitive murine L cells (H2-$D^b$ haplotype) at 2.5ng/ml. L cells treated with the toxins were tested for sensitisation for lysis by Nucleoprotein 366-374-specific CTLs (Figure.7.6). Infection of L cells with a vaccinia virus encoding influenza Nucleoprotein sensitises them for lysis by matched CTL albeit at a relatively low level of 20%. However no killing is observed with L cells treated with the ricin-NP chimeras indicating that in this assay, ricin at this low concentration, is unable to deliver sufficient NP epitope into the MHC class-1 presentation pathway.

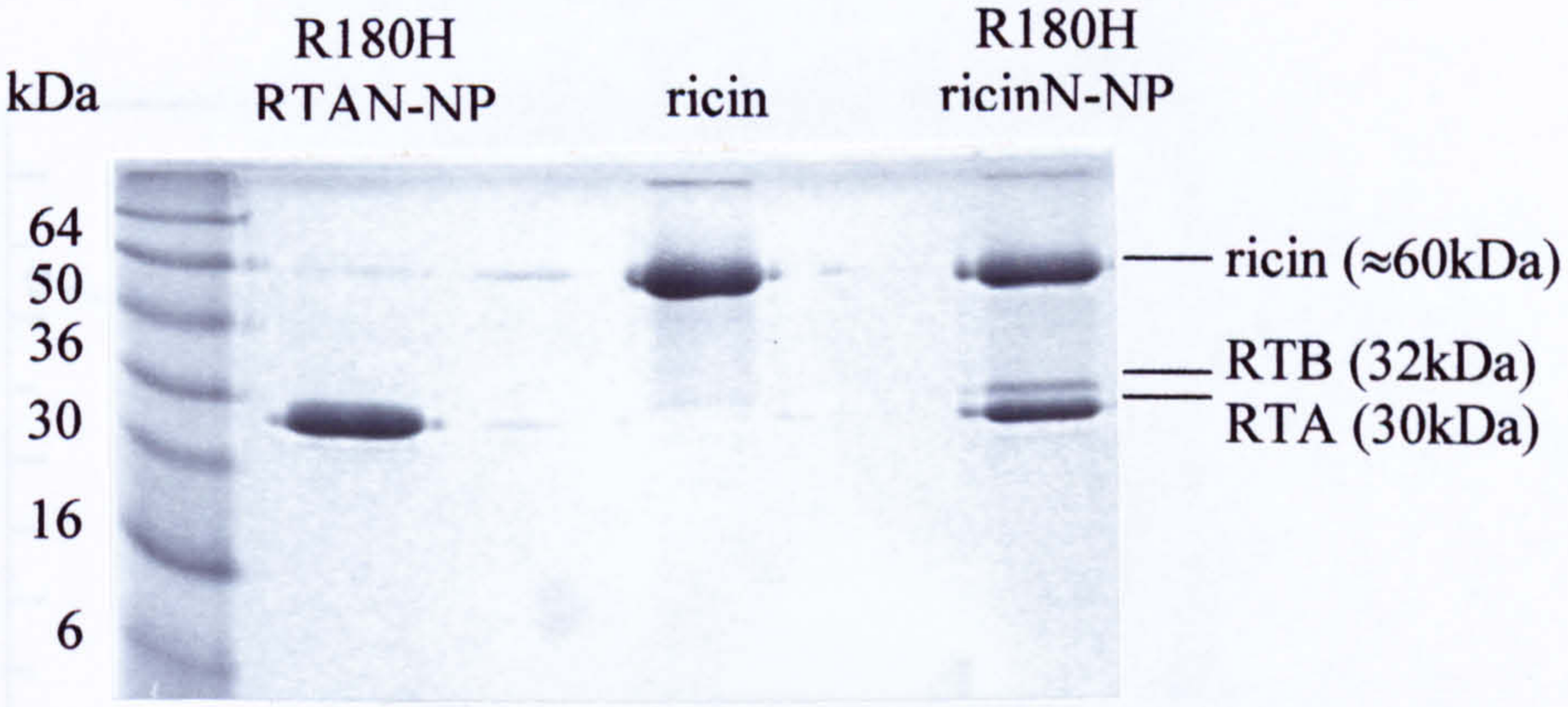


***Figure 7.5 Reassociation of purified RTA-NP fusion with RTB.***

Typically 50μg of ricin A-chain (RTA) was mixed with 50μg of ricin B-chain (RTB)(Inland Labs) in a total volume of 200μl in PBS, by gentle agitation on a tumbler at 4°C for 4 hours. *Reassociation of RTA with* RTB was confirmed by non-reducing SDS-PAGE. The R180H ricinN-NP reassociation mixture above (compared with control reassociated native ricin) consists of reassociated ricin together with remaining RTA and RTB. Free RTA may then be removed by applying the sample to a 0.5ml α-lactose (insolubilized on 6% beaded agarose) column equilibrated with PBS.

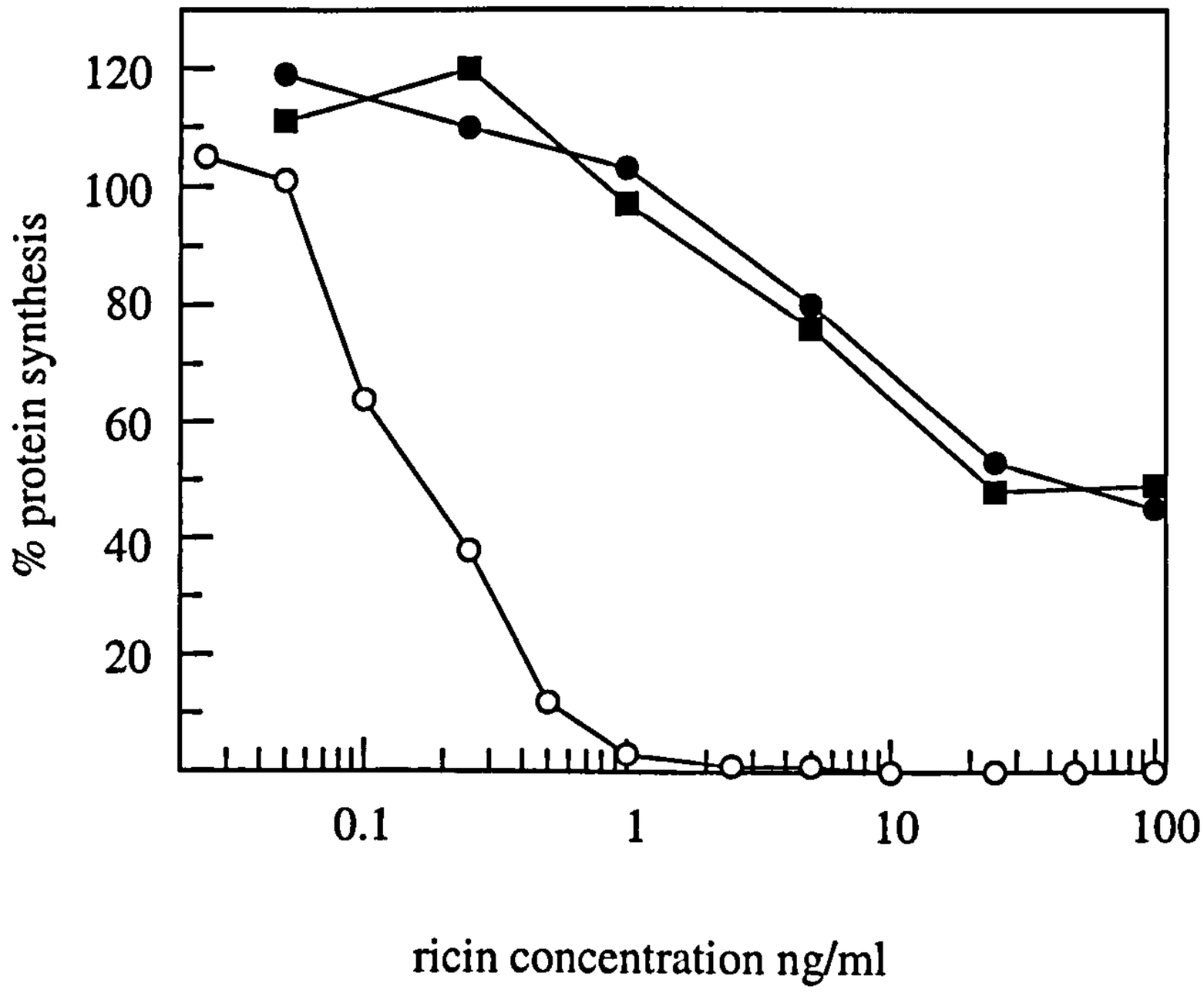


***Figure 7.6 Cytotoxicity comparison of wt ricin and R180H ricin-NP fusion proteins***

Cytotoxicity of ricin (○ ), R180H ricinN-NP (● ) and R180H ricinClaI-NP (■ ) towards L cells. Cells were incubated with various concentrations of ricin proteins, in quadruplicate, for 16 hours at 37°C before adding [$^{35}$S]-Methionine (1μCi/well) and incubating for a further 2 hours. Cell proteins were precipitated by washing with 5% trichloroacetic acid and radioactivity measured by liquid scintillation counting. Protein synthesis was measured by the incorporation of [$^{35}$S]-Methionine into protein and a percentage calculated in relation to toxin-free control cells.

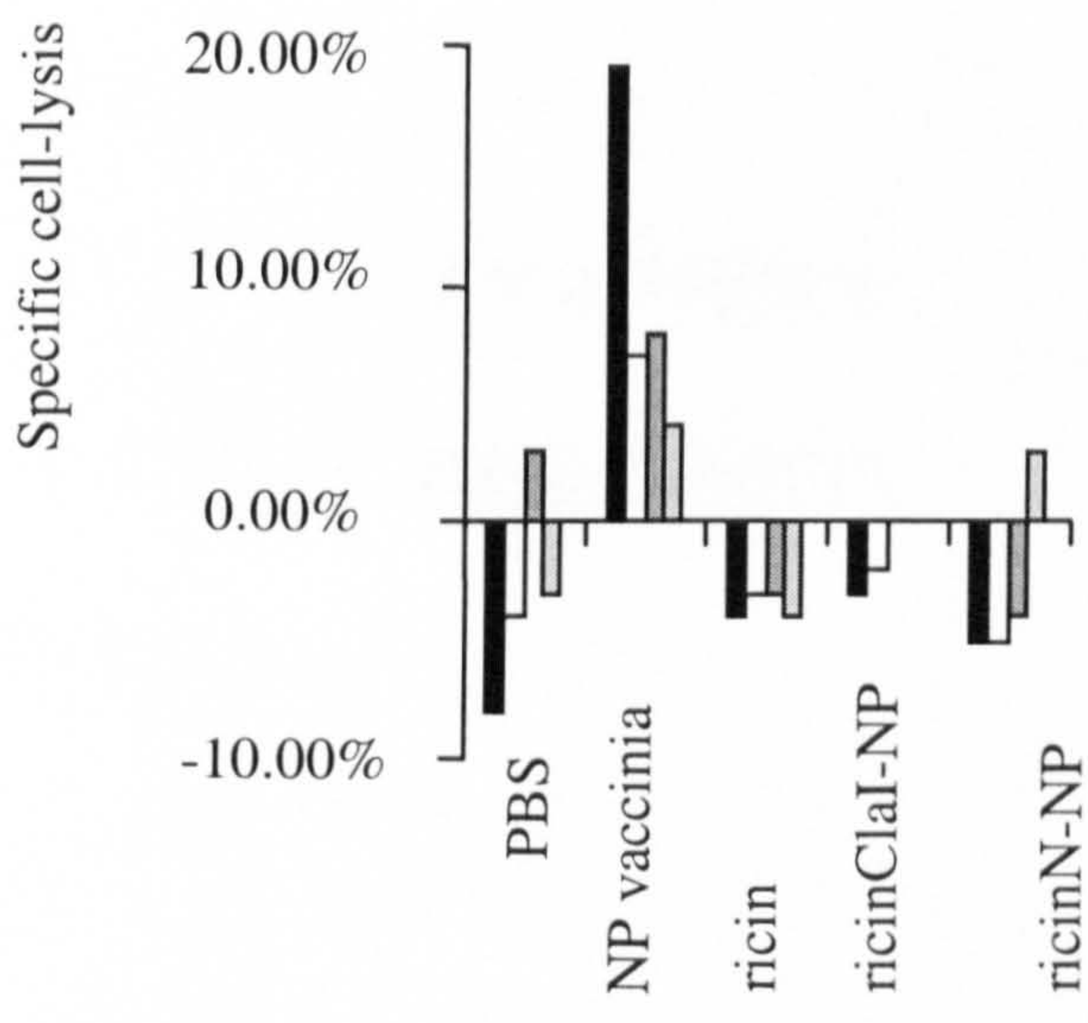


***Figure 7.7 $^{51}$ Cr-release CTL assay to assess the ability of ricin-NP fusions to deliver peptide to H2-D$^{b}$ class-1 molecules.***

L cells with an H2-D$^{b}$ haplotype were incubated overnight with H180 ricin-NP fusion proteins at 2.5ng/ml. The cells were then washed and labelled with $^{51}$ Chromium. Cells were then plated with CTLs at 20:1 (black bars), 10:1 (white bars), 5:1 (dark grey) or 2.5:1 (light grey) effector:target ratios and incubated for 4 hours at 37°C before $^{51}$ Cr-release counting. L cells were infected for 90 minutes with 5 plaque forming units (pfu)/cell of vaccinia virus encoding influenza Nucleoprotein (NP) at the same time as chromium labelling. Cells were then washed and allowed to express influenza Matrix protein for 3 hours prior to plating with CTLs.

# CHAPTER 8

# DISCUSSION

# Chapter 8

# Discussion

## 8.1 Overview.

These results describe how a disarmed SLT holotoxin, carrying a well defined peptide epitope for influenza virus Matrix protein at the N-terminus of SLT A-chain, can be used to deliver antigens for intracellular processing and presentation by MHC class-I molecules in cultured cells.

Other toxins (diphtheria (DT), anthrax toxin and *Pseudomonas* exotoxin A (PE)) have been used to deliver peptide epitopes to class-I MHC molecules (Stenmark *et al.*, 1991; Donelly *et al.;* 1993, Ballard *et al.;* 1996, Goletz *et al.;* 1997). DT and anthrax toxin lethal factor (LF) are known to translocate into the cytosol from acidified endosomes which is therefore the likely site of entry into the cytosol for the toxin-peptide chimeras. Presumably, these become processed cytosolically and the released peptides then delivered to MHC class-1 molecules via TAP transporters in the ER membrane.

PE, like SLT A-chain, is believed to translocate from the ER but unlike SLT, has never been visualised there. When PE was used to deliver antigenic peptides, treatment of target cells with brefeldin A had no effect on antigen presentation, although a requirement for PE-peptide internalisation had been shown by fixing cells at 4°C, thus blocking endocytosis and preventing sensitisation of target cells for lysis by CTLs. (Donelly *et al.*, 1993;Ulmer *et al.*, 1994). BFA inhibits both the transport

of PE to the ER and the association and transport of processed peptides with nascent HLA class-1 molecules. The authors proposed that the processing of PE-peptide fusions and the loading of peptide onto MHC class-1 molecules occurred in endosomes and that recycling of these complexes to the cell surface resulted in MHC-peptide presentation. It is still unclear whether MHC class-1 molecules can recycle via endosomes. Work by Neefjes *et al.*, (1990) suggests that only MHC class-II molecules recycle between endosomes and the cell surface. Using neuraminidase to cleave sialic acid from cell surface MHC class-I and class-II molecules, it was found that only MHC class-II molecules become resialated (an indication of recycling back to the trans Golgi network). Other results (Reid and Watts, 1990) using primaquine, a reagent known to slow the recycling of endocytosed receptors, suggest that both MHC class-I and class-II molecules recycle from the cell surface. However, whereas MHC class-II molecules load peptide well at low pH, the affinity for class-I molecules and peptide decreases 100 fold below pH7. It would therefore seem unlikely for MHC class-I molecules to load with peptide in acidic endosomes (pH6), which may suggest that in the PE fusion study by Ulmer *et al.*, (1994), the BFA used was not disrupting the Golgi totally.

The results from this study suggest that the processing and subsequent presentation of a peptide epitope delivered to class-I molecules by SLT involves the trafficking of the SLT-peptide chimeras to the ER of target cells. Treatment of HeLa-A2 cells with BFA successfully blocked the presentation of the M58-66 epitope by class-1 molecules at the cell surface.

## 8.2 Characterisation of E167DSLT and E167DSLT-Ma chimeras.

The activity of E167D SLT, purified to homogeneity from *E.coli* by receptor-ligand based chromatography, was assessed by *in vitro* ribosome-inactivation assays and *in vivo* cytotoxicity comparisons with wild-type SLT (Chapter 4). The $ID_{50}$ value of a toxin is the concentration of toxin which depurinates 50% of ribosomes. The $ID_{50}$ of wtSLT is 50pg/µl, when incubated with rabbit reticulocyte ribosomes (20-30µg) for 30 minutes at 30°C. Under the same conditions, the $ID_{50}$ of E167D SLT was calculated to be 5180pg/µl, a 100 fold decrease in *in vitro* ribosome depurination activity compared to wtSLT. The $IC_{50}$ value of a toxin is the concentration of toxin causing 50% inhibition of cellular protein synthesis under the assay conditions used. The $IC_{50}$ of E167D SLT was calculated to be 10ng/ml compared to 0.01ng/ml for wtSLT when incubated overnight with HeLa-A2 cells. This represents a 1000 fold loss in activity.

To ensure that the presence of the M58-66 peptide did not interfere with normal trafficking of the toxin moiety, the peptide was genetically fused to the wild type toxin and its activity compared to that of naked wtSLT. The modified holotoxins were designated SLTN-Ma or SLTC-Ma, depending whether M58-66 is located at the N- or C-terminus of the A-chain. The wtSLT fusions were as potent as wtSLT with an $IC_{50}$ value of 0.01ng/ml on HeLa-A2 cells. The peptide chimeras engineered using E167D SLT were, as expected, approximately 1000 fold less toxic. Furthermore, the toxicity of wtSLTN-Ma was completely blocked when HeLa-A2 cells were pre-treated with brefeldin A to collapse the Golgi stack. This implies that the uptake pathway of the SLT-Ma chimeras is identical to that of native toxin.

To confirm the entirety of the influenza Matrix peptide within the SLT-Ma fusion proteins, the toxin chimeras were analysed by electrospray ionization (ESI) mass spectrometry. The presence of the full influenza Matrix nonamer in both constructs was confirmed with molecular masses of 33148.47 +/- 0.31 and 33148.08 +/- 2.83 Da for SLT N-Ma and C-Ma respectively (predicted mass 33148.47) when the fusion proteins were purified in the presence of a protease inhibitor cocktail (Boehringer Mannheim).

## 8.3 HeLa-A2 cells incubated with SLTN-Ma but not SLTC-Ma are sensitised for lysis by Matrix specific CTL.

Hela-A2 cells treated with 20ng/ml SLTN-Ma (equivalent to 0.6nM) were sensitised for lysis by Matrix 58-66 specific CTL (Chapter 5). In contrast, no lysis was observed after the addition of SLTC-Ma, even though it was shown by cytotoxicity assays to be internalised by HeLa-A2 cells. Presentation of the M58-66 epitope contained within the full length Matrix protein and SLTN-Ma was enhanced by interferon-γ treatment. This is consistent with a IFN-γ-dependent upregulation of the class-1 processing and presentation pathway. Indeed, expression of the MHC-encoded proteasomal subunits, LMP2 and LMP7, was significantly enhanced after incubation of HeLa cells with IFN-γ as shown by Western blotting using anti-LMP2 and anti-LMP7 mouse monoclonal antibodies. FACS analysis of IFN-γ treated HeLA-A2 cells also confirmed that MHC class 1 molecules are generally upregulated by IFN-γ.

An additional effect of IFN-γ treatment, which may contribute to the enhancement of delivery and presentation of the M58-66 epitope by SLTN-Ma, is that wtSLTN-Ma cytotoxicity is increased 3-fold when HeLa-A2 cells are pretreated with interferon-γ. This is likely to be due to an overall upregulation of trafficking in the cell by IFN-γ .

## 8.4 The M58-66 epitope must be internalised to sensitise target cells for lysis.

To confirm that the M58-66 epitope of SLTN-Ma was generated by intracellular proteases rather than serum proteases, the melanoma line Skmel-29, which is naturally resistant to SLT was used as target cells. Skmel-29, whilst sensitised for lysis when free A2-MAGE-3 peptide 271-279 was applied, were not sensitised for lysis by the addition of 20ng/ml SLTN-Ma to cells. In addition, treatment of HeLa-A2 cells with BFA successfully blocked the presentation of the M58-66 epitope by class-1 molecules at the cell surface. The finding that BFA also blocks the cytotoxicity of wild-type SLTN-Ma suggests that the fusions follow the same pathway as native SLT, a route via the Golgi to the ER. Since BFA could inhibit both the transport of SLTN-Ma to the ER and the association and transport of processed peptides with nascent class-I molecules to the cell surface, its exact mode of inhibition remains unclear. However as described earlier (section 8.1), it seems unlikely that peptide loading of MHC class-1 molecules can occur in endosomes as the affinity for class-1 molecules and peptide is low below pH7.

## 8.5 The generation of the M58-66 epitope from SLTN-Ma is independent of proteasomal processing.

The proteasomal inhibitor lactacystin did not block the processing and presentation of the M58-66 epitope from SLTN-Ma as has also been shown for the full length influenza Matrix protein (V. Cerundolo, personal communication). This suggests that non-proteasomal cytosolic proteases may be involved in the generation of the M58-66 epitope. Although it is clear that proteasomes play an important role in the processing of antigens for presentation by the MHC class-I pathway it has become apparent that there are other proteolytic systems that compensate for the loss of proteasomal activity, induced by the addition of proteasomal inhibitors such as lactacystin (Glas *et al.*, 1998). Alternative processing in the ER has been suggested (Elliot *et al.*, 1995, Snyder *et al.*, 1997). Studies with minigenes encoding peptide epitope precursors, preceded by the influenza hemagglutinin ER translocation sequence, have shown that processing of polypeptides of at least 40 residues can occur in the ER of TAP-negative cell-lines. Recently antigen processing in the secretory pathway has been investigated with a role for the Golgi-resident protease, furin in alternative processing pathways (Gil-Torregrosa *et al.*, 1998), which is of interest for SLT fusion proteins which reach the ER via the Golgi. Furin is the cellular enzyme responsible for the proteolytic cleavage and separation of the two A-chain domains necessary for the full activity of SLT (Garred *et al.*, 1995).

It is unclear where in the cell (ER or cytosol), the SLT-Ma chimeras are being processed. If processing of the SLT-Ma fusions is dependent on cytosolic proteases, this may explain why peptide presentation by class-1 molecules did not occur when

cells were treated with SLTC-Ma. SLTC-Ma has M58-66 located at the C-terminal end of the A2 fragment, a region that is unlikely to translocate from the ER to the cytosol. This observation is made from studies of cholera toxin, (Majoul *et al.*, 1996), another $AB_5$ structure bacterial toxin where the A1 fragment alone is known to translocate to the cytosol after its reduction from the A2 fragment in the ER lumen. SLTN-Ma contains the antigenic peptide on the A1 fragment which is normally the catalytic portion of the toxin that is capable of reaching the cytosol. Therefore a fusion with Ma at the N-terminus of SLT would be predicted to reach the cytosol for processing if this event were not possible in the ER lumen.

## 8.6 Catalytic activity and stability measurements of a novel 'double' active-site substitution of ricin A-chain.

The advantage of creating ricin fusion proteins is the potential to deliver peptide to all cells, including professional antigen presenting cells, such as dendritic cells. In addition, a drawback to using any 'carrier' system as a vaccine is that eventually the recipient will raise an immune response against the carrier protein itself and the vaccine will no longer be effective. It is therefore important to test as many delivery vehicles as possible for their ability to deliver exogenous antigen MHC to class-1 molecules. A long-term protective CTL-vaccine programme may necessitate the use of alternate antigen-carriers.

Ideally, a peptide delivery system should be non-toxic. This can be achieved using SLT by fusing peptides to the SLT B-chain and expressing the B-chain chimera alone but this is impossible with ricin as the B-chain is unstable when expressed

without ricin A-chain. The catalytic mutations E177D and R180H of ricin A-chain were combined in an attempt to produce a catalytically inactive mutant ricin. The *in vitro* ribosome depurination activity of E177D R180H was assessed by aniline-cleavage assays and the catalytic activity of E177D R180H RTA estimated to be a 1000-fold down from wild-type RTA (Chapter 7). At 100ng/ml reassociated E177D R180H ricin, no activity was seen against HeLa cells compared to an $IC_{50}$ of 0.1ng/ml calculated for wild-type ricin.

However E177D R180H RTA was found to be unstable, lasting only 2-3 weeks at 4°C before precipitating. This instability was confirmed by testing the thermal stability of the mutant RTA and its sensitivity to proteolysis over a range of pH values. The addition of a peptide (M58-66 or NP366-374) at the N-terminus of E177D R180H RTA further destabilised the protein and altered the binding affinity of RTA for CM-Sepharose leading to the conclusion that E177D R180H ricin was an unsuitable vehicle for peptide delivery.

## 8.7 Construction of R180H ricin chimeras for the delivery of NP 366-374 epitope to MHC class-1 molecules.

R180H RTA fusion proteins placing influenza Nucleoprotein 366-374 (NP) peptide at the N-terminus of RTA or within the *Cla*I site of RTA were reassociated with ricin B-chain. The generation of the NP366-374 epitope from full length influenza Nucleoprotein has been shown to be dependent on proteasomal processing (V. Cerundolo, personal communication). Thus the ricin fusion proteins are of interest as their processing requirements can be studied using the proteasome inhibitor

lactacystin. In addition, the importance of epitope position (at the end or within a toxin subunit) can be investigated.

Murine L cells (H-2D$^b$ haplotype) treated with the ricin-NP chimeras (2.5ng/ml) were tested for sensitisation to lysis by Nucleoprotein 366-374-specific CTL. Infection of L cells with a vaccinia virus encoding influenza Nucleoprotein sensitises them for lysis by matched CTL albeit at a low level. However no killing is observed with L cells treated with a low concentration of ricin-NP chimeras indicating that in this assay and at the toxin concentration tested, ricin is unable to deliver NP into the MHC class-1 pathway. Further experiments are necessary to determine whether cells are sensitised for lysis by CTL when treated with higher concentrations of ricin-NP fusions. Successful SLT or ricin fusions could then be titrated to calculate the maximum concentration limit of each toxin and the highest obtainable percentage specific cell lysis.

## 8.8 Future directions for the exploitation of RIPs in antigen delivery.

The delivery of a single peptide epitope to MHC class-1 molecules is clearly only useful as a model system, which was the intent of this research project. An effective CD8+ T cell-vaccine should generate a range of antigenic peptides suitable for presentation by a number of class-1 haplotypes present in the population. Thus a useful vaccine approach would be to deliver a whole antigenic protein into the MHC class-1 processing pathway.

Recently, the B chain of Shiga-toxin (ST) has been used to successfully deliver a peptide from the Mage 1 tumour antigen to MHC class-1 molecules (Lee *et al.*., 1998). Processing and presentation appeared to involve trafficking of toxin chimeras to the ER of target cells. Both subunits of the ST/SLT family have therefore been shown to deliver peptide to class-1 molecules. The B fragment of ST/SLT has the advantage of being non toxic to cells but is believed not to translocate to the cytosol from the ER (unpublished observations from the toxin group laboratory). SLT holotoxin with its membrane translocating A chain component may therefore be of greater utility when whole antigens are to be delivered if there is a requirement for conventional proteasomal degradation.

SLT holotoxin vaccines may be of additional value; It is interesting to note that a theory has been suggested that the immune system only responds to a threat when cell damage or death occurs in the host (Matzinger *et al.*, 1998) It is at this point that damaged or dying cells send out an additional signal that allows the initiation of an immune response. If this is the case then low level cytotoxicity may be beneficial, for instance, in certain tumour vaccines.

As noted above (section 6.8) it is important to test other toxins for their use in peptide delivery since the recipient of a vaccine will eventually raise an immune response against the carrier protein itself (or may have been vaccinated against the vaccine vehicle). Ricin fusion proteins offer the potential to deliver peptide to all cells. Professional antigen presenting cells (APCs), such as dendritic cells appear to be critical for the initiation of an immune response (Cayeux *et al.*, 1999), providing

the necessary non-specific co-stimulatory signal, required to prime antigen-specific CTL. The sensitivity of APCs to SLT and ricin should be investigated.

The antigenic properties of the carrier toxins are also important in vaccine design. MHC class-II peptide presentation and induction of CD4+ T helper cell signalling is thought to be required for the production of long-lived memory CTLs (Ridge *et al.*, 1996). Class-II-specific epitopes may be generated from the processing of the carrier toxin. Alternatively class-II specific peptides may be encoded within the toxin. These issues may be better addressed by investigating the delivery of peptides by SLT and ricin using an animal model. This is the long term goal of future research in this area.

## 8.9 The future of vaccines

Although live or attenuated virus vaccines such as polio, measles, mumps and rubella, have been very successful. For certain pathogens, such as HIV, there have been safety concerns about the reversion of attenuated vaccine strains to virulent phenotypes. In addition there have been concerns over the potential side-effects of certain vaccines, for example the combination measles/mumps/rubella (MMR) vaccine that may out-way the benefits of the vaccine. This has led to the research for safer vaccine vehicles, some of which have reached the stage of clinical trials.

DNA vaccines in clinical trials include vaccines against hepatitis B, genital herpes and an influenza virus vaccine. The advantages of DNA vectors in vaccine design is that they encode multiple epitopes for many HLA allelles. This is also true for

mRNA-based vaccines. A disadvantage of plasmid DNA encoded vaccines is that chromosomal intergration of foreign DNA may occur. If after vaccination, DNA is taken up by fetal or germ-line cells, immunological tolerance may be induced in the progeny. Tolerant progeny would be more susceptible to infection or may become carriers which would affect the whole population. RNA-vaccines are a safer option but RNA itself is extremely labile, in contrast to DNA vaccines that are stable and do not require cold-storage. In addition, DNA-vaccines that encode antigens under the control of a strong eukaryotic promoter (usually cytomegalovirus enhancer-promoter) have generated a sustained humoral and cell-mediated response. Thus the benefits of DNA-based vaccines may outweigh the potential risks of chromosomal integration.

In animal models (mice and chimpanzees), protection against Ebola virus (Xu *et al.*, 1998), malaria (Schneider *et al.*, 1998) and HIV (Hanke *et al.*,1999) have been reported by use of DNA-based vaccination that correlate with high levels of activated CTLs in the spleens of animals. T cell induction has been enhanced by the subsequent boosting of DNA vaccines with a modified vaccinia virus (MVA) (Hanke *et al.*, 1999). Used together, the level of CTL induction is far greater than if either of the vectors were used as both the priming and boosting vaccine. If combinations of vaccine vectors raises the protective immune response against pathogens then it is important to have a number of vaccine vehicles capable of eliciting a MHC class I restricted CTL response. Disarmed toxins may therefore in the future be used in combination with other vaccines. Another important factor is that if boosting is required to maintain protective cellular immunity then eventually antibodies against the vaccine vector will be raised upon subsequent immunization.

One of the drawbacks to viral or bacterial based vaccines is that neutralizing antibodies already exist for example by previous exposure to crossreacting viruses (a problem with adenovirus vectors) or previous immunization (vaccinia) (Pardoll *et al.*, 1998). Therefore the continued study of alternative T-cell vaccine vehicles is an important aspect in the progress towards safe and protective immunization regimes

# CHAPTER 9

# REFERENCES

## Chapter 9

## References


**Argent, R.H., Roberts, L.M., Wales, R., Robertus, J.D. and Lord, J.M.** (1994). Introduction of a disulfide bond into ricin A chain decreases the cytotoxicity of the ricin holotoxin. *J. Biol. Chem.* **269**, 26705-26710.

**Austin, P.R., Jablonski, P.E., Bohach, G.A., Dunker, A.K. and Hovde, C.J.** (1994). Evidence that the A2 fragment of Shiga-like toxin type 1 is required for holotoxin integrity. *Infect. Immun.* **62**, 1768-1775.

**Ballard, D.J., Collier, R.J. and Starnbach, M.N.** (1996). Anthrax-toxin mediated delivery of a cytotoxic T-cell epitope *in vivo*. *Proc. Natl. Acad. Sci. USA* **93**, 12531-12534.

**Ballard, J.D., Doling, A.M., Beauregard, K., Collier, R.J. and Starnbach, M.N.** (1998). Anthrax-toxin mediated delivery *in vivo* and *in vitro* of a cytotoxic T-lymphocyte epitope from ovalbumin. *Infect. Immun.* **66**, 615-619

**Bijlmakers, M.E., Benaroch, P. and Ploegh, H.L.** (1994). Mapping functional regions in the luminal domain of the class II-associated invariant chain. *J. Exp. Med.* **180**, 623-629.

**Boes, B., Hengel, H., Ruppert, T., Multhaup, G., Koszinowski, U.H. and Kloetzel, P.M.** (1994). Interferon gamma stimulation modulates the proteolytic activity and cleavage site preference of 20S mouse proteasomes. *J. Exp. Med.* **179**, 901-909.

**Bona, C.A., Casares, S. and Brumeanu, T-D.** (1998). Toward development of T-cell vaccines. *Immunol. Today* **19**, 126-133.

**Brachet, V., Raposo, G., Amigorena, S. and Mellman, I.** (1997). Ii controls the transport of major histocompatibility class II molecules to and from lysosomes. *J. Cell Biol.* **137**, 51-65.

**Bradley, J.L. and Mcguire, P.M.** (1990). Sire-directed mutagenesis of a ricin A chain Trp-211 to Phe. *Int. J. Pept. Protein Res.* **35**, 365-366.

**Brodsky, J.L. and McCracken, A.A.** (1997). ER-associated and proteasome mediated protein degradation: how two topologically restricted events come together. *Trends Cell Biol.* **7**, 151-156.

**Brown, M.G., Driscoll, J. and Monaco, J.J.** (1991). Structural and serological similarity of MHC-limked LMP and proteasome (multicatalytic proteinase) complexes. *Nature* **353**, 355-357.

**Calderwood, S.B., Auclair, F., Donohue-Rolfe, A., Keusch, G.T. and Mekalanos, J.J.** (1987). Nucleotide sequence of the Shiga-like toxin genes of *Escherichia coli*. *Proc. Natl. Acad. Sci. USA* **84**, 4364-4368.

**Cayeux, S., Richer, G., Becker, C., Pezzutto, A., Dorken, B. and Blankenstein, T.** (1999). Direct and indirect T cell priming by dendritic cell vaccines. *Eur. J. Immunol.* **29**, 225-234.

**Cerundolo, V. and Braud, V.** (1996). Cell biology of MHC class-I molecules. In *HLA and MHC*, pp.193. Edited by Browning and A.J. McMichael. Oxford: BIOS Scientific publishers.

**Cerundolo, V., Benham, A., Braud, V., Mukherjee, S., Gould, K., Macino, B., Neefjes, J. and Townsend, A.** (1997). The proteasome-specific inhibitor lactacystin blocks presentation of cytotoxic T lymphocytes epitopes in human and murine cells. *Eur. J. Immunol.* **27**, 336-341.

**Chapman, H.** (1998). Endosomal proteolysis and MHC class II function. *Curr. Opin. Immunol.* **10**, 57-58.

**Chaudhary, V., Jinno, K.Y., Fitzgerald, D. and Pastan, I.** (1990). *Pseudomonas* exotoxin contains a specific sequence at the carboxyl terminus that is required for cytotoxicity. *Proc. Natl. Acad. Sci. USA* **87**, 308-312.

**Cohen A., Hannigan, G.E., Williams, B.R.G. and Lingwood, C.A.** (1987). Roles of globotriosyl and galabiosylceramide in verotoxin binding and high affinity interferon receptor. *J. Biol. Chem.* **262**, 17088-17091.

**Cresswell, P.** (1994). Assembly, transport and function of MHC class II molecules. *Annu. Rev. Immunol.* **12**, 259-293.

**Day, P.J., Ernst, S.R., Frankel, A.E., Monzingo, A.F., Pascal, J.M., Molina-Svinth, M.C. and Robertus, J.D.** (1996). Structure and activity of an active site substitution of ricin A chain. *Biochemistry* **35**, 11098-11103.

**Degen, E., Cohen-Doyle, M.F., Williams, D.B.** (1992). Efficient dissociation of the p88 chaperone from major histcompatibility complex class I molecules requires both $\beta_2$–microglobulin and peptide. *J. Exp. Med.* **180**, 2163-2171.

**Deng, H., Apple, R., Clare-Salzler, M., Trembleau, S., Mathis, D., Adorini, L. and Sercarz, E.** (1993). Determinant capture as a possible mechanism of protection afforded by major histocompatibility complex class II molecules in autoimmune disease. *J. Exp. Med.* **178**, 1675-1680.

**Deresiewicz, R.L., Calderwood, S.B., Robertus, J.D. and Collier, R.J.** (1992). Mutations affecting the activity of the Shiga-like toxin 1 A-chain. *Biochem.* **31**, 3272-3280.

**Donelly, J.J., Ulmer, J.B., Hawe, L.A., Friedman, A., Shi, X-P, Leander, K.R., Shiver, J.W., Oliff, A.I., Martinez, D., Montgommery, D. and Liu, M.A.** (1993). Targeted delivery of peptide epitopes to class-I major histocompatibility molecules by a modified *Pseudomonas* exotoxin. *Proc. Natl. Acad. Sci. USA* **90**, 3530-3534.

**Driscoll, J., Brown, M., Finley, D. and Monaco, J.** (1993). MHC-linked LMP gene products specifically alter peptidase activities of the proteasome. *Nature* **365**, 252-264.

**Elliott, T., Smith, M., Driscoll, P. and McMichael, A.J.** (1993). Peptide selection by class 1 molecules of the major histocompatibility complex. *Curr. Biol.* **3**, 854-864

**Elliott, T., Willis, A., Cerundolo, V. and Townsend, A.** (1995). Processing of Major Histocompatibility Class-1 restricted antigens in the Endoplasmic Reticulum. *J. Exp. Med.* **181**, 1481-1491.

**Endo, Y., Mitsui, K., Motizuki, M. and Tsurugi, K.** (1987). The mechanism of ricin and related toxins on eukaryotic ribosomes. *J. Biol. Chem.* **262**, 5908-5912

**Endo, Y. and Tsurugi, K.** (1988). The RNA-N-glycosidase activity of ricin A chain-The characteristics of the enzymatic-activity of ricin A-chain with ribosomes and with ribosomal-RNA. *J. Biol. Chem.* **263,** 8735-8739.

**Fehling, H., Swat, W., Laplace, C., Kuhn, R., Rajewsky, K., Muller, U. and Boehmer, H.V.** (1994). MHC class I expression in mice lacking the proteasome subunit LMP7. *Science* **265**, 1234-1237.

**Fraser, M.E., Chernaia, M.M., Kovlov, Y.V. and James, M.N.G.** (1994). Crystal structure of the holotoxin from *Shigella dysenteriae* at 2.5 Å resolution. *Struc. Biol.* **1**, 59-64.

**Gareed, O., Deurs, B. and Sandvig. K.,** (1995a). Furin-induced cleavage and activiation of Shiga toxin. *J. Biol. Chem.* **270,** 10817-10821.

**Gareed, O., Dubinina, E., Holm, P.K., Olsnes, S., van Deurs, B., Kozlov, J.V. and Sandvig, K.** (1995). Role of processing and intracellular transport for optimal toxicity of Shiga toxin and toxin mutants. *Exp. Cell Res.* **218**, 39-49.

**Gaczynska, M., Rock, K.L. and Goldberg, A.L.** (1993). Gamma-interferon and expression of MHC genes regulate peptide hydrolysis by proteasomes. *Nature* **365**, 264-267.

**Gaczynska, M., Rock, K.L., Spies, T. and Goldberg, A.L.** (1994). Peptidase activities of proteasomes are differentially regulated by the major histocompatbility complex-encoded genes for LMP2 and LMP7. *Proc. Natl. Acad. USA* **91**, 9213-9217.

**Gil-Torregrosa, B.C., Castaño, A.R. and Del Val, M.** (1998). Major Histocompatibility Complex class I viral antigen processing in the secretory pathway defined by the *trans*-Golgi network protease furin. *J. Exp. Med.* **6**, 1105-1116.

**Glas, R., Bogyo, B., McMaster, J.S., Gaczynska, M and Ploegh, H.L.** (1998). A proteolytic system that compensates for loss of proteasome function. *Nature* **392**, 618-622.

**Goletz, T.J., Klimpel, K.R., Arora, N., Leppla, S.H., Keith, J.M. and Berzofsky, J.A.** (1997). Targeting HIV proteins to the major histocompatibility complex class-I processing pathway with a novel gp120-anthrax toxin fusion protein. *Proc. Natl. Acad. Sci. USA* **94**, 12059-12064.

**Groettrup, M., Ruppert, T., Kuehn, L., Seeger, M., Standera, S., Koszinowski, U. and Kloetzel, P.M.** (1995). The interferon-gamma-inducible 11S regulator (PA28) and the LMP2/LMP7 subunits govern the peptide production of the 20S proteasome *in vitro*. *J. Biol. Chem.* **270**, 23808-23815.

**Halling, K.C., Halling, A.C., Murray, E.E., Ladin, B.F., Houston, L.L. and Weaver R.F.** (1985). Genomic cloning and characterisation of a ricin gene from *Ricinus communis*. *Nucleic Acids Res.* **13**, 8019-8033.

**Hanke, T., Neumann, V.C., Blanchard, T.J., Sweeney, P., Hill, A.V.S., Smith, G.L. and McMichael, A.** (1999). Effective induction of HIV-specific CTL by multiple-epitope gene gun in a combined vaccine regime. *Vaccine* **17**, 589-596.

**Harding, C.V., France, J., Song, R., Farah, J.M., Chatterjee, S., Iqbal, M. and Simon, R.** (1995). Novel dipeptide aldehydes are proteasome inhibitors and block the MHC-I antigen processing pathway. *J. Immunol.* **155**, 1767-1775.

**Hartley, M.R., Legname, G., Osborn, R., Chen, Z. and Lord, J.M.** (1991). Single-chain ribosome inactivating proteins from plants depurinate *E.coli* 23S ribosomal-RNA. *FEBS Lett.* **290**, 65-68.

**Heus, H.A. and Pardi, A.** (1991). Structural features that give rise to the unusual stability of RNA hairpins containing GRNA loops. *Science* **253**, 191-194

**Hiller, M.M., Finger, A., Schweiger, M. and Wolf, D.** (1996). ER degradation of a misfolded luminal protein by the cytosolic ubiquitin-proteasome pathway. *Science* **273**, 1725-1728.

**Hovde, C.J., Calderwood, S.B., Mekalanos, J.J. and Collier, R.J.** (1988). Evidence that glutamic acid 167 is an active-site residue of Shiga-like toxin-1. *Proc. Natl. Acad. Sci.* **85**, 2568-2572.

**Hughes, E.A., Ortmann, B., Surman, M. and Cresswell, P.** (1996). The protease inhibitor, *N*-acetyl-L-leucyl-L-norleucinal, decreases the pool of major histocompatibility complex class I binding peptides and inhibits peptide trimming in the endoplasmic reticulum. *J. Exp. Med.* **183**, 1569-1578.

**Hughes, E.A. and Cresswell, P.** (1998). A role for the thiol-dependent reductase Erp57 in the assembly of MHC class-I molecules. *Curr. Biol.* **8**, 709-712.

**Jackson, M.R., Cohen-Doyle, M.F., Peterson, P.A. and Williams, D.** (1994). Regulation of MHC class I transport by the molecular chaperone, calnexin. *Science* **263**, 384-387.

**Jardetzky, T.S., Brown, J.H., Gorga, J.C., Stern, L.J., Urban, R.G., Strominger, J.L. and Wiley, D.C.** (1996). Crystallographic analysis of endogenous peptides associated with HLA-DR1 suggests a common, polyproline II-like conformation for bound peptides. *Proc. Natl. Acad. Sci. USA* **93**, 734-738.

**Johannes, L., Tenza, D., Anthony, C. and Goud, B.** (1997). Retrograde transport of KDEL-bearing B-fragment of Shiga toxin. *J. Biol. Chem.* **272**, 19554-19561.

**Joseph, K.C., Kim, S.U., Stieber, A. and Gonatas, N.K.** (1978). *Proc. Natl. Acad. Sci., USA* **75**, 2815-2819.

**Joyce, S.** (1997). Traffic control of completely assembled MHC class I molecules beyond the Endoplasmic reticulum. *J. Mol. Biol.* **266**, 993-1001.

**Kaufman, S.,** (1999). Cell-mediated immunity: Dealing a direct blow to pathogens. *Curr. Biol.* **9**, 97-99.

**Kirberg, J., Baron, A., Jakob, S., Rolink, A., Karjalainen, K. and von Boehmer, H.** (1994). Thymic selection of CD8+ single positive cells with a class-II major histcompatibility complex-restricted receptor. *J. Exp. Med.* **180**, 25-34.

**Kuckelhorn, U., Frentzel, S., Kraft, R., Kostka, S., Groettrup, M. and Kloetzel, P.M.** (1995). Incorporation of major histcompatibility complex encoded subunits LMP2 and LMP7 changes the quality of the 20S proteasome polypeptide processing products independent of interferon-gamma. *Eur. J. Immunol.* **25**, 2605-2611.

**Lee, R.S., Tartour, E., van der Bruggen, P., Vantomme, V., Joyeux, I., Goud, B., Fridman, W.H. and Johannes, L.** (1998). Major histocompatibility complex class 1 presentation of exogenous soluble tumor antigen fused to the B-fragment of Shiga-toxin. *Eur. J. Immunol.* **28**, 2726-2737.

**Lippincott-Schwartz, J., Donaldson, J.G., Schweizer, A., Berger, E.G., Hauri, H-P., Yuan, L.C. and Klausner, R.D.** (1990). Microtubule-dependent retrograde transport of proteins into the ER in the presence of brefeldin A suggests an ER recycling pathway. *Cell* **60**, 821-836.

**Lord, J.M., Roberts, L.M. and Robertus, J.D.** (1994). Ricin: structure, mode of action, and some current applications. *FASEB J.* **8**, 201-208.

**Llorente, A., Rapak, A., Schmid, S.L., van Deurs, B. and Sandvig, K.** (1998). Expression of mutant dynamin inhibits toxicity and transport of endocytosed ricin to the Golgi apparatus. *J. Cell Biol.* **140**, 553-563.

**Luckey, C.J., King, G.M., Venketeswaran, S., Maier, B.F., Crotzer, V.L., Colella, T.A., Shabanowitz, J., Hunt, D.F. and Englehard, V.H.** (1998). Proteasomes can either generate or destroy MHC class 1 epitopes: Evidence for non proteasomal epitope generation in the cytosol. *J. Immunol.* **161**, 112-121.

**Matzinger, P.** (1998). An innate sense of danger. *Seminars in Immunol.* **10**, 399-415.

**Magnusson, S., Kjeken, R. and Berg, T.** (1993). Characterisation of 2 distinct pathways of endocytosis of ricin by rat-liver endothelial cells. *Exp. Cell. Res.* **205**, 118-125.

**May, M.J., Hartley, M.R., Roberts, L.M., Krieg, P.A., Osborn, R.W. and Lord, J.M.** (1989). Ribosome inactivation by ricin A chain: a sensitive method to assess the activity of wild-type and mutant polypeptides. *EMBO J.* **8**, 301-308.

**Meir, U.C., Klenerman, P., Griffen, P., James, W., Koppe, B., Larder, B., Mcmichael, A.J. and Philips, R.** (1995). Cytotoxic T lymphocyte lysis inhibited by viable HIV mutants. *Science* **270**, 1360-1363.

**Mellman, I., Turley, S.J. and Steinman, R.M.** (1998). Antigen processing for amateurs and professionals. *Trends Cell Biol.* **8**, 231-237.

**Merril C.R., Goldman, D., Sedman, S.A. and Ebert, M.H.** (1981). Ultrasensitive stain for proteins in polyacrylamide gels shows regional variation in cerebrospinal fluid proteins. *Science* **211**, 1437-1438.

**Michalek, M.T., Grant, E.P. and Rock, K.L.** (1996). Chemical denaturation and modification of ovalbumin alters its dependence on ubiquitin conjugation for class 1 antigen presentation. *J. Immunol.* **155**, 617-624.

**Mitsumi, Y., Miki, A., Takatsuki, A., Tamura, G. and Ikehara, Y.** (1986). Novel blockade by brefeldin A of intracellular transport of secretory proteins in cultured rat hepatocytes. *J. Biol. Chem.* **261**, 11398-11403.

**Montford, W., Villafranca, J.E., Monzingo, A.F., Ernst, S.R., Katzin, B., Rutenber, E., Xuong, N.H., Hamlin, R. and Robertus, J.D.** (1987). The three dimensional structure of ricin at 2.8 Å. *J. Biol. Chem.* **262**, 5398-5403.

**Mosse, C.A., Meadows, L., Luckey, C.J., Kittlesen, D.J., Huczko, E.L., Slingluff, C.L., Shabanowitz, J., Hunt, D.F. and Engelhard, V.H.** (1998). The class 1 antigen-processing pathway for the membrane protein tyrosinase involves translation in the endoplasmic reticulum and processing in the cytosol. *J. Exp. Med.* **187**, 37-48.

**Moya, M., Dautry-Varsat, A., Gould, B., Louvard, D. and Boquet, P.** (1985). Inhibition of coated pit formation in Hep2 cells blocks the cytotoxicity of diphtheria toxin but not that of ricin. *J. Cell Biol.* **101**, 548-559.

**Nair, S.K., Boczkowski, D., Morse, M., Cumming, R.I., Lyerly, K. and Gilboa. E.** (1998). *Nature Biotechnology* **16**, 364-369.

**Neefjes, J.J., Stollorz, V., Peters, P.J., Geuze, H.J. and Ploegh, H.L.** (1990). The biosynthetic pathway of MHC class II but not class I molecules intersects the endocytic route. *Cell* **61**, 171-183.

**Neefjes, J.J., Momburg, F. and Hammerling, G.J.** (1993). Selective and ATP-dependent translocation of peptides by the MHC-encoded peptide transporter. *Science* **261**, 769-771.

**Neefjes, J., Gottfried, E., Roelse, J., Gromme, M., Obst, R., Hammerling, G.J. and Momberg, F.** (1995). Analysis of the fine specifity of rat, mouse and human TAP peptide transporters. *Eur. J. Immunol.* **25**, 1133-1136.

**Neisig, A., Wubbolts, R., Zang, X., Melief, C. and Neefjes, J.** (1996). Allele-specific differences in the interaction of MHC class I molecules with transporters associated with antigen processing. *J. Immunol.* **156**, 3196-3206.

**Nijenhuis, M., Schmitt, S., Armandola, E.A., Obst, R., Brunner, J. and Hammerling, G.J.** (1996). Identification of a contact region for peptide on the TAP1 chain of the transporter associated with antigen processing. *J. Immunol.* **156**, 2186-2195.

**Nuchtern, J.G., Biddison, W.E. and Klausner, R.D.** (1990), Pathway of antigen presentation. *Nature*, **343**, 74-76.

**Orlandi, P.A.** (1997). Protein disulfide isomerase-mediated reduction of the A-subunit of cholera toxin in a human intestinal cell line. *J. Biol. Chem.* **272**, 4591-4599.

**Osborn, R.W. and Hartley, M.R.** (1990). Dual effects of ricin A chain on protein synthesis in rabbit reticulocyte lysate. *Eur. J. Biochem.* **193** 401-407.

**Pardel, D.M.** (1998). Cancer vaccines. *Nature Medicine Supplement* **4**, 525-531.

**Pilon, M.R., Schekman, R. and Rimisch, K.** (1997). Sec61p mediates export of a misfolded secretory protein from the endoplasmic reticulum to the cytosol for degradation. *EMBO J.* **16**, 4540-4548.

**Plemper, R.K., Bîhmler, S., Bordollo, J., Sommer, T. and Wolf, D.H.** (1997). Mutant analysis links the translocon and BiP to retrograde protein transport for ER degradation. *Nature* **388**, 891-895.

**Ready, M.P., Katzin, B.J. and Robertus, J.D.** (1991). Site-directed mutagenesis of ricin A chain and implications for the mechanism of action. *Proteins:Struct. Funct. Genet.* **10**, 270-278.

**Rapak, A., Falnes, P.O. and Olsnes, S.** (1997). Retrograde transport of mutant ricin to the endoplasmic reticulum with subsequent translocation to the cytosol. *Proc. Natl. Acad. Sci. USA.* **94**, 3783-3788.

**Reid, P.A. and Watts, C.** (1990). Cycling of cell-surface MHC glycoproteins through primaquine-sensitive intracelular compartments. *Nature* **346**, 655-657.

**Reise. R.J., Wolf, P.R., Bromme, D., Natkin, L.R., Villadangos, J.A., Ploegh, H.L. and Chapman, H.A.** (1996). Essential role for cathepsin S in MHC class II-associated invariant chain processing and peptide loading. *Immunity* **4**, 357-365.

**Ridge, J.P., Di Rosa, F. and Matzinger, P.** (1998). A conditioned dendritic cell can be a temporal bridge between a CD4+ T-helper and a T-killer cell. *Nature* **393**, 474-477.

**Rivett, A.J.** (1998). Intracellular distribution of proteasomes. *Curr. Opin. Immun.* **10**, 110-114.

**Rock, K.L., Gramm, C., Rothstein, L., Clark, K., Stein, R., Dick, L., Hwang, D. and Goldberg, A.L.** (1994). Inhibitors of the proteasome block the degradation of most cell proteins and the generation of peptides on MHC class I molecules. *Cell* **78**, 761-771.

**Romero, P., Dunbar, R., Valmori, D., Pittet, M., Ogg, G., Rimoldi, D., Chen, J-L., Lienard, D., Cerottini, J.C. and Cerundolo, V.** (1998). Ex-vivo staining of metastatic lymph nodes by class-I MHC tetramers reveals high numbers of antigen-experienced tumour specific CTL. *J. Exp. Med.* **188**, 1641-1644.

**Sadasivan, B., Lehner, P.J., Ortmann, B., Spies, T. and Cresswell, P.** (1996). Roles for calreticulin and a novel glycoprotein, tapasin, in the interaction of MHC class I molecules with TAP. *Immunity* **5**, 103-114.

**Sambrook, J., Fritsch, E.F. and Maniatis, T.** (1989). Molecular Cloning, a Laboratory Manual (2nd edition). Cold Spring Harbour Laboratory Press.

**Sandvig, K., Sundan, A. and Olsnes, S.** (1984). Evidence that diphtheria toxin and modeccin enter the cytosol from different vesicular compartments. *J. Cell Biol.* **98** 963-970.

**Sandvig, K., Olsnes, S., Brown, J.E., Peterson, O.W. and van Deurs, B.** (1989). Endocytosis from coated pits of Shiga toxin: a glycolipid-binding protein from *Shigella dysenteriae* 1. *J. Cell Biol.* **108** 1331-1343.

**Sandvig, K., Prydz, K., Ryd, M. and van Deurs, B.** (1991a). Endocytosis and intracellular transport of the glycolipid-binding ligand Shiga toxin in polarized MDCK cells. *J. Cell Biol.* **113**, 553-562.

**Sandvig, K., Prydz, K., Hansen, S.H. and van Deurs, B.** (1991b). Ricin transport in brefeldin A treated cells: correlation between Golgi structure and toxic effect. *J. Cell Biol.* **115**, 971-981.

**Sandvig, K., Garred, Ø., Prydz, K., Kozlov, J.V., Hansen, S.H. and van Deurs, B.** (1992a). Retrograde transport of endocytosed Shiga toxin to the endoplasmic reticulum. *Nature* **358**, 510-511.

**Sandvig, K., Ryd, M., Garred, Ø., Schweda, E., Holm, P.K. and van Deurs, B.** (1994). Retrograde transport from the Golgi complex to the ER of both Shiga toxin and the nontoxic Shiga B-fragment is regulated by butyric acid and cAMP. *J. Cell Biol.* **126**, 53-64.

**Sandvig, K. and van Deurs, B.** (1996). Endocytosis, intracellular transport, and cytotoxic action of Shiga toxin and ricin. *Physiol. Rev.* **76**, 949-966.

**Schlossman, D., Withers, D., Welsh, P., Alexander, A., Robertus, J. and Frankel, A.** (1989). Role of glutamic acid-177 of the ricin toxin A-chain in enzymatic inactivation of ribosomes. *Mol. Cell Biol.* **9**, 5012-5021.

**Schneider, J., Gilbert, S.C., Blanchard, T.J., Hanke, T., Robson, K.J., Hannan, C.M., Becker, M., Sinden, R., Smith, G.L. and Hill, A.V.S.** (1998). Enhanced immunogenicity for CD8+ T cell induction and complete protective efficacy of malaria DNA vaccination by boosting with modified vaccinia virus Ankara. *Nature Medicine* **4**, 397-402.

**Schwartz, R.H.** (1992). Costimulation of lymphocytes T-The role of CD28, CTLA-4 and B7/BB1. *Cell* **71**, 1065-1068.

**Scott, C.A., Peterson, P.A., Teyton, L. and Wilson, I.A.** (1998). Crystal structures of two I-ad-peptide complexes reveal that high affinity can be achieved without large anchor residues. *Immunity* **8**, 319-322.

**Silverman, J.A., Mindell, J.A., Finkelstein, A., Shen, W.H. and Collier, R.J.** (1994). Mutational analysis of the helical hairpin region of diphtheria toxin transmembrane domain. *J. Biol. Chem.* **269**, 22524-22532

**Simmons, B.M., Stahl, P.D. and Russel, J.H.** (1986). Mannose receptor mediated uptake of ricin toxin and ricin A chain by macrophages. Multiple intracellular pathways for A chain translocation. *J. Biol. Chem.* **261**, 7912-7920.

**Simpson, J.C., Dascher, C., Roberts, L.M., Lord, J.M. and Balch, W.E.** (1995). Ricin cytotoxicity is sensitive to recycling between the endoplasmic reticulum and the Golgi complex. *J. Biol. Chem.* **270**, 20078-20083.

**Simpson, J.C., Lord, J.M. and Roberts, L.M.** (1995). Point mutations in the hydrophobic C-terminal region of ricin A chain indicate that Pro250 plays a key role in membrane translocation. *Eur. J. Biochem.* **232**, 458-463.

**Simpson, J.C., Smith, D.C., Roberts, L.M. and Lord, J.M.** (1998). Expression of mutant dynamin protects cells against diptheria toxin but not against ricin. *Expl. Cell Res.* **239**, 293-300.

**Sloan, V.S., Cameron, P., Porter, G., Gammon, M., Amaya, M., Mellins, E. and Zaller, D.M.** (1995). Mediation by the HLA-DM of dissociation of peptides from HLA-DR. *Nature* **375**, 802-806.

**Smith, K.J., Reid, S.W., Harlos, K., McMichael, A.J., Stuart, D.I., Bell, J.I. and Jones, E.Y.** (1996). Bound water structure and polymorphic amino acids act together to allow the binding of different peptides to MHC class I HLA-B53. *Immunity* **4**, 215-228.

**Snyder, H.L., Bacik, I., Bennink, J.R. and Kearns, G.** (1997). Two novel routes of transporter associated with antigen processing (TAP)-independent major histcompatibility complex class 1 processing. *J. Exp. Med.* **186**, 1087-1098.

**Spomer, W.E. and Wooton, J.F.** (1971). *Biochim. et Biophys. Res. Acta* **235**, 164-171.

**Suh, W-K, Mitchell, E.K., Yang, Y., Peterson, P.A., Waneck, G.L. and Williams, D.B.** (1996). MHC class I molecules form ternary complexes with calnexin and TAP and undergo peptide-regulated interaction with TAP via their extracellular domains. *J. Exp. Med.* **184**, 337-348.

**Tanaka, K., Tanahshi, N., Tsurumi, C., Yokata, K.Y. and Shimbara, N.** (1997). Proteasomes and antigen processing. *Adv. Immunol.* **64**, 1-38.

**Tighe, H., Corr, M., Ronan, M. and Raz, E.** (1998). Gene vaccination: plasmid DNA is more than just a blueprint. *Immunol. Today* **19**, 89-97.

**Townsend, A., Bastin, J., Gould, K., Brownlee, G., Andrew, M., Coupar, B., Boyle, D., Chan, S. and Smith, G.** (1988). Defective presentation to class I restricted cytotoxic T lymphocytes in vaccinia-infected cells is overcome by enhanced degradation of antigen. *J. Exp. Med.* **168**, 1211-1224.

**van Deurs, B., Pedersen, L.R., Sundan, S., Olsnes, S. and Sandvig, K.** (1985). Receptor-mediated endocytosis of a ricin-colloidal gold conjugate in Vero cells. Intracellular routing to vacuolar and tibulo-vesicular portions of the endosomal system. *Exp. Cell Res.* **159**, 287-304.

**van Deurs, B., Tonnessenm T.L., Petersen, O.W., Sandvig, K. and Olsnes, S.** (1986). Routing of internalized ricin and ricin conjugates to the Golgi complex. *J. Cell Biol.* **102**, 37-47.

**van Deurs, B., Peterson, O.W., Olsnes, S. and Sandvig, K.** (1987). Delivery of internalized ricin from endosomes to cisternae Golgi elements is a discontinuous, temperature-sensitive process. *Exp. Cell Res.* **171**, 137-152.

**van Deurs, B., Sandvig, K., Peterson, O.W., Olsnes, S., Simons, K. and Griffiths, G.** (1988). Estimation of the amount of internalized ricin that reaches the trans-Golgi network. *J. Cell Biol.* **106** 253-267.

**van Keur, L.V., Ashton-Rickardt, P., Eichelberger, M., Gaczynska, M., Nagashima, K., Rock, K., Goldberg, A.L., Doherty, P. and Tonegawa, S.** (1994). Altered peptidase and viral specific response in LMP2 mutant mice. *Immunity* **1**, 533-541.

**Vinitsky, A., Anton, L., Snyder, H.L., Orlowski, M., Bennink, J.R. and Yewdell, J.W.** (1997). The generation of nonproteasomal cytosolic proteases in antigen processing? *J. Immunol.* **159**, 554-564.

**Wales, R., Chaddock, J.A., Roberts, L.M. and Lord, J.M.** (1992). Addition of an ER retention signal to the ricin A chain increases the cytotoxicity of the holotoxin. *Exp. Cell Res.* **203**, 1-4.

**Watts, C.** (1997). Capture and processing of exogenous antigens for presentation on MHC molecules. *Annu. Rev. Immunol.* **15**, 821-850.

**Weiss, S. and Brogen, B.** (1991). MHC class-II restricted presentation of intracellular antigen. *Cell* **64**, 767-776.

**Werner, E.D., Brodsky, J.L. and McCracken, A.A.** (1996). Proteasome dependent, endoplasmic reticulum associated protein degradation: an unconventional route to a familiar fate. *Proc. Natl. Acad. Sci. USA.* **93**, 13792-13801.

**Wiertz, E.J.H.J., Jones, T.R., Bogyo, M., Geuze, H.J. and Ploegh, H.** (1996a). The human cytomegalovirus US11 gene product dislocates MHC class-1 heavy chains from the endoplasmic reticulum to the cytosol. *Cell* **84**, 769-779.

**Wiertz, E.J.H.J., Tortorella, D., Bogyo, M., Yu, J., Mothes, W., Jones, T.R., Rapoport, T.A. and Ploegh, H.** (1996b). Sec61-mediated transfer of a membrane protein from the endoplasmic reticulum to the proteasome for degradation. *Nature* **384**, 432-438.

**Wool, I.G., Glück, A. and Endo, Y.** (1992). Ribosomal recognition of ribosomal RNA and a proposal for the mechanism of translocation. *Trends Biochem. Sci.* **17**, 266-269.

**Xu, L., Sanchez, A., Yang, Z-Y., Zaki, S., Nabel, E.G., Nichol, S.T. and Nabel, G.J.** (1998). Immunization for Ebola virus infection. *Nature Medicine* **4**, 37-42.

**Yoshida, T., Chen, C., Zhang, M. and Wu, H.C.** (1991). Disruption of the Golgi apparatus by brefeldin A inhibits the cytotoxicity of ricin, modeccin, and *Pseudomonas* exotoxin. *Exp. Cell Res.* **192**, 389-395.

**Zinkernagel, R.M., Bachmann, M.F., Kundig, T.M., Oehen, S., Pirchet, H. and Hengarter, H.** (1996). Immunological memory. *Annu. Rev. Immunol.* **14**, 333-336

# Appendix 1

DNA and amino acid sequences of the SLT operon from *E.coli* phage H19B (Calderwood *et al.*, 1987). Shine-Dalgarno sequences are underlined and indicated by SD. Proposed signal peptide cleavage sites are indicated by vertical arrows. Numbers refer to amino acid residues in each polypeptide. Negative numbers designate residues in the signal peptide, and positive numbers designate residues in the mature protein.

```
GCTCAAGGAG TATTGTGTAA T ATG AAA ATA ATT ATT TTT AGA GTG CTA ACT TTT -12
      SD                Met Lys Ile Ile Ile Phe Arg Val Leu Thr Phe

TTC TTT GTT ATC TTT TCA GTT AAT GTG GTG GCG AAG GAA TTT ACC TTA GAC   6
Phe Phe Val Ile Phe Ser Val Asn Val Val Ala Lys Glu Phe Thr Leu Asp

TTC TCG ACT GCA AAG ACG TAT GTA GAT TCG CTG AAT GTC ATT CGC TCT GCA  23
Phe Ser Thr Ala Lys Thr Tyr Val Asp Ser Leu Asn Val Ile Arg Ser Ala

ATA GGT ACT CCA TTA GAG ACT ATT TCA TCA GGA GGT ACG TCT TTA CTG ATG  40
Ile Gly Thr Pro Leu Gln Thr Ile Ser Ser Gly Gly Thr Ser Leu Leu Met

ATT GAT AGT GGC TCA GGG GAT AAT TTG TTT GCA GTT GAT GTC AGA GGG ATA  57
Ile Asp Ser Gly Ser Gly Asp Asn Leu Phe Ala Val Asp Val Arg Gly Ile

GAT CCA GAG GAA GGG CGG TTT AAT AAT CTA CGG CTT ATT GTT GAA CGA AAT  74
Asp Pro Glu Glu Gly Arg Phe Asn Asn Leu Arg Leu Ile Val Glu Arg Asn

AAT TTA TAT GTG ACA GGA TTT GTT AAC AGG ACA AAT AAT GTT TTT TAT CGC  91
Asn Leu Tyr Val Thr Gly Phe Val Asn Arg Thr Asn Asn Val Phe Tyr Arg

TTT GCT GAT TTT TCA CAT GTT ACC TTT CCA GGT ACA ACA GCG GTT ACA TTG 108
Phe Ala Asp Phe Ser His Val Thr Phe Pro gly Thr Thr Ala Val Thr Leu

TCT GGT GAC AGT AGC TAT ACC ACG TTA CAG CGT CTT GCA GGG ATC AGT CGT 125
Ser Gly Asp Ser Ser Tyr Thr Thr Leu Gln Arg Val Ala Gly Ile Ser Arg

ACG GGG ATG CAG ATA AAT CAG CAT TCG TTG ACT ACT TCT TAT CTG GAT TTA 142
Thr Gly Met Gln Ile Asn Arg His Ser Leu Thr Thr Ser Tyr Leu Asp Leu

ATG TCC CAT AGT GGA ACC TCA CTG ACG CAG TCT GTG GCA AGA GCG ATG TTA 159
Met Ser His Ser Gly Thr Ser Leu Thr Gln Ser Val Ala Arg Ala Met Leu

CGG TTT GTT ACT GTG ACA GCT GAA GCT TTA CGT TTT CGG CAA ATA CAG AGG 176
Arg Phe Val Thr Val Thr Ala Glu Ala Leu Arg Phe Arg Gln Ile Gln Arg

GGA TTT CGT ACA ACA CTG GAT GAT CTC AGT GGG CGT TCT TAT GTA ATG ACT 193
Gly Phe Arg Thr Thr Leu Asp Asp Leu Ser Gly Arg Ser Tyr Val Met Thr

GCT GAA GAT GTT GAT CTT ACA TTG AAC TGG GGA ACG TTG AGT AGC GTC CTG 210
Ala Glu Asp Val Asp Leu Thr Leu Asn Trp Gly Arg Leu Ser Ser Val Leu

CCT GAC TAT CAT GGA CAA GAC TCT GTT CGT GTA GGA AGA ATT TCT TTT GGA 227
Pro Asp Tyr His Gly Gln Asp Ser Val Arg Val Gly Arg Ile Ser Phe Gly

AGC ATT AAT GCA ATT CTG GGA AGC GTG GCA TTA ATA CTG AAT TGT CAT CAT 244
Ser Ile Asn Ala Ile Leu Gly Ser Val Ala Leu Ile Leu Asn Cys His His

CAT GCA TCC CGA GTT GCC AGA ATG GCA TCT GAT GAG TTT CCT TCT ATG TGT 261
His Ala Ser Arg Val Ala Arg Met Ala Ser Asp Glu Phe Pro Ser Met Cys

CCG GCA GAT GGA AGA GTC CGT GGG ATT ACG CAC AAT AAA ATA TGT TGG GAT 278
Pro Ala Asp Gly Arg Val Arg Gly Ile Thr His Asn Lys Ile Leu Trp Asp

TCA TCC ACT CTG GGG GCA ATT CTG ATG CGC AGA ACT ATT AGC AGT TGAGGGGG
Ser Ser Thr Leu Gly Ala Ile leu Met Arg Arg Thr Ile Ser Ser  SD

TA AA ATG AAA AAA ACA TTA TTA ATA GCT GCA TCG CTT TCA TTT TTT TCA    -6
      Met Lys Lys Thr Leu Leu Ile Ala Ala Ser Leu Ser Phe Phe Ser

GCA AGT GCG CTG GCG ACG CCT GAT TGT GTA ACT GGA AAG GTG GAG TAT ACA  11
Ala Ser Ala Leu Ala Thr Pro Asp Cys Val Thr Gly Lys Val Glu Tyr Thr

AAA TAT AAT GAT GAC GAT ACC TTT ACA GTT AAA GTG GGT GAT AAA GAA TTA  28
Lys Tyr Asn Asp Asp Asp Thr Phe Thr Val Lys Val Gly Asp Lys Glu Leu

TTT ACC AAC AGA TGG AAT CTT CAG TCT CTT CTT CTC AGT GCG CAA ATT ACG  45
Phe Thr Asn Arg Trp Asn Leu Gln Ser Leu leu Leu Ser Ala Gln Ile Thr

GGG ATG ACT GTA ACC ATT AAA ACT AAT GCC TGT CAT AAT GGA GGG GGA TTC  62
Gly Met Thr Val Thr Ile Lys Thr Asn Ala Cys His Asn Gly Gly Gly Phe

AGC GAA GTT ATT TTT CGT TGA
Ser Glu Val Ile Phe Arg STOP
```

# Appendix 2

DNA and amino acid sequences of mature ricin from *Ricinus communis* (Roberts *et al.*, 1985). Numbers refer to amino acid residues in each polypeptide.

**ATA TTC CCC AAA CAA TAC CCA ATT ATA AAC TTT ACC ACA GCG GGT GCC ACT 17**
Ile Phe Pro Lys Gln Tyr Pro Ile Ile Asn Phe Thr Thr Ala Gly Ala Thr

**GTG CAA AGC TAC ACA AAC TTT ATC AGA GCT GTT CGC GGT CGT TTA ACA ACT 34**
Val Gln Ser Tyr Thr Asn Phe Ile Arg Ala Val Arg Gly Arg Leu Thr Thr

**GGA GCT GAT GTG AGA CAT GAA ATA CCA GTG TTG CCA ACC AGA GTT GGT TTG 51**
Gly Ala Asp Val Arg His Glu Ile Pro Val Leu Pro Asn Arg Val Gly Leu

**CCT ATA AAC CAA CGG TTT ATT TTA GTT GAA CTC TCA AAT CAT GCA GAG CTT 68**
Pro Ile Asn Gln Arg Phe Ile Leu Val Glu Leu Ser Asn His Ala Glu Leu

**TCT GTT ACA TTA GCC CTG GAT GTC ACC AAT GCA TAT GTG GTC GGC TAC CGT 85**
Ser Val Thr Leu Ala Leu Asp Val Thr Asn Ala Tyr Val Val Gly Tyr Arg

**GCT GGA AAT AGC GCA TAT TTC TTT CAT CCT GAC AAT CAG GAA GAT GCA GAA 102**
Ala Gly Asn Ser Ala Tyr Phe Phe His Pro Asp Asn Gln Glu Asp Ala Glu

**GCA ATC ACT CAT CTT TTC ACT GAT GTT CAA AAT CGA TAT ACA TTC GCC TTT 119**
Ala Ile Thr His Leu Phe Thr Asp Val Gln Asn Arg Tyr Thr Phe Ala Phe

**GGT GGT AAT TAT GAT AGA CTT GAA CAA CTT GCT GGT AAT CTG AGA GAA AAT 136**
Gly Gly Asn Tyr Asp Arg Leu Glu Gln Leu Ala Gly Asn Leu Arg Glu Asn

**ATC GAG TTG GGA AAT GGT CCA CTA GAG GAG GCT ATC TCA GCG CTT TAT TAT 153**
Ile Glu Leu Gly Asn Gly Pro Leu Glu Glu Ala Ile Ser Ala Leu Tyr Tyr

**TAC AGT ACT GGT GGC ACT CAG CTT CCA ACT CTG GCT CGT TCC TTT ATA ATT 170**
Tyr Ser Thr Gly Gly Thr Gln Leu Pro Thr Leu Ala Arg Ser Phe Ile Ile

**TGC ATC CAA ATG ATT TCA GAA GCA GCA AGA TTC CAA TAT ATT GAG GGA GAA 187**
Cys Ile Gln Met Ile Ser glu Ala Ala Arg Phe Gln Tyr Ile Glu Gly Glu

**ATG CGC ACG AGA ATT AGG TAC AAC CGG AGA TCT GCA CCA GAT CCT AGC GTA 204**
Met Arg Thr Arg Ile Arg Tyr Asn Arg Arg Ser Ala Pro Asp Pro Ser Val

**ATT ACA CTT GAG AAT AGT TGG GGG AGA CTT TCC ACT GCA ATT CAA GAG TCT 221**
Ile Thr Leu Glu Asn Ser Trp Gly Arg Leu Ser Thr Ala Ile Gln Glu Ser

**AAC CAA GGA GCC TTT GCT AGT CCA ATT CAA CTG CAA AGA CGT AAT GGT TCC 238**
Asn Gln Gly Ala Phe Ala Ser Pro Ile Gln Leu gln Arg Arg Asn Gly Ser

**AAA TTC AGT GTG TAC GAT GTG AGT ATA TTA ATC CCT ATC ATA GCT CTC ATG 255**
Lys Phe Ser Val Tyr Asp Val Ser Ile Leu Ile Pro Ile Ile Ala Leu Met

**GTG TAT AGA TGC GCA CCT CCA CCA TCG TCA CAG TTT**
Val Tyr Arg Cys Ala Pro Pro Pro Ser Ser Gln Phe